Enhancing Optimization in Building Performance: Simplified Models, Parallel Computing, and Neural Networks

By

Yasaman Dadras

Under the supervision of

Dr. Miroslava Kavgic

Thesis submitted to the University of Ottawa in partial fulfillment of the requirements for the degree of Doctor of Philosophy in Civil Engineering

Department of Civil Engineering

Faculty of Engineering

University of Ottawa

February 2026

Abstract

Accurate and computationally efficient building energy models are essential for retrofit decision-making under climate uncertainty. This study evaluates the use of simplified building energy models within simulation-based multi-objective optimization frameworks. Detailed models provide high predictive accuracy but impose substantial computational costs when optimization requires large numbers of simulations. Simplified models reduce computational effort but may introduce errors that affect the identification and ranking of energy conservation measures. This research quantifies these trade-offs, evaluates climate sensitivity, and proposes methods to improve predictive accuracy without modifying physical structure.

The study is organized into three phases. The first phase assesses the effects of common simplification strategies, including thermal zone aggregation, HVAC abstraction, material property reduction, and geometry simplification, on model accuracy and optimization performance. A commercial building case study shows that simplification reduces simulation and optimization time by more than an order of magnitude. Error magnitude and direction depend strongly on building typology and abstraction type. HVAC idealization and excessive zoning aggregation distort Pareto-optimal solutions and lead to suboptimal retrofit recommendations. Parallel computing further improves efficiency, enabling large-scale optimization using both detailed and simplified models.

The second phase examines the sensitivity of simplified models to climate inputs, including typical and actual meteorological years, future climate projections, and extreme hot and cold conditions. Using a mid-rise dormitory as a case study, results indicate that simplification-induced errors vary across climate scenarios and may intensify during extreme events or seasonal transitions, highlighting the importance of climate-aware model selection.

The third phase introduces an external artificial neural network adjustment that improves the predictive accuracy of simplified models without altering their physical structure. The approach restores hourly load and objective-function accuracy across all case studies, particularly for complex buildings where simplification effects are most pronounced. Embedded within a prNSGA-III framework, the method preserves Pareto-front structure while maintaining computational efficiency.

Overall, the results demonstrate that simplified models can support efficient and reliable retrofit optimization when their limitations are explicitly evaluated and addressed. The proposed methodology offers a structured framework for assessing simplified models under climate uncertainty and enhancing accuracy through data-driven correction, supporting scalable retrofit planning for existing buildings.

Acknowledgements

I would like to express my deepest gratitude to my supervisor, Dr. Miroslava Kavgic, for her exceptional guidance, unwavering support, and remarkable dedication throughout my doctoral journey. Her expertise, insightful advice, and patience shaped every stage of this work. Her encouragement and confidence in my abilities made this experience not only academically enriching but also profoundly meaningful. It has been a true privilege to learn under her mentorship.

I also extend my sincere appreciation to the members of my examination committee, Dr. Mamadou Fall, Dr. Ahmad Jrade, Dr. Ousmane Seidou, and Dr. Tareq Abuimara, for their time, thoughtful feedback, and constructive suggestions, which significantly strengthened this thesis. I gratefully acknowledge the financial support provided by the Natural Sciences and Engineering Research Council of Canada, without which this research would not have been possible.

My sincere thanks go to Dr. Mehdi Ghobadi for his valuable guidance, collaboration, and insightful input throughout this research. I am also thankful to my colleague Farzad for his collaboration, encouragement, and engaging discussions that enriched my doctoral experience.

I am deeply grateful for the love and encouragement of my fiancé, Lyubomyr, whose constant support and kindness carried me through every challenge. His presence has been an enduring source of strength and happiness. My heartfelt gratitude goes to my parents, Shahrzad and Bijan, for their lifelong sacrifices, unconditional love, and steadfast belief in me. Their guidance shaped who I am today. I also thank my brother, Hooman, for his constant encouragement and for always standing by my side.

I would further like to acknowledge my grandparents, Abbas and Fakhrozaman, as well as Zahra and Houshang; my aunts, Tahmineh, Shadi and Mehrzad; my uncles, Mehdi, Hossein,

and Ahmadreza; and my cousins, Reza, Parto, Rojan, Rohan, Mehrsa, and Mahour. Their love, pride, and continuous encouragement provided reassurance and strength throughout this journey.

Finally, I am grateful to my friends, Shima, Mozhgan, John, Igor, Borzou, and Mohammad, for their kindness, understanding, and companionship. The meaningful moments we shared brought balance, perspective, and positivity to this experience.

Preface

Across all the journal and conference papers included in this dissertation, the research direction, core ideas, and overall methodological framework were initiated and led by Yasaman Dadras under the supervision of Dr. Miroslava Kavgic. The integrated thesis structure retains only the articles that directly support the central research narrative, while additional publications completed during the PhD, including MEVO-related journal and conference papers, are not included as chapters to preserve coherence and thematic alignment.

Journal papers:

- Article 1: R. Batres, Y. Dadras, F. Mostafazadeh, M. Kavgic, MEVO: A Metamodel-Based Evolutionary Optimizer for Building Energy Optimization, Energies 2023, Vol. 16, Page 7026 16 (2023) 7026. https://doi.org/10.3390/EN16207026.
- Article 2: Y. Dadras, F. Mostafazadeh, M. Kavgic, M. Ghobadi, Enhancing Building Energy Optimization Efficiency: A Performance Analysis of Simplification Approaches, Journal of Building Engineering 105 (2025). https://doi.org/10.1016/j.jobe.2025.112559.
- Article 3: Y. Dadras, F. Mostafazadeh, M. Kavgic, M. Ghobadi, Evaluating Simplified Building Models' Sensitivity to Climate Data for Energy Retrofit Optimization, Building and Environment Evaluating 287 (2026). https://doi.org/10.1016/J.BUILDENV.2025.113885.
- Article 4: Y. Dadras, F. Mostafazadeh, M. Kavgic, M. Ghobadi, Enhancing Retrofit Optimization with ANN-Corrected Simplified Building Energy Models: *ready to be submitted.*

Conference papers:

- Conference paper 1: Y. Dadras, M. Kavgic, The applicability of simplified whole-building energy model for energy-efficiency retrofit analysis, (2022). (eSim Conference in Ottawa, Ontario, Canada).
- Conference paper 2: Y. Dadras, M. Kavgic, O. Alaei, Investigation of the thermal transmittances calculated using new infrared technology developed by QEA Tech, (2022). (CCBST Conference in Vaughan, Ontario, Canada).
- Conference paper 3: F. Mostafazadeh, Y. Dadras, M. Kavgic, R. Batres, Application of Metamodel-Based Evolutionary Optimizer (MEVO) to Improve Energy Efficiency of a Dormitory Building in Canada, in: Lecture Notes in Civil Engineering, Springer Science and Business Media Deutschland GmbH, 2025: pp. 479–485. https://doi.org/10.1007/978-981-97-8309-0_65. (2024). (IBPC Conference in Toronto, Ontario, Canada).
- Conference paper 4: Y. Dadras, F. Mostafazadeh, M. Kavgic, Y.D. Ca, Impact of Modeling Simplification on Energy Simulation Speed and Accuracy Considering Climate Change: A Case Study of a Dormitory Building, CIB Conferences 1 (2025) 171. https://doi.org/10.7771/3067-4883.1926. (2025). (CIB Conference in West Lafayette, Indiana, USA).
- Conference paper 5: Y. Dadras, F. Mostafazadeh, M. Kavgic, Y.D. M. Ghobadi, A Multi-Location Assessment Framework for Simplified Building Energy Models in Canada, (2026). (Submitted).

Article 1:

R. Batres conducted the algorithm development. The building energy modeling, simulation setup, case-study analysis, result interpretation, and manuscript preparation were carried out by Yasaman Dadras under the supervisory guidance of Dr. Kavgic. Farzad Mostafazadeh contributed to methodological discussions, review, and refinement of the final manuscript.

Articles 2, 3, and 4:

These studies were designed, developed, and led by Yasaman Dadras. The simplification framework, energy modeling workflows, climate scenario evaluations, result interpretation, and manuscript drafting were primarily carried out by the candidate. Farzad Mostafazadeh provided support for selected components of the methodology, contributed to software implementation and analytical refinement, and participated in the review and improvement of the manuscripts. Supervisory input was provided consistently by Dr. Kavgic and Dr. Ghobadi.

The contribution breakdown for these articles is summarized as:

- **Yasaman Dadras:** Writing – original draft; Writing – review and editing; Visualization; Validation; Software; Methodology; Investigation; Formal analysis; Data curation; Conceptualization.
- **Farzad Mostafazadeh:** Writing – review and editing; Software support; Methodology support; Visualization support; Analytical feedback.
- **Miroslava Kavgic:** Writing – review and editing; Writing – original draft; Supervision; Resources; Project administration; Methodology; Funding acquisition; Conceptualization.
- **Mehdi Ghobadi:** Writing – review and editing; Supervision; Project administration; Methodology; Conceptualization.

In summary, while the research benefited from meaningful collaboration, the primary intellectual leadership, model development, analytical design, and integration of methods across all included studies were carried out by Yasaman Dadras as the lead researcher.

Minor revisions have been applied to the included articles to improve consistency and alignment with the thesis structure. Use of copyrighted material complies with the corresponding publishers' guidelines.

Table of Contents

List of Tables

List of Figures

List of Abbreviations

Abbreviations	*Definition*
AMY	Actual Meteorological Year
AHU	Air Handling Unit
ANN	Artificial Neural Network
BC	Best Cost
BEM	Building Energy Model
BPO	Building Performance Optimization
BPS	Building Performance Simulation
CWEC	Canadian Weather for Energy Calculations
CE	Carbon Emissions
CCWorldWeatherGen	Climate Change World Weather Generator
CV	Coefficient of Variation
CV(RMSE)	Coefficient of Variation of the Root Mean Square Error
CDD	Cooling Degree Day
EGO	Efficient Global Optimization
ECM	Energy Conservation Measure
EC	Energy Consumption
EPW	EnergyPlus Weather File
EUI	Energy Use Intensity
GHI	Global Horizontal Irradiance
GA	Genetic Algorithm
HVAC	Heating Ventilation and Air Conditioning
IDF	EnergyPlus Input Data File
IEQ	Indoor Environmental Quality
IWEC	International Weather for Energy Calculations
IQR	Interquartile Range

Abbreviations	*Definition*
JMIM	Joint Mutual Information Maximization
KPIs	Key Performance Indicators
LHS	Latin Hypercube Sampling
LCC	Lifecycle Cost
NPV	Maximizing Net Present Value
MB	Mixed-use Building
MBC	Mean Best Cost
MCT	Mean Computation Time
MSE	Mean Square Error
MFNN	Multi-Layer Feedforward Neural Network
MLP	Multilayer Perceptron
NCM	National Calculation Methodology
NG	Natural Gas
NMBE	Normalized Mean Bias Error
NRC	National Research Council
NSGA-II	Non-dominated Sorting Genetic Algorithm II
NSGA-III	Non-Dominated Sorting Genetic Algorithm-III
prNSGA-III	Parallel Non-Dominated Sorting Genetic Algorithm-III
PEC	Primary Energy Consumption
RB	Residential Building
RCP	Representative Concentration Pathways
RMSE	Root Mean Square Error
RH	Relative Humidity
SBMO	Simulation-Based Multi-Objective Optimization
SHGC	Solar Heat Gain Coefficient
SD	Standard Deviation

Abbreviations	*Definition*
T_{eq}	Equivalent Temperature
TMY	Typical Meteorological Year
UBEM	Urban Building Energy Model
CV(RMSE)	Coefficient of Variation of the Root Mean Square Error
WWR	Window-to-Wall Ratio
WC	Worst Cost

Chapter 1: Introduction

The building sector accounts for about 39% of global energy consumption and carbon emissions worldwide [1]. This impact is particularly pronounced in existing buildings, many of which were constructed before modern energy-efficiency standards were implemented. As these older structures are gradually replaced, retrofitting emerges as a crucial measure to reduce emissions and promote sustainability [2]. Retrofitting typically involves improving building envelopes and upgrading mechanical systems to enhance energy performance [3]. Building Performance Simulation (BPS) plays a pivotal role in retrofitting efforts by providing advanced tools to assess the potential impacts of various energy efficiency measures. By enabling building designers and decision-makers to model existing energy consumption, BPS facilitates accurate predictions of the benefits associated with proposed interventions. This capability ensures retrofit decisions are well-informed and based on reliable data. However, optimizing these strategies presents challenges, particularly in balancing multiple, often conflicting objectives, such as minimizing costs, maximizing energy savings, and enhancing occupant comfort. This balancing act becomes increasingly complex when considering the wide array of available retrofit strategies [4–7].

To address these challenges, Building Performance Optimization (BPO) is employed to identify the most effective retrofit strategies. BPO utilizes objective functions focused on specific performance metrics, including energy efficiency, cost-effectiveness, and occupant satisfaction [8]. However, the computational cost of direct optimization can be prohibitively high, often requiring hundreds or thousands of simulations to evaluate potential solutions [9,10]. This challenge is particularly pronounced in Simulation-Based Multi-Objective Optimization (SBMO), where model complexity and the sheer volume of required simulations create a substantial computational burden [11–13]. Given these constraints, there is a pressing

need to improve the optimization process's efficiency. One effective strategy is to simplify the building energy model, thereby reducing both development time and computational demand. Recent studies have explored the impact of simplification techniques on prediction accuracy and computational requirements, demonstrating that strategic model simplifications can yield significant efficiency gains without substantially compromising accuracy [14,15].

Additionally, optimization efficiency can be improved by employing techniques such as multi-stage optimization algorithms and parallel computing. These techniques are increasingly integrated into BPO methodologies, enabling the simultaneous evaluation of multiple solutions and dramatically reducing the time to convergence [16,17]. Such advancements in computational techniques are essential for overcoming the limitations of traditional simulation-based approaches, especially in complex scenarios with multiple objectives.

While optimizing for multiple objectives, such as cost and energy consumption, improves the reliability of retrofit strategies, climate change introduces additional uncertainty. As global temperatures rise, the increased frequency and intensity of heat waves will drive higher cooling demand, especially in older buildings with outdated energy systems. This strains energy infrastructure and exacerbates thermal discomfort, particularly during hot seasons. Therefore, incorporating climate change scenarios into BPO ensures retrofits remain effective under future climate conditions. Without accounting for climate risks, energy performance simulations may underestimate future energy demands, leading to inadequate retrofit strategies that fail to meet sustainability goals.

To improve the efficiency of building performance optimization, this reserach examines acceleration methods, including strategies to reduce the complexity and development time of energy models and enhance the optimization process. The review also explores how BPO can incorporate climate resilience, ensuring that retrofit strategies are effective under future climate conditions. This review provides the foundation for an optimization framework that enhances

energy retrofit efficiency and long-term sustainability by identifying trends, assessing effectiveness, and addressing gaps.

1.1 Research Objectives

This research aims to investigate the reliability, efficiency, and applicability of simplified building energy models within simulation-based multi-objective optimization frameworks for retrofit decision-making under climate uncertainty. The study seeks to systematically quantify the trade-offs between model fidelity and computational performance, and to develop methods that improve the predictive accuracy of simplified models while preserving their underlying physical structure.

To achieve this overall goal, the following research objectives were pursued:

• *Evaluate the impact of common building energy model simplification strategies*
This objective examines how reductions in thermal zoning resolution, HVAC system representation, material property definition, and geometric detail influence prediction accuracy, computational cost, and optimization outcomes in simulation-based retrofit analysis.

• *Quantify simplification-induced errors within multi-objective optimization frameworks*
This objective assesses how simplification affects Pareto-optimal solutions, decision variable selection, and objective trade-offs, rather than focusing solely on isolated energy prediction errors.

• *Assess the performance of simplified models under diverse climate conditions*
This objective investigates the sensitivity of detailed and simplified models to different weather datasets, including typical meteorological years, actual meteorological years, future climate projections, and extreme hot and cold events.

• *Examine the interaction between climate uncertainty and model simplification*
This objective identifies whether simplification-related inaccuracies remain stable or intensify

under changing climate conditions, particularly during seasonal transitions and extreme weather periods.

• *Develop and validate a data-driven external correction approach for simplified models*
This objective introduces an artificial neural network-based adjustment method that improves the predictive accuracy of simplified models without altering their physical configuration.

• *Integrate ANN-enhanced simplified models into multi-objective optimization*
This objective evaluates whether the proposed ANN correction restores the accuracy and structural integrity of Pareto fronts in cost, energy, and environmental optimization problems.

1.2 Contribution to the Field

This thesis makes several original contributions to the field of building energy modeling and retrofit optimization, particularly in the context of computational efficiency and climate uncertainty:

• *Systematic evaluation of simplification strategies within optimization, not standalone simulation*
Unlike most prior studies that evaluate simplified models through single-scenario energy comparisons, this research quantifies the impacts of simplification directly within multi-objective optimization workflows, capturing their influence on Pareto fronts and retrofit decision-making.

• *Demonstration that simplification errors propagate nonlinearly through optimization processes*
The study shows that simplification-induced inaccuracies distort Pareto-optimal solution spaces, potentially leading to suboptimal retrofit recommendations even when average energy errors appear modest.

• *Climate-sensitive assessment of simplified building energy models*

This work is among the first to evaluate how simplified models perform across multiple climate representations, including future climate scenarios and extreme weather years, highlighting that simplification robustness is climate-dependent.

• *Identification of building typology and system complexity as key drivers of simplification reliability*

The findings demonstrate that the suitability of simplified models varies significantly across building types, with complex, heterogeneous buildings exhibiting greater sensitivity to zoning and HVAC abstraction.

• *Introduction of an external ANN-based correction framework that preserves physical modeling structure*

Rather than replacing physics-based models with surrogate models, this research is the first to propose a hybrid approach that enhances simplified model outputs while retaining interpretability and physical consistency.

• *Validation of ANN-enhanced simplified models within multi-objective optimization*

The integrated ANN–prNSGA-III framework successfully restores the accuracy and structural characteristics of Pareto fronts, ensuring reliable optimization outcomes with substantially reduced computational cost.

• *Provision of a practical decision-support framework for early retrofit analysis*

By linking simplification level, climate condition, and building complexity, this thesis offers actionable guidance for practitioners seeking efficient yet reliable modeling strategies in the early stages of retrofit decision-making.

• *Validation across three real-world case studies with distinct building typologies*

This research evaluates simplified and detailed building energy models using three real existing

buildings, including a commercial building, a mid-rise residential dormitory, and a single-family detached house. The use of multiple real case studies with different scales, functions, and system complexities strengthens the general applicability of the findings and allows cross-comparison of simplification effects across building typologies.

1.3 Outline of the Thesis

This thesis is structured into six chapters, combining a general methodological framework with three research articles that address different aspects of simplified building energy modeling and retrofit optimization under climate uncertainty.

Chapter 1 introduces the research context and motivation, highlighting the challenges associated with computational cost and accuracy in simulation-based multi-objective optimization for building retrofits. It presents a critical review of the relevant literature, identifies key research gaps, and defines the research objectives and the thesis's contributions.

Chapter 2 presents the general methodology adopted across all studies. This chapter describes the selected case studies, including a commercial building, a mid-rise residential dormitory, and a single-family detached house. It outlines the development of detailed and simplified building energy models and describes the applied simplification strategies related to thermal zoning, HVAC system representation, material properties, and geometry.

Chapter 3 investigates the influence of model simplification on computational efficiency and optimization outcomes. Using simulation-based multi-objective optimization, this chapter evaluates how different simplification strategies affect prediction accuracy, computational time, Pareto-optimal solutions, and retrofit decision-making. The chapter also examines the role of parallel computing in accelerating optimization processes.

Chapter 4 examines the sensitivity of detailed and simplified building energy models to different climate datasets. This chapter evaluates model performance under typical

meteorological years, actual meteorological years, future climate projections, and extreme hot and cold weather conditions. The implications of future climate projections on optimization results and retrofit strategy selection are discussed.

Chapter 5 presents an artificial neural network-based external adjustment framework designed to improve the predictive accuracy of simplified models. This chapter evaluates the training performance of the neural networks and assesses their integration into multi-objective optimization, focusing on restoring accuracy in monthly predictions and objective functions while maintaining computational efficiency.

Chapter 6 summarizes the thesis's overall findings, highlighting the main conclusions from each research article. It discusses the limitations of the current work and provides recommendations for future research directions, including simplified modeling, climate-aware optimization, and data-driven enhancement methods.

1.4 Review of Literature

1.4.1 Model Simplifications

A practical approach to addressing computational challenges in SBMO is to simplify building energy models, thereby minimizing both model complexity and the time required for development and simulation. This approach also facilitates the evaluation of various technologies and design strategies during the early [18]. Recent studies have explored how commonly used simplification techniques affect prediction accuracy and computational requirements [14,15]. One of the most common methods is thermal zone abstraction. A thermal zone is a building section where HVAC demand is sufficiently uniform to be controlled by a single unit or thermostat [19,20]. Standards such as ASHRAE 90.1, Canada's EE4, and the BRE National Calculation Methodology (NCM) provide guidelines for using simplified thermal

zoning, HVAC, and geometric representations to balance computational efficiency and predictive accuracy.

The UK's BRE NCM [31] provides guidelines for dividing buildings into thermal zones to ensure consistency in energy performance assessments for regulatory compliance. Zoning must align with the building's operational control strategy, ensuring that each zone uses the same heating and cooling setpoints, ventilation systems, and plant operating schedules. Setback conditions, such as reduced heating during unoccupied periods, must also be consistently applied across the zone. Furthermore, the same types of HVAC terminal units (e.g., radiators or air-handling units) and primary plant systems must serve all areas within a zone, and the control strategy should be uniformly applied. The NCM permits combining adjoining thermal zones with similar characteristics, but the influence of partitions must be considered.

ASHRAE 90.1 (2019) [19], a widely used standard in North America, provides zoning guidelines to ensure energy-efficient designs comply with regulations. Spaces with identical functions served by the same HVAC system can be grouped into a single thermal zone if their orientations are similar or differ by no more than 45 degrees. Within the ASHRAE framework, a "space" is a subdivision of an HVAC zone, and HVAC zones represent thermal concepts rather than physical boundaries. Figure 1-1 illustrates the hierarchical relationship between spaces, HVAC zones, and thermal blocks, with similar zones grouped into thermal blocks for streamlined modeling. Residential buildings require at least one thermal block per unit, particularly for corner units and those with roof or floor loads. Although plenums are typically modeled separately, they can be combined with conditioned spaces for simplicity.

Canada's EE4 standard [21] focuses on modeling energy performance in commercial and institutional buildings, particularly in response to the challenges of the Canadian climate. It advocates grouping spaces with similar HVAC systems, schedules, and internal loads into a single thermal zone. Auxiliary spaces, such as corridors, stairwells, equipment rooms, and

laundry rooms, are excluded from zoning to concentrate on areas with higher HVAC demands. This approach effectively captures significant thermal variations, especially between north- and south-facing zones, which are critical in heating-dominated climates. However, excluding auxiliary spaces can underestimate total energy use, potentially affecting the accuracy of optimization efforts.

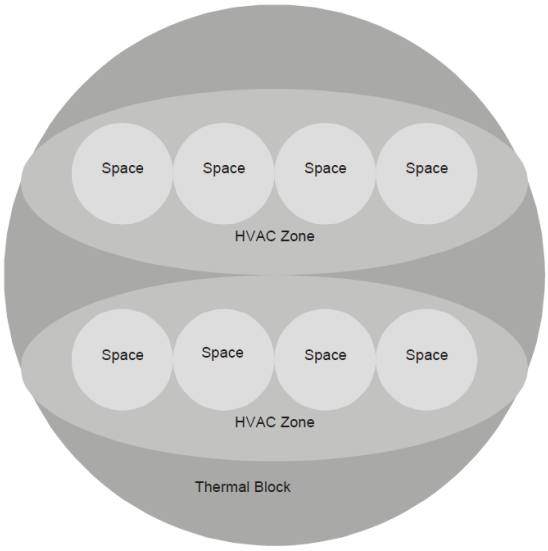

Figure 1-1: Structure of Spaces, HVAC Zones, and Thermal Blocks based on ASHRAE 90.1 (2019) [20].

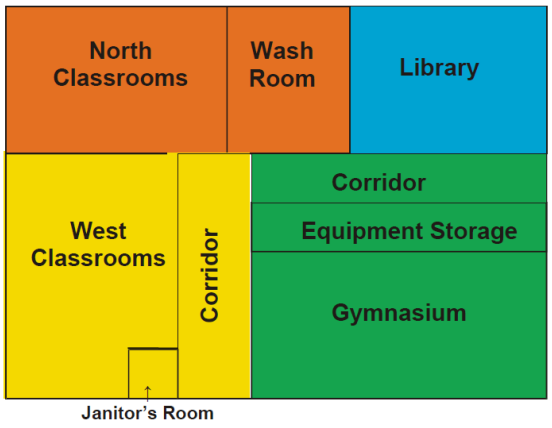

Figure 1-2: Zoning strategy for a typical school building based on EE4 [21].

While these standards provide a foundation for regulatory compliance, they may not always offer the detail needed for more complex simulations. Assigning too many thermal zones can increase complexity, slow simulations, and increase computational costs. Simplifying thermal zones can significantly reduce simulation time. [22,23].

Elhadad et al. [14] examined the effects of thermal zone simplification in residential buildings within hot, arid climates by comparing a detailed model with four simplified scenarios. Scenario S1, which grouped spaces by use and orientation, reduced modeling time by 79% and simulation time by 63% while underestimating energy use by 12.7% and thermal comfort by 21.4%. The most simplified model (S4) saved 95% of modeling time and 94% of simulation time but resulted in larger deviations, underestimating energy use by 35.8% and thermal comfort by 63.3%. Klimczak et al. [24] investigated the impact of thermal zone and shading simplifications in building energy simulations through four variants of varying complexity, focusing on low-energy residential buildings in Poland. The simplified model, which excluded bathroom zones and reduced the number of zones from 70 to 25, achieved a 3.5% reduction in energy consumption compared to the baseline (133.1 GJ). This model also showed a peak hourly power demand nearly identical to the baseline, with only a 0.08% difference (26.03 kW versus 26.01 kW). Larsen et al. [25] explored the impact of model simplification on energy and Indoor Environmental Quality (IEQ) in Nordic climates. While energy demand was relatively insensitive to zoning complexity (3% average deviation), non-energy Key Performance Indicators (KPIs), such as thermal comfort, showed deviations of up to 23.7% during heating seasons with simplified models.

In large-scale models, simplifications become even more critical. For example, Johari et al. [15] compared energy performance and zoning configurations for three multifamily buildings using IDA ICE, TRNSYS, and EnergyPlus. Simplifications affected results differently across tools, with EnergyPlus underestimating and IDA ICE overestimating heat demand in single-zone models (variation within ±5%). Deviations of up to 9% in heating demand were observed between the simplest (LoD1) and most detailed (LoD3) models. The study favored LoD1 models for Urban Building Energy Models (UBEMs), balancing computational efficiency and accuracy. Chen et al. [26] evaluated 940 office and retail buildings in San Francis and compared

three zoning methods: OneZone, AutoZone, and Prototype. The OneZone method, using a single thermal zone per floor, reduced fan capacity by 15.2%, cooling capacity by 11.1%, heating capacity by 11.0%, space heating load by 16.9%, and cooling load by 7.5% compared to the more complex AutoZone method. It achieved 50% faster simulation times using floor multipliers, albeit at the cost of reduced accuracy.

Geometry simplifications also improve simulation efficiency. Heidarinejad et al. [27] introduced a framework to balance accuracy and complexity in building energy models, demonstrating that variations in shape and zoning can affect simulation results by up to 10%. They identified 14 typical building shapes that represent over 80% of neighborhood-scale buildings and 60% of city-scale buildings, and proposed a method to model the remaining 20%. Santos et al. [28] conducted experiments on the simplification of complex geometry. The first experiment focused on simplifying double-curved building envelopes, achieving a 112-fold reduction in simulation time (from 15,407 seconds to 3 minutes and 53 seconds) with minimal error in hourly energy predictions (CVRMSE = 3.4%, NMBE = 0.1%). The second experiment involved simplifying multi-zone models, with one model reducing simulation time by 95.8% and another by 99.4%, completing simulations in just 89 seconds. The first model reported errors of 6.4% and -1.4% for CVRMSE and NMBE, respectively, while the second model reported errors of 7.2% and -1.7%.

Beyond thermal zones and geometry, simplifications in HVAC systems, materials, and internal load schedules also accelerate simulations. Al-Janabi et al. [29] highlighted the impact of HVAC system simplification on the accuracy of energy predictions, showing that oversimplified approaches can lead to significant discrepancies. Using an ideal air load system, a common simplification in the early design phase, introduced a 96.9% error in cooling energy predictions for a Canadian university facility compared to a detailed HVAC model. This research emphasizes that while such simplifications improve simulation efficiency, they

sacrifice prediction accuracy, especially in cooling and heating loads. When comparing EnergyPlus and IES for the ideal air load system scenario, they revealed discrepancies of 1.7% in heating and 7.8% in cooling loads between the two tools, despite identical input parameters. Picco et al. [30] emphasized the importance of accurate HVAC modeling, showing that omitting humidity control can skew energy predictions, with total differences of 9.63% for heating and 4.72% for cooling loads. Peak heating and cooling power differences were 3.7% and 2.4%, respectively. Simplifying geometry led to an overestimate of heating energy by 15%, while simplifying material properties resulted in only a 0.2% difference. Ren et al. [31] investigated the effects of thermal zoning and internal load scheduling on decision-making for heating-related retrofit in British semi-detached houses. Combining rooms with similar thermal characteristics underestimated annual heating demand by approximately 7% while modeling the entire house as a single zone resulted in a 24% underestimation compared to the detailed model. Using actual internal load profiles derived from smart meter data showed significant variations in energy predictions, with errors reaching up to 325% for electricity and 69% for heating demand when simplified schedules were used.

While simplification strategies significantly accelerate simulation time, they might compromise predictive accuracy, particularly in optimization workflows that explore a wide range of retrofit combinations. To address this limitation, researchers have explored calibration methods to improve the reliability of building energy models before optimization [32–42]. These calibration techniques, often grounded in statistical modeling or machine learning, seek to align simulation outputs with measured or high-fidelity reference data. Recent efforts have focused on developing automated and semi-automated calibration frameworks that improve model accuracy while maintaining simplified configurations. For instance, Herbinger et al. [38] introduced a surrogate-based neural network calibration method employing a multilayer perceptron to infer uncertain building parameters, integrating external drivers such as weather

and internal schedules. Similarly, Chong et al. [35,41] applied Bayesian calibration methods that leverage large datasets, combining information-theoretic subset selection with a No-U-Turn Sampler (NUTS) to efficiently navigate the parameter space. Sun et al. [33] proposed a pattern-based automated calibration strategy that links parameter tuning to systematic bias detection in load profiles, reducing reliance on manual input while maintaining physical interpretability. Other researchers, including Asadi et al. [32] and Pachano and Bandera [36], implemented optimization-based and multi-step calibration procedures using genetic algorithms and staged approaches to meet ASHRAE Guideline 14 and IPMVP criteria.

Despite these advances, significant challenges remain in achieving consistently reliable calibration outcomes. Yang and Becerik-Gerber [42] highlighted that the large number of independent and interdependent parameters, coupled with dynamic interactions among building subsystems, introduces uncertainties that are difficult to resolve empirically. Herbinger et al. [38] further noted that neural network–based calibration, while powerful, may produce physically implausible parameter values when the model structure or available data is insufficiently robust. These issues raise concerns about the physical interpretability of calibrated parameters and the adequacy of relying solely on statistical metrics such as CV(RMSE) to assess model quality.

Moreover, while existing calibration methods can substantially improve model accuracy, they often do so by adjusting key physical parameters, such as material properties, internal gains, or HVAC setpoints. Although statistically effective, such changes risk altering the core behavior and assumptions of the building energy model, undermining its consistency, traceability, and generalizability across retrofit scenarios. This limitation is particularly problematic in optimization contexts, where preserving the model's original abstraction is essential to ensure interpretable and actionable retrofit recommendations. Despite growing interest in model

calibration, little attention has been paid to approaches that improve the predictive accuracy of simplified models during optimization without modifying their inherent structure.

1.4.2 Optimization Process Enhancement

While simplifying building models can significantly reduce computational costs, additional strategies are needed to further enhance SBMO's efficiency. One effective approach is multi-level optimization, which breaks down complex optimization problems into smaller, more manageable subproblems [43,44]. This method involves optimizing building elements in a series of level-dependent stages. The optimal solutions identified in the initial stage serve as design options for more detailed exploration in subsequent phases, ensuring a systematic and efficient optimization process.

Bichiou et al. [43] developed a simulation environment to optimize building envelope features and HVAC systems in residential buildings across five U.S. cities. They evaluated four optimization approaches: HVAC optimization only, envelope optimization only, optimization of all elements, and multi-stage optimization, which first optimized building geometry and envelope variables before selecting HVAC systems. The multi-stage approach proved more efficient, reducing CPU time by 33% to 95% while minimizing life-cycle costs. While full optimization provided slightly more accurate results, it required more computational resources. Ascione et al. [44] introduced the Harlequin framework, a novel multi-stage approach for the multi-objective optimization of building energy design. It comprises three phases: the first employs a genetic algorithm for Pareto optimization of building geometry, envelope, and conditioning setpoints; the second uses smart exhaustive sampling to identify optimal energy systems; and the third provides stakeholders with categorized design solutions based on sustainability, cost, and investment efficiency. The multi-stage design optimization process was found to yield better performance than the benchmark design. In a separate study, Ascione et al. [45] developed a two-stage optimization approach utilizing genetic algorithms to enhance

building energy conservation. The first stage identifies effective Energy Conservation Measures (ECMs) to minimize heating and cooling demand. The second stage integrates these ECMs with supplementary strategies to boost system efficiency and incorporate renewable energy sources. The study employs smart exhaustive sampling to assess investment costs, primary energy consumption, and global costs. This innovative methodology significantly reduces computational time, requiring only about 76.1 hours to evaluate 596,700 design packages, in stark contrast to traditional simulation methods, which are often much more time-consuming.

Despite the benefits of multi-stage optimization, this method may undermine the integrity of the overall process by dividing decision variables and the search space across different optimization stages. Waibel et al. [46] presented a co-simulation framework for optimizing building geometries and multi-energy systems, emphasizing the need for simultaneous design to enhance energy efficiency. The bi-objective optimization, applied to four office buildings in Zurich, aimed to minimize operational costs and carbon emissions while integrating building design with energy systems early in the planning process. By comparing the nested optimization procedure with a traditional consecutive approach (Figure 1-3), the study demonstrated that simultaneous evaluation of building energy demands, solar potentials, and optimal energy system design is crucial, as these factors are interdependent. Findings indicated that a nested formulation significantly impacts construction decision-making, leading to different design choices that affect energy demands, renewable energy potential, and optimal building characteristics aligned with environmental targets. Ferrara et al. [47] introduce a methodology for simultaneously optimizing energy demand and supply to design nearly zero-energy single-family homes in Northern Italy. By comparing a single-stage optimization approach with a multi-stage method, the study showed that simultaneous consideration of energy demand and supply leads to a broader set of optimal solutions. Compared to the multi-

stage approach, the single-stage method resulted in a slight decrease in total primary energy consumption (from 95.47 kWh/m² to 90.83 kWh/m²) and a reduction in global costs (from €915.59/m² to €906.47/m²), demonstrating its effectiveness in delivering more optimal results. The one-stage approach enabled designers to explore the design space more effectively, account for interdependencies among building elements, and achieve higher-performing solutions. A further limitation of multi-stage optimization is that fixing the design variables in the first stage may limit the ability to find optimal solutions in the second stage. Gagnon et al. [48] compared the performance of multi-stage and single-stage building design approaches using multi-objective optimization. In their case study, the single-stage approach, which simultaneously optimized 39 design variables related to architecture and HVAC systems, was more efficient than the sequential approach. The single-stage method found about 59% of optimal solutions within 100 computational hours, while the sequential approach took 765 hours to find approximately 40.8%.

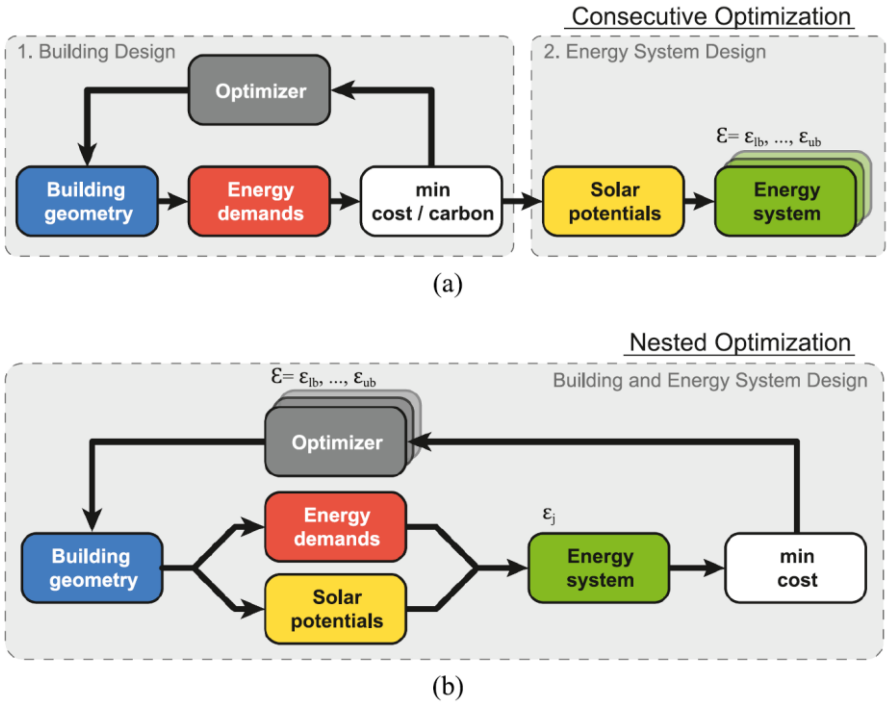

Figure 1-3: Consecutively optimizing the building geometry followed by the energy system; (b) Nested (or coupled) optimization of both the building geometry and energy system [46].

Another approach to enhance SBMO's efficiency is parallel computing, which distributes tasks across multiple processors, significantly accelerating the optimization process. Karatas et al. [49] presented an expandable, scalable parallel computing framework to optimize the environmental and economic performance of housing units. The framework integrates a multi-objective genetic algorithm with EnergyPlus to enable precise energy performance modeling while minimizing the trade-offs between environmental sustainability and upfront construction costs. The framework is divided into four main stages: defining metrics and decision variables, implementing the genetic algorithm, utilizing parallel computing for efficient data processing, and conducting extensive performance testing (Figure 1-4). The study's results demonstrated that employing multiple processors significantly reduced computational time, from 12 days to approximately 1.7 days when eight processors were used. Brea et al. [50] presented a computational multi-objective optimization method designed to enhance energy efficiency and thermal comfort in residential buildings, emphasizing the importance of parallel computing (Figure 1-5). The integrated NSGA-II with EnergyPlus simulation software evaluated various design parameters, such as roof and wall types, solar orientation, and ventilation strategies.

By utilizing a high-performance computing cluster, the study significantly reduces analysis time from nearly 12 days to approximately 4.4 hours, showcasing the efficiency of parallel computing in complex simulations. Tavakolan et al. [51] presented a parallel-structured NSGA-II optimization framework (Figure 1-6) tailored to the Iranian building sector, which faces distinct challenges due to highly subsidized energy prices and a step utility tariff system. By integrating MATLAB as the optimization engine and EnergyPlus as the dynamic energy simulator, the study aimed to optimize key performance indicators, including primary energy consumption, net present value, and discounted payback period. The framework’s parallel processing structure and result-saving feature significantly reduced computational time from 500 to 200 seconds per generation, enabling efficient exploration of various retrofit solutions.

Mostafazadeh et al. [52] introduced a simulation-based multi-objective optimization framework using a modified version of the Non-Dominated Sorting Genetic Algorithm-III (NSGA-III), named Parallel Non-Dominated Sorting Genetic Algorithm-III (prNSGA-III), to address building energy retrofitting in the context of climate change and energy price variations. This framework integrates EnergyPlus for energy simulation with MATLAB for optimization and uses parallel computing to significantly reduce computational time. The study applied this framework to a residential building in Tehran, Iran, and investigated various active, passive, water-conservation, and renewable-energy retrofit measures. The optimization aimed to maximize environmental performance while minimizing thermal discomfort and life cycle costs. The findings revealed that implementing the proposed retrofits could result in up to 73% reduction in carbon emissions and a 46% reduction in thermal discomfort.

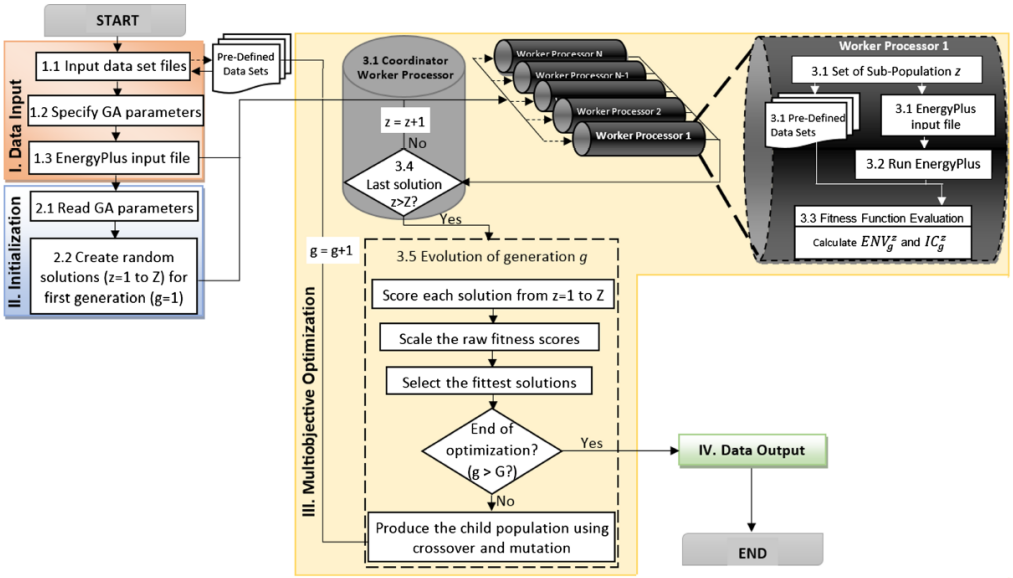

Figure 1-4: The multi-objective optimization framework was developed by Karatas et al. [49].

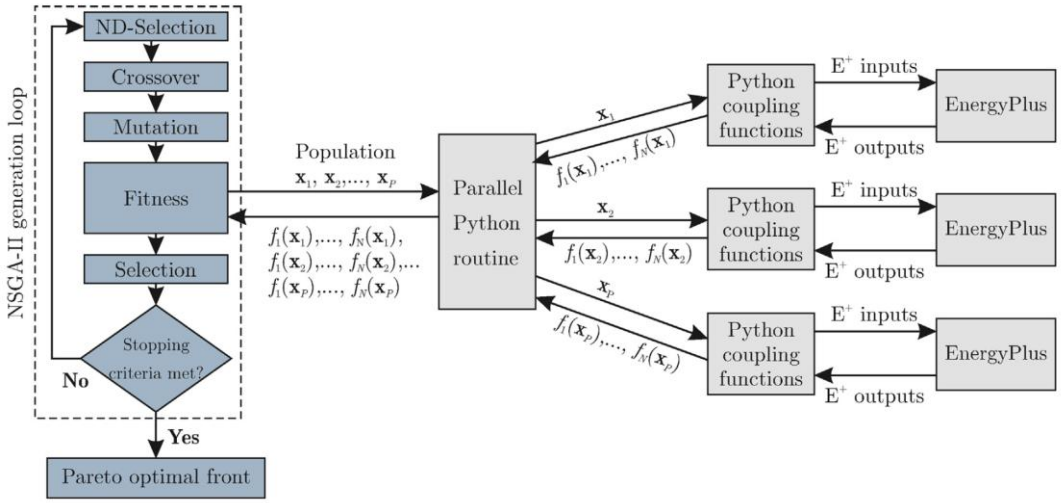

Figure 1-5: The multi-objective optimization framework was developed by Bre et al. [50].

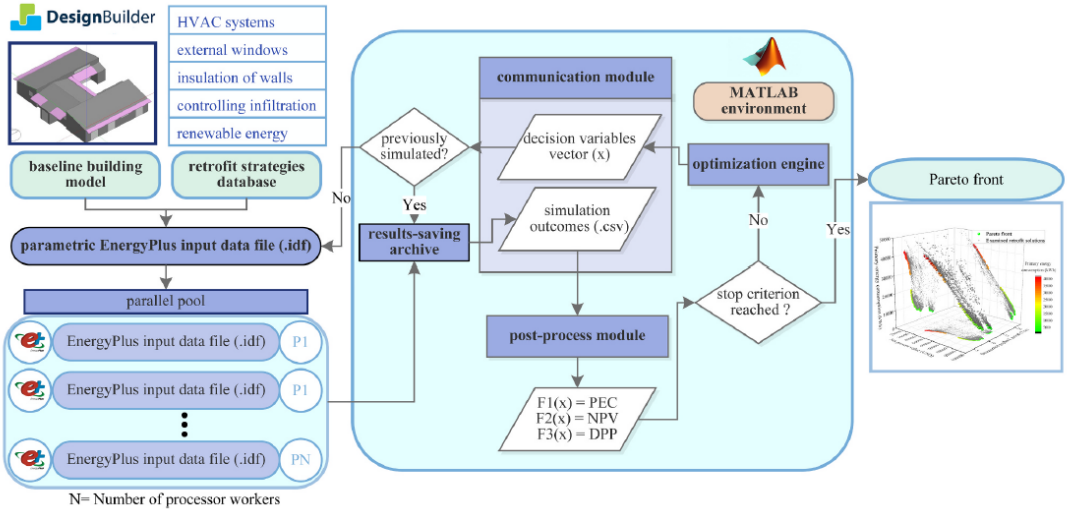

Figure 1-6: The multi-objective optimization framework was developed by Tavakolan et al. [51].

1.4.3 Climate Change and Its Impact on Building Retrofits

While recent optimization techniques have substantially lowered energy use and computation time, an equally important consideration is the increasing influence of climate change on building performance [53,54]. While traditional retrofitting strategies primarily focus on optimizing energy use and minimizing costs, the increasing unpredictability of weather patterns and rising global temperatures introduce new challenges that demand a more dynamic approach to building energy systems. Climate change affects thermal loads in buildings and necessitates retrofitting measures to adapt to more extreme weather conditions, higher energy demands, and

the need for resilience [55,56]. Consequently, optimization frameworks, which have been centered on energy efficiency and cost-effectiveness, must now integrate climate-responsive solutions that account for the present and future climatic shifts. Addressing these challenges will require advanced simulation tools and innovative retrofitting strategies to ensure long-term sustainability and occupant comfort.

Streicher et al. [57] investigated various deep energy retrofit pathways for the Swiss residential building stock by combining dynamic stock modeling, bottom-up energy modeling, and optimization for different climate scenarios. Their study found that while replacing older buildings with more energy-efficient ones will result in some reductions in energy demand and greenhouse gas emissions, these reductions will likely fall short of the Swiss target of a 60% decrease in energy demand by 2050. The research demonstrated that partial retrofitting and cost-minimized pathways would not be sufficient to meet long-term climate goals. Instead, Streicher et al. found that early and comprehensive retrofitting offers the greatest energy savings and greenhouse gas reduction potential, but requires a higher upfront investment. Shen et al. [58] investigated the feasibility and importance of incorporating climate change impacts in building retrofit analysis. Their research introduced a framework for assessing different ECMs for existing buildings under future climate conditions. By developing a Python-based tool that integrates EnergyPlus simulations with a parametric study, the authors applied LHS and a Joint Mutual Information Maximization (JMIM) feature selection method to identify the most impactful ECMs regarding NPV and energy use. Their findings demonstrated that global climate change would alter the optimal selection of ECM combinations over time, with the effect varying by building type and location. Shen et al. validated their model using future extreme weather data from Philadelphia and San Francisco, emphasizing that the ranking and performance of ECMs under future climate conditions differed significantly from those in the current climate. Berardi et al. [59] studied the impact of future climate scenarios on building

energy demand, focusing on heating and cooling requirements in Canada. By employing statistical and dynamical downscaling methods, they projected significant shifts in energy consumption for 16 ASHRAE prototype buildings in Toronto. Their simulations showed a decrease in heating Energy Use Intensity (EUI) by 18%–33% and an increase in cooling EUI between 15%–126% by 2070, depending on the building typology and baseline climate data. The study underscored the importance of selecting appropriate baseline climate files and using high-resolution regional climate models to accurately capture local conditions. The results indicated that incorporating future weather files in energy simulations is crucial for designing resilient, energy-efficient buildings that can adapt to the extreme conditions expected from climate change.

Ascione et al. [16] explored the resilience of cost-optimal energy retrofits of buildings to global warming by applying a multi-stage, multi-objective optimization approach. The study focused on identifying robust retrofit solutions for a typical Mediterranean residential building in Naples, Italy, across various global warming and economic scenarios. The study demonstrated that the resilience of energy retrofits to climatic and economic changes can be significantly improved through robust optimization methodologies, ensuring cost-effectiveness and sustainable building performance over time. Luo et al. [60] developed a life-cycle optimization strategy to determine optimal retrofit solutions for office buildings, explicitly integrating climate change impacts into their analysis. By combining a hybrid genetic algorithm with an artificial neural network, they accurately predicted future energy demand using projected weather profiles generated by the HadCM3 model. Their approach evaluated the cumulative performance of various retrofitting measures, revealing significant discrepancies when contrasting current and future weather conditions. Notably, the study found that relying solely on current weather data to select optimal retrofitting solutions could lead to underestimates of lifetime costs, energy use, and carbon emissions by as much as 54.7%. Tomrukcu et al. [61]

investigated the impacts of climate change on residential buildings in Istanbul and Izmir, Turkey, focusing on the effectiveness of energy-efficient retrofitting strategies. By creating future weather scenarios and conducting dynamic simulations under RCP 4.5 and RCP 8.5, the study revealed significant temperature increases of 4.3 °C in Istanbul and 5 °C in Izmir. These changes are expected to dramatically affect energy consumption, with Cooling Degree Days (CDDs) potentially doubling in July, reaching 292 in Izmir and quadrupling to 158 in Istanbul. The research found that primary heating energy consumption could decrease by 36–41% without retrofitting, while primary cooling energy consumption could triple in both cities. Implementing energy-efficient improvements reduced summer temperatures by approximately 5–6 °C in naturally ventilated spaces in Istanbul and 4–5 °C in Izmir, highlighting the need for tailored retrofit strategies that account for regional climate conditions to enhance building performance and occupant comfort.

1.5 Knowledge Gaps

1.5.1 Model Simplifications

Despite advances in simplifying building energy models, a significant gap persists in applying them within optimization processes. While various simplification techniques have been developed, their integration into simulation-based multi-objective optimization frameworks remains underexplored. Specifically, little research has focused on identifying which simplification methods can significantly reduce computational effort without compromising accuracy. Addressing this gap is essential to improving optimization efficiency, particularly in large-scale simulations that demand substantial computational resources.

Furthermore, although the impact of climate change on building energy consumption is well documented, its effect on the accuracy of simplified models remains insufficiently studied. Rising global temperatures and shifting weather patterns alter external thermal loads, affecting

energy demand for heating and cooling [62,63]. However, how simplified models respond to these climatic variations, particularly in the context of energy efficiency assessments and retrofitting projects, remains unclear. This gap is crucial, as inaccuracies in predicting future energy performance could lead to suboptimal retrofit decision-making, affecting both cost-effectiveness and environmental sustainability. Consequently, more research is needed to evaluate the reliability of simplified models under evolving climate conditions, ensuring that energy predictions remain accurate and useful for long-term planning.

1.5.2 Calibration of Simplified Models in Optimization

A parallel gap emerges in the calibration of simplified models used within optimization processes. Although calibration techniques, particularly data-driven and neural network-based methods, can substantially improve model accuracy, several limitations constrain their applicability in optimization settings. Prior studies have shown that calibration often involves adjusting key physical parameters, such as material properties, internal gains, or HVAC settings, to match measured data. While statistically effective, these adjustments risk altering the model's fundamental structure and physical meaning, thereby reducing transparency, interpretability, and consistency across retrofit scenarios. This is especially problematic in optimization workflows, where preserving the original modeling abstraction is essential for ensuring that recommended retrofit measures remain credible and actionable.

Despite growing attention to calibration techniques, limited research has explored methods to enhance the predictive accuracy of simplified models without altering their underlying physics, geometry, or assumptions, particularly in computationally intensive optimization. This gap motivated the development of the parallel neural network-based adjustment framework presented in the accompanying research: a strategy that improves prediction accuracy externally, preserves the model’s structural integrity, and maintains computational efficiency.

However, broader evaluation of such external-adjustment approaches within multi-objective optimization remains scarce.

1.6 Study Plan

This study aims to address research gaps in building energy optimization by assessing the accuracy, time efficiency, and practical applications of simplified models in the optimization process, leveraging advanced computational methods. The study integrates parallel computing and machine learning to further enhance efficiency and predictive accuracy. The three key phases of this research are summarized below, each answering specific research questions.

I. Phase 1: Simplified Building Energy Models (chapter 3)

The first phase assesses how simplified models, developed based on common building energy modeling simplifications, perform in terms of accuracy and computational efficiency within an optimization framework. This phase also investigates how parallel computing can further improve optimization efficiency.

In addition to simulation-based investigations, this research incorporates an expert-informed perspective through a structured survey of professional building energy modelers. The survey was designed to identify commonly used simplification practices in industry and research, ensuring that the evaluated model abstractions reflect real-world modeling approaches rather than purely theoretical simplifications.

Research Questions:

1. How does model simplification affect its prediction accuracy, and which simplification strategies effectively reduce the computational demands of multi-objective optimization while maintaining acceptable accuracy?
2. Which commonly used simplification methods may hinder the selection of optimal energy efficiency measures?

3. How can parallel computing enhance efficiency by reducing computational time in the optimization process?
4. What are the standard practices and benefits of using simplified models in building energy modeling?

II. Phase 2: Climate Change and Energy Performance of Simplified Models (chapter 4)

The second phase investigates the impact of climate change on the performance of simplified energy models. This phase evaluates various weather scenarios and their effects on energy consumption predictions during energy efficiency assessments and retrofitting projects.

Research Questions:

1. How do variations in climatic data, such as TMY data, extreme weather years, and future climate projections, affect the predictive accuracy of simplified building energy models?
2. Do the error trends between simplified and detailed models remain consistent across different types of weather files?
3. Do simplified models retain similar error patterns compared to detailed models after optimization using future climate scenarios?
4. Which simplification methods (e.g., thermal zone abstraction, HVAC system simplification, material property reduction) are most affected in terms of accuracy under extreme climate change conditions?

III. Phase 3: Improving the Accuracy of Simplified Models in the Optimization Process (chapter 5)

In this phase, the focus shifts to enhancing the predictive accuracy of simplified models during optimization. The study evaluates how different simplifications affect accuracy and the

identification of optimal energy-efficiency measures for retrofitting, and proposes methods to enhance the accuracy of simplified building energy models.

Research Questions:

1. To what extent can artificial neural networks correct simplification-induced errors in hourly and aggregated energy predictions of simplified building energy models?
2. How does integrating ANN-adjusted simplified models into multi-objective optimization affect the accuracy and structure of Pareto-optimal solutions?
3. Which simplification types and building characteristics benefit most from ANN-based external correction?

Chapter 2: General Methodology

This research seeks to enhance the efficiency of building energy optimization by simplifying the physical model, improving the optimization workflow, and advancing the optimization algorithm. Because several components of the overall framework are shared across the published papers on model simplification and the optimization process, presenting the entire methodology separately in each chapter would lead to unnecessary repetition. To maintain clarity and avoid duplication, all common methodological elements are described in full detail in this chapter. The variations specific to each phase of the research, along with the corresponding results and discussions, are provided in Chapters 3 through 5.

2.1 Case Studies Overview

2.1.1 Case Study 1: Commercial Building in Markham, Ontario, Canada

The first case study building is a single-story office building in Markham, Ontario, Canada. This building was selected because, first, it is characterized by a common building layout, construction, and HVAC system typical of Canadian office buildings. As illustrated in Figure 2-1, the buildings in the selected area share a similar architectural style. Given their widespread presence, single-story mixed-use office buildings serve as important archetypes for energy modeling and retrofit strategies [64]. Notably, in 2020, office buildings accounted for 33.3% of total energy consumption and 32.5% of greenhouse gas emissions in Canada's commercial and institutional sectors, highlighting their significant role in overall energy performance [65].

Furthermore, its mixed-use, composed of office space and warehouse, introduces unique simplification challenges that require careful examination. The office space occupies 36% of the total building area, with a plenum space above it. A detailed building model for the case study was developed in SketchUp, with EnergyPlus as the simulation engine to assess the building's energy performance. In the detailed model, the warehouse area is divided into five

Figure 2-1: First case study building, commercial building.

thermal zones to account for variations in orientation and accommodate the distinct operation of independent HVAC systems. As shown in Figure 2-1, virtual airwalls rather than physical walls were introduced in the warehouse to enhance modeling precision. The office area is further segmented into 14 zones, including a plenum zone at the top of the office, resulting in a detailed model with 19 thermal zones in total. The office walls comprise gypsum board, fiberglass insulation, concrete, and brick veneer, yielding a U-value of 1.2-1.4 W/m²K. The warehouse walls lack insulation and have a total thickness of 30 cm with a U-value of 2.8 W/m²K. This poor thermal performance across the envelope, including windows, roofs, and floors, suggests significant potential for energy savings through retrofitting.

The building is conditioned by two rooftop air handling units (AHUs). One serves the office area, providing heating (37,000 W) and cooling (21,000 W) via natural gas and electricity. The second AHU provides cooling (53,000 W) for the warehouse, supplemented by two 65,000 W industrial heaters for space heating in core and perimeter zones. Energy consumption is divided between grid electricity, used for lighting, cooling, and appliances, and natural gas, used for domestic hot water and heating. Occupied by 15 people on weekdays (10:00–18:00), the building maintains seasonal setpoints of 22°C in winter and 24°C in summer.

Since the building was constructed in 1985, it predates Canada's first national energy code (1997) [66] and thus features a poorly insulated envelope, contributing to high energy consumption. Accordingly, an energy model of the building was developed using SketchUp [67] and simulated in EnergyPlus [68]. The model was validated against 2020 natural gas consumption and assessed using the normalized mean bias error (NMBE) and the coefficient of variation of the root mean square error (CV(RMSE)), as per ASHRAE Guideline 14 [71]. These metrics were calculated using Equations 2-1 and 2-2:

$$NMBE = \frac{\frac{1}{N}\sum_{i}^{N}(V_i - \hat{V}_i)}{V} \times 100 \qquad \text{Equation 2-1}$$

$$CV(RMSE) = \frac{\sqrt{\frac{1}{N}\sum_{i}^{N}(V_i - \hat{V}_i)^2}}{\bar{V}} \times 100 \qquad \text{Equation 2-2}$$

where N denotes the number of data points, V_i represents the measured value, $\hat{V}_i$ is the model prediction, and V is the mean of the observed values. ASHRAE Guideline 14 [69] recommends thresholds of ±5% for NMBE and 15% for CV(RMSE) when monthly data are used. In this case, the NMBE for natural gas and electricity consumption predicted by the detailed model were 4.6% and -4.3%, respectively, while the CVRMSE values were 12.6% for natural gas and 9.7% for electricity, indicating satisfactory accuracy in predicting energy consumption patterns.

2.1.2 Case Study 2: Residential Dormitory Building in Ottawa, Ontario, Canada

The second case study building is a five-story residential dormitory located in Ottawa, Canada, constructed in 1965 (Figure 2-2). The building shares key characteristics with mid-rise residential apartment buildings across Canada. In addition to construction technology, it is comparable in terms of building height, window-to-wall ratio, insulation levels, and typical envelope and mechanical system configurations, particularly for buildings constructed in the same period. These similarities support considering the case study as representative of apartment buildings from that era. Furthermore, according to [70], approximately 2.5 million

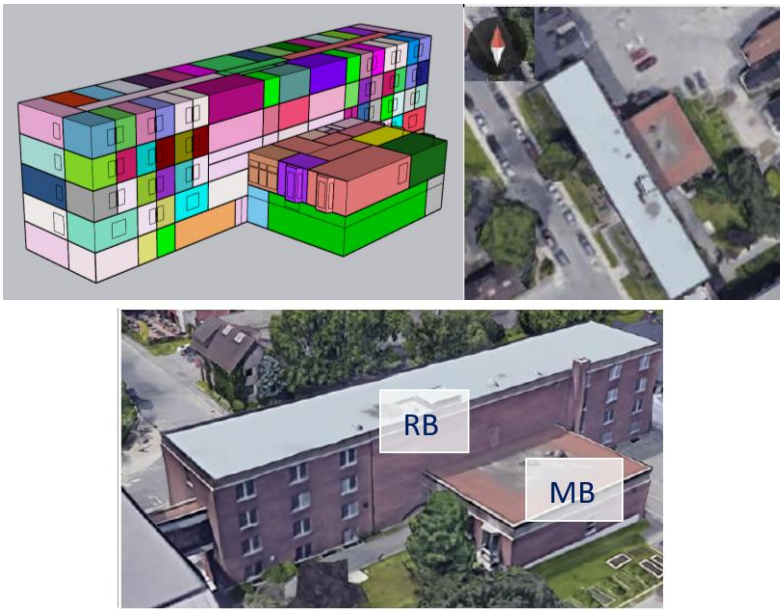

Figure 2-2. Second case study building, dormitory building (divided into two main sections (RB and MB)).

residential buildings constructed in Canada between 1960 and 1977 were still standing in 2022, with apartments accounting for 33% of the residential building stock that year. These statistics further support the representativeness of the case study building for a significant portion of the Canadian residential building stock.

The building comprises a primary residential section (residential building, RB) and a smaller, mixed-use component (mixed-use building, MB). The building model is separated into two distinct parts because of their distinct functions; the occupancy schedules in the mixed-use building differ significantly from those in the residential building. The mixed-use zones follow daytime operational patterns typical of office and event spaces, contrasting with the more constant occupancy patterns in the dormitory zones. With a total floor area of 3,850 m^2, the facility contains 183 zones, 163 of which are conditioned. The residential building primarily accommodates dormitory-style living spaces, including bedrooms, laundry rooms, and washrooms. The mixed-use building features public and service areas, such as conference halls and offices.

The building is equipped with a radiant heating system for space heating during colder months but lacks a dedicated cooling system, as it remains unoccupied in summer. The two main zones in the mixed-use building (conference rooms and the main hall) are served by both the radiant system and an additional air handling unit (AHU), offering greater flexibility for spaces with variable occupancy. The input parameters for the detailed model were obtained from multiple sources, including building walkthroughs, on-site surveys, sensor and meter readings, and data from the centralized HVAC management system (for example, heating setpoints of 22 °C). For parameters where direct measurements were unavailable, such as occupant, lighting, and equipment schedules, standard profiles from NECB 2020 [71] were adopted. All simulations were conducted using the default EnergyPlus timestep of six per hour. Constructed before the introduction of Canada's first national energy code (1997) [66], the envelope is poorly insulated and not air-tight, resulting in high heat loss and elevated heating demand. These inefficiencies present a strong opportunity for retrofit.

The model yields a CV(RMSE) of 11.4% and an NMBE of -0.12% for the monthly natural gas consumption of 2018 during occupied months, both of which fall within the recommended limits. These results support the model's reliability and its applicability for further performance analysis. In addition, the annual natural gas consumption predicted by the detailed model was 63,332 m^3, compared to the measured utility value of 62,812 m^3.

2.1.3 Case Study 3: Single Family Detached House in Ottawa, Ontario, Canada

The third case study building is a single-family detached house located in Ottawa, Canada, originally constructed in 1910 (Figure 2-3). The building is occupied by university students and reflects the characteristics of early twentieth-century residential construction common across Ontario. The dwelling exhibits features that are consistent with older low-rise detached homes across Canada. Its structural form, window proportions, insulation quality, and the

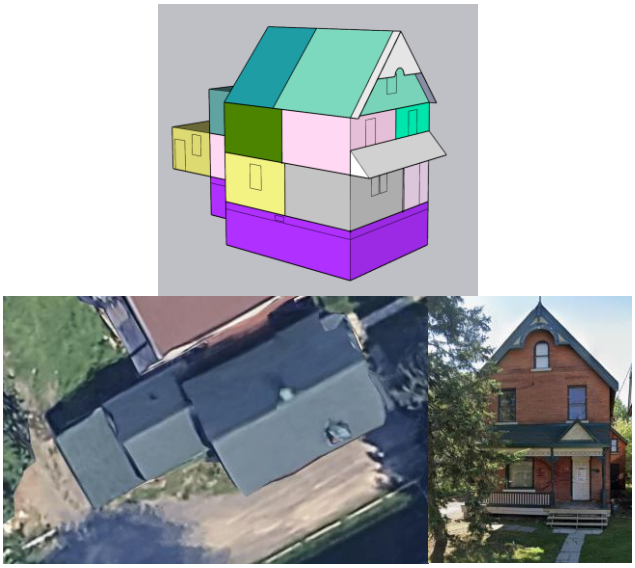

Figure 2-3. Third case study: building a single-family detached house.

nature of its envelope and mechanical systems all correspond to the construction practices typical of its period. These similarities support considering the case study as representative of detached single-family houses from that era. Moreover, according to national housing statistics, approximately 9% of Canada's residential dwellings that were still standing in 2022 were built before 1946, a category that includes all homes constructed before 1920 [70]. Many of these older detached houses remain in active use, particularly in long-established urban neighborhoods. The selected case study house, therefore, represents a historically common building type with persistent energy-performance challenges. Its age, construction characteristics, and current occupancy profile make it a relevant example for evaluating retrofit strategies in older low-rise Canadian housing.

The house includes six bedrooms and a single bathroom, with additional finished space in the basement. The total conditioned floor area is approximately 320 m², represented in the model using 17 thermal zones to capture the distinct occupancy patterns and envelope conditions. The dwelling functions as a student residence and follows residential-style schedules throughout the occupied months. Space heating is provided through a forced-air furnace, while no active cooling system is installed. Summer cooling is not required because the building is typically

vacant during the warm months. Model validation results show CV(RMSE) values of 9.2% for monthly natural gas and 10.7% for monthly electricity, with corresponding NMBE values of 1.1% and 2.8% for the 2022 monthly data. All metrics fall within recommended performance thresholds by ASHRAE Guideline 14 [69].

2.2 Model Simplifications

This research investigates four simplification methods commonly used in building energy modeling to reduce computational burden while maintaining acceptable levels of predictive accuracy. These approaches include thermal zone abstraction, HVAC system simplification, material property simplification, and geometry simplification. Each method reflects practices widely used by researchers and industry professionals. Thermal zone abstraction is commonly employed in academic research and architectural design firms to simplify multi-zone simulations while maintaining reasonable accuracy [14,15,22,23,72,73]. HVAC system simplification is frequently used by mechanical engineers and energy modelers in early-stage design assessments to approximate thermal loads without the complexity of detailed system dynamics [29]. Material property simplification is widely applied in both research and industry, particularly in large-scale energy simulations where precise material characterization may be impractical due to data limitations or time constraints [30]. Geometry simplification aims to streamline the building model by reducing geometric details that have a limited impact on energy performance. These simplification techniques are applied differently across the three case study buildings, depending on each building's purpose within the research and the phase-specific objectives. The following sections describe each simplification method in general terms.

2.2.1 Thermal Zoning

Thermal zoning defines how a building is partitioned into spaces with distinct thermal conditions, occupancy patterns, internal gains, and HVAC controls. Detailed building energy models typically follow ASHRAE guidelines, which recommend one thermal zone per distinct space [20]. However, excessively detailed zoning can increase computational complexity without necessarily enhancing accuracy. On the other hand, insufficient zoning can result in inaccurate energy consumption predictions as it may neglect localized heat gains, airflows, and occupancy variations, leading to underestimated or overestimated energy use [14,15,22,23,72,73]. Thus, the decision on the number of thermal zones in a BEM should consider the trade-off between accuracy and computational speed based on the simulation's objectives.

In this research, thermal zoning simplification is implemented as a sequence of scenarios that span from detailed multi-zone configurations to increasingly aggregated models, up to a single-zone representation. Intermediate scenarios merge spaces that share similar functions, schedules, or thermal characteristics, while the most abstract scenarios treat the entire building, or large building sections, as a single thermal zone. This tiered strategy enables quantification of how progressive reductions in spatial resolution affect both computational effort and model accuracy. The specific zoning simplification scenarios used for each case study are described in the following subsections.

2.2.1.1 Thermal Zoning for Case Study 1: Commercial Building

The commercial building includes a detailed model with nineteen thermal zones, comprising fourteen in the office area and five in the warehouse. This representation captures variations in occupancy, HVAC operation, and envelope exposure. To evaluate the effect of spatial aggregation, three levels of zoning simplification were applied relative to the detailed model. As illustrated in Figure 2-4, the base scenario (A_{10}) maintained the maximum zoning

granularity, modeling each space as an independent thermal zone to ensure the highest level of spatial resolution. Scenario A_{11} introduced the first level of simplification by consolidating zones with similar thermal characteristics and functions into a three-zone model, categorizing the building into warehouse, office, and plenum space. This approach reflects common industry practices, grouping spaces with similar occupancy, heat gains, and ventilation needs to reduce computational demand while preserving localized thermal behavior. In Scenario A_{12}, further simplification was applied by merging the plenum space with the office area, creating a two-zone model, one representing the combined office-plenum space and the other for the warehouse. This method reflects real-world modeling assumptions commonly made in early design phases, in which plenums are assumed to be thermally coupled to adjacent zones due to their air exchange and similar temperature profiles. Finally, Scenario A_{13} simplified the entire building into a single thermal zone, assuming uniform temperature distribution across all spaces. While this approach significantly enhances computational efficiency, it introduces the greatest potential for discrepancies in energy predictions, as it neglects internal temperature gradients, varying heat loads, and airflow between functional areas. Despite its limitations, single-zone models are frequently used in early-stage energy simulations and large-scale parametric studies, where speed and ease of comparison outweigh fine-grained accuracy. This tiered simplification framework enables a systematic evaluation of how thermal zoning decisions affect energy predictions, balancing simulation accuracy, computational efficiency, and practical modeling considerations.

The schedule for the merged zones is determined using a weighted average of the individual zone schedules. For example, the warehouse area has 11 occupants, while the office area has 16, with shared spaces such as the kitchen and washrooms contributing only a small fraction to overall occupancy and time distribution. When consolidating all zones into a single-zone model, the total number of occupants remains consistent with the detailed model at 27.

However, the schedules are averaged and applied to the single-zone model, while the minor influence of shared spaces is not explicitly accounted for. The only parameter that is not weighted-averaged is the material definition of exterior surfaces. To ensure consistency when comparing envelope retrofit scenarios, all exterior surfaces are defined identically across models. For instance, in the single-zone model, the total area of exterior walls remains the same as in the detailed model. Consequently, after merging zones into a single-zone model, the characteristics of the exterior walls in the warehouse and office areas are preserved without averaging, maintaining their exact properties as defined in the detailed model.

2.2.1.2 Thermal Zoning for Case Study 2: Residential Dormitory Building

The dormitory building comprises two distinct sections: a residential block and a mixed-use block. The detailed model contains 183 zones, of which 163 are conditioned, to represent the large number of individual rooms, service spaces, and public areas. Given the size and complexity of the building, zoning simplification was applied by merging rooms based on function, occupancy schedules, and envelope exposure. Scenario A evaluates the impact of zone simplification on simulation accuracy and computational performance using four levels of thermal zone aggregation (A_{21} to A_{24}), as shown in Figure 2-5. Among the zone-simplified models, the most detailed is the thirty-five-zone configuration (A_{21}), which divides each floor into five zones, one core, and four perimeter zones, preserving a high degree of spatial granularity. The seven-zone model (A_{22}) assigns one zone per floor: five for RB and two for MB. The two-zone model (A_{23}) aggregates each building into a single zone, while the one-zone model (A_{24}) represents the entire facility as a single thermal zone, reflecting the highest level of simplification. To isolate the impact of zoning abstraction, all models share identical internal loads, occupancy density, equipment schedules, and infiltration rates.

2.2.1.3 Thermal Zoning for Case Study 3: Single Family Detached House

The single-family detached house is represented by a detailed model with 17 thermal zones to capture variations in occupancy, envelope exposure, and construction characteristics across the dwelling. Because the house is relatively small and exhibits limited functional diversity compared to the other case study buildings, zoning simplification was carried out by directly merging all individual spaces into a single thermal zone (A_{31}), shown in Figure 2-6. This level of aggregation is common in residential energy modeling, where houses of similar size and layout are often represented using a one-zone configuration, especially when the objective is to reduce computational effort in optimization-driven studies. The simplified one-zone model maintains the same envelope properties and overall occupancy patterns as the detailed model, allowing meaningful comparisons of heating energy predictions while enabling faster simulation during the optimization process.

2.2.2 HVAC System

Modeling complex HVAC configurations in EnergyPlus can be challenging, mainly when multiple systems, such as fan-coil units combined with electric heaters, serve the same thermal zone. In such cases, EnergyPlus's pre-defined HVAC templates may not suffice, requiring manual creation and interconnection of each component using the node system. While this approach provides greater flexibility for representing complex HVAC configurations, it also demands a deeper understanding of the components and their interactions, thereby significantly increasing modeling effort [29].

The ideal loads air system is a common simplification approach to streamline HVAC modeling. Instead of defining individual physical components such as chillers, boilers, fans, ducts, and pumps, this system assumes an idealized, infinitely responsive unit that supplies the exact amount of heating or cooling needed to maintain setpoint and setback temperatures. This approach is particularly useful in early design phases, where detailed HVAC specifications are

often unavailable, and in parametric studies, where multiple design scenarios must be evaluated quickly. However, while the ideal loads air system enhances computational efficiency, it introduces accuracy limitations by neglecting real-world inefficiencies, part-load performance, and energy losses. As a result, this simplification can lead to overly optimistic energy consumption predictions, as it does not account for equipment inefficiencies, fan power consumption, or distribution losses. Despite these drawbacks, it remains a widely used approximation in conceptual design, benchmarking studies, and early-stage energy modeling, where its benefits in reducing modeling complexity and simulation time outweigh the loss of HVAC system fidelity. HVAC simplifications are applied to the detailed model while preserving all other aspects, including thermal zoning, internal gains, and schedules. The only modification is replacing the detailed HVAC system with an ideal loads air system. This substitution maintains the same setpoints and setbacks for each zone, ensuring that the impact of HVAC simplification is isolated from other building parameters.

In this research, HVAC simplification is applied by replacing the detailed systems with an ideal load air system while keeping all other inputs consistent, including zoning configuration, setpoints, internal gains, and schedules. This approach isolates the effect of system-level simplification and allows direct comparison between detailed and simplified models. The application of this simplification corresponds to scenarios B_{11}, B_{21}, and B_{31}, which represent HVAC abstraction for Case Study 1, Case Study 2, and Case Study 3, respectively.

2.2.3 Material Definition

In building energy modeling, envelope elements such as walls, roofs, and floors are represented by defining the specific properties of each material layer within a construction assembly. Key parameters include thickness, thermal conductivity, specific heat capacity, and density, all of which contribute to the assembly's thermal resistance (R-value) and thermal mass. Thermal

mass plays a crucial role in temperature regulation and energy performance, as it influences a building's ability to store and release heat over time [74].

In this research, scenario C applies material property simplification by replacing multi-layered constructions with single-layer equivalents that preserve the original assembly's total R-value. This method reduces the number of material definitions and eliminates the need to specify properties for each layer. By retaining only the overall thermal resistance, the approach simplifies the model and improves computational efficiency. However, this process also removes thermal mass effects because the simplified construction lacks specific heat capacity and density. As a result, the model may not accurately represent dynamic thermal behavior, including temperature lag, thermal storage, and responsiveness to short-term weather fluctuations. These limitations can affect peak load predictions and may be more pronounced in buildings with heavy construction.

Material simplification is implemented while maintaining all other aspects of the model, including zoning, HVAC definitions, internal gains, and setpoints. Only the envelope material definitions are altered. This ensures that any observed changes in energy performance can be attributed directly to the reduction in material detail rather than to interactions with other modeling inputs. This approach corresponds to scenarios C_{11}, C_{21}, and C_{31}, which apply material simplification to Case Study 1, Case Study 2, and Case Study 3, respectively.

2.2.4 Geometry

Geometry directly influences building energy performance by affecting exposure to solar gains, shading patterns, surface-to-volume ratios, and thermal interactions across envelope elements. In detailed energy models, accurate geometry requires defining all vertices, surfaces, window placements, and façade irregularities. While this level of detail improves the representation of the building’s physical form, it also increases modeling effort, complexity, and simulation time.

In this research, geometry simplification is implemented only for Case Study 1, which has a more complex mix of office and warehouse volumes (Figure 2-4). The other two case study buildings, the dormitory and the detached house, have simple rectangular forms with no curved or irregular façade elements, so geometry simplification would offer little computational advantage and is therefore not applied to them. As a result, only two geometric simplification scenarios are used, designated as D_{11} and D_{12}.

In Scenario D_{11}, curved and angular façade segments are replaced with straight-line approximations, reducing the number of surfaces and vertices in the EnergyPlus model. This process simplifies geometric input while removing self-shading effects along irregular façade edges. To further streamline the model, windows are not placed individually. Instead, a Window-to-Wall Ratio is assigned uniformly across each façade, preserving the total fenestration proportion without modeling the exact window locations.

In Scenario D_{12}, a more aggressive form of geometry simplification is introduced using a shoebox modeling approach. The building is represented as a simple rectangular volume with the same total floor area as the original design. This method is widely used in early design analysis and large-scale parametric studies because it greatly reduces modeling time and simulation costs while maintaining a basic representation of thermal behavior. However, the shoebox form removes architectural features, shading conditions, and airflow patterns that influence localized energy performance. As a result, Scenario D_{12} provides significant computational efficiency but at the expense of reduced accuracy in representing detailed geometric interactions.

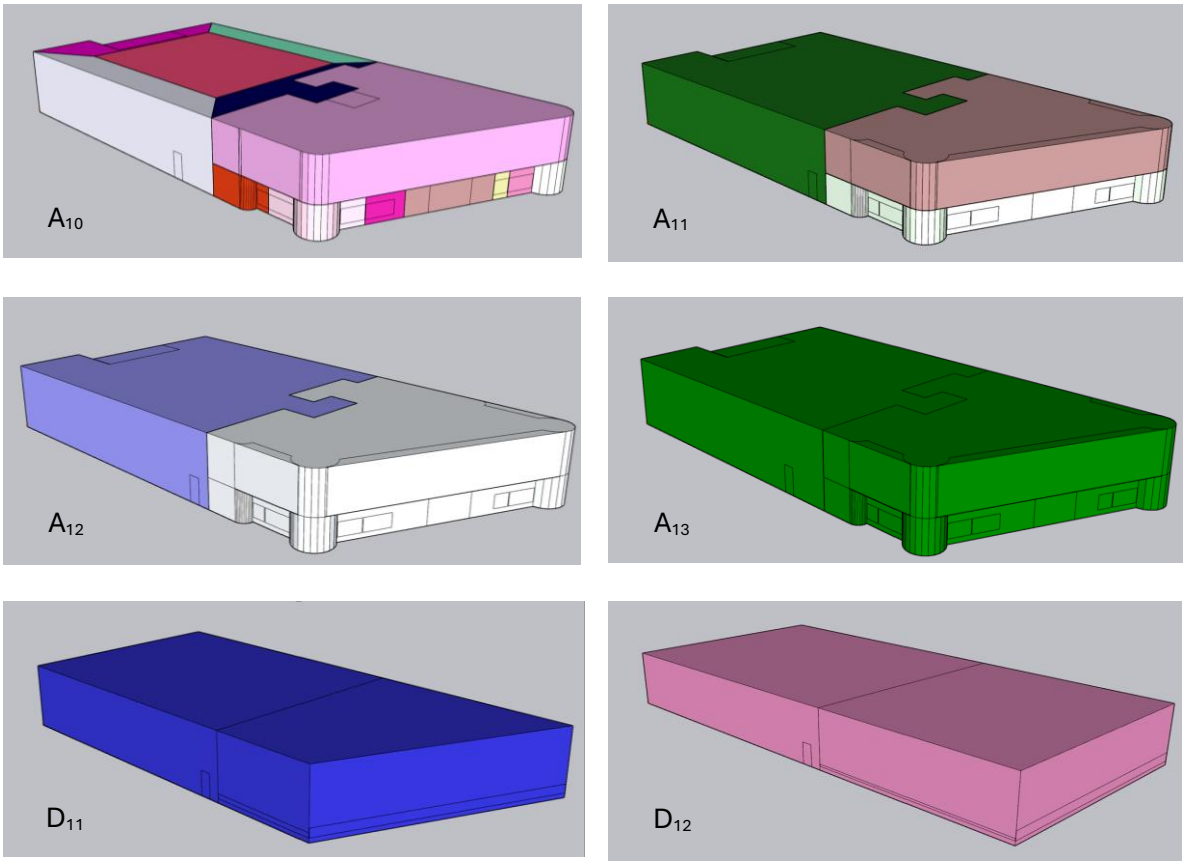

Figure 2-4: Detailed and simplified models' geometry and zoning. Scenario A_{10}: detailed, scenario A_{11}: three-zone, scenario A_{12}: two-zone, scenario A_{13}: one-zone, scenario D_{11}: simple geometry, scenario D_{12}: shoebox models.

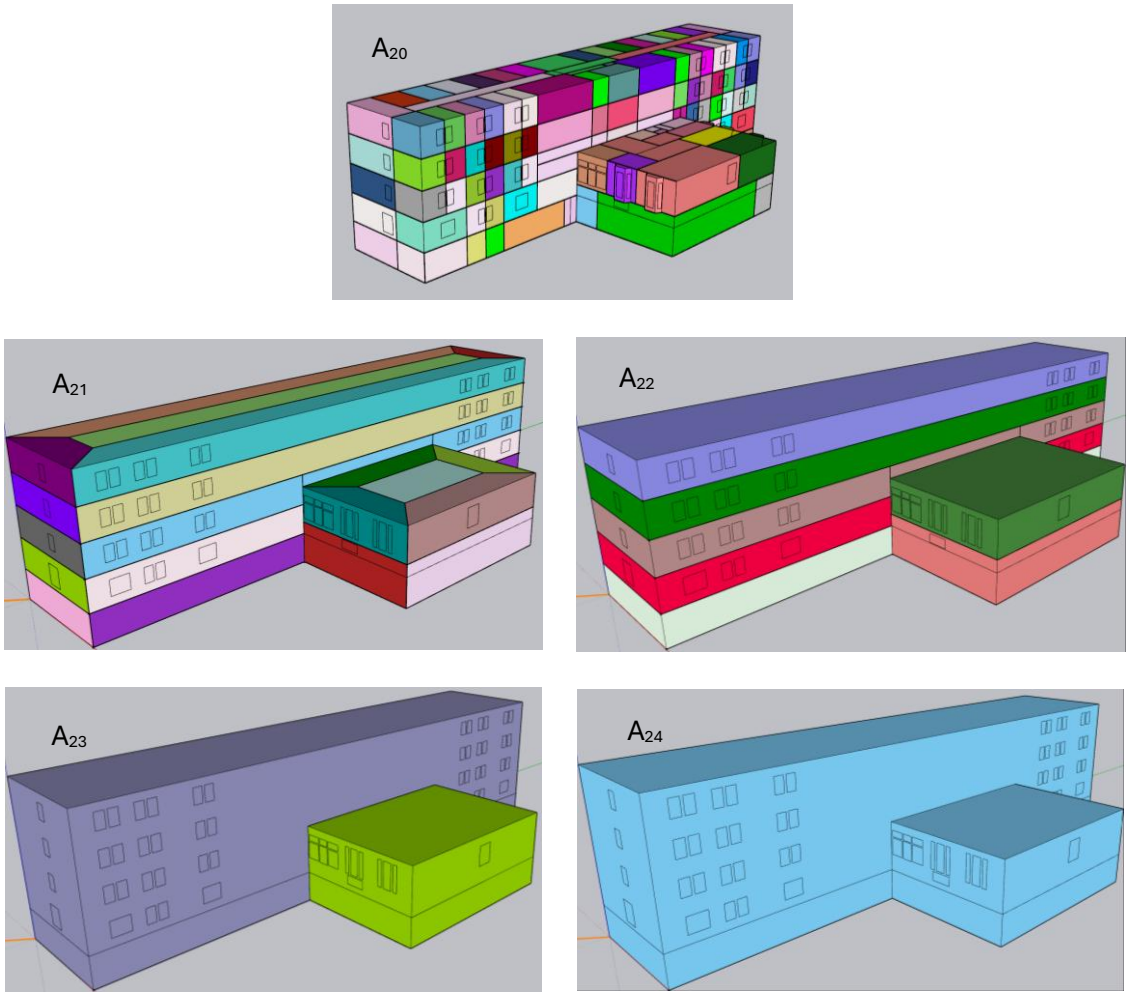

Figure 2-5: Detailed and simplified models' zoning. Scenario A_{20}: detailed, scenario A_{21}: thirty-five-zone (five zones per floor), scenario A_{22}: seven-zone (one zone per floor), scenario A_{23}: two-zone, scenario A_{24}: one-zone.

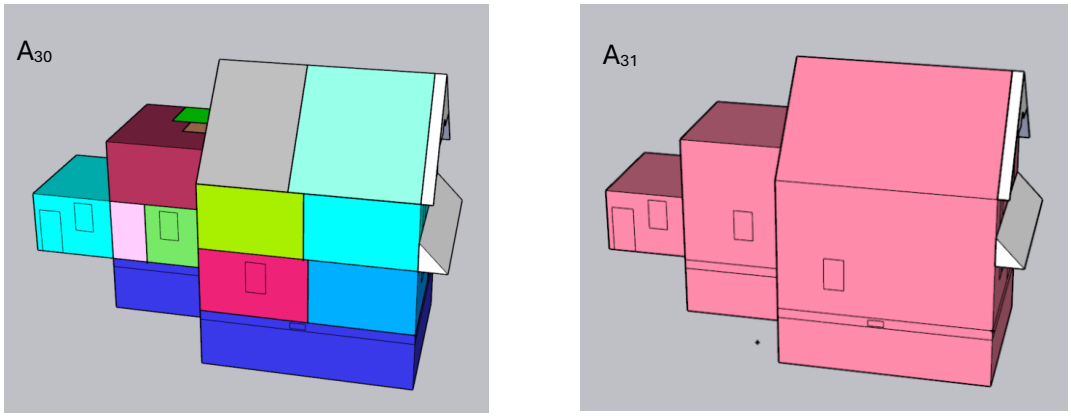

Figure 2-6: Detailed and simplified models' zoning. Scenario A_{30}: detailed, scenario A_{31}: one-zone.

Chapter 3: Enhancing Building Energy Optimization Efficiency: A Performance Analysis of Simplification Approaches

This chapter has been published as:

- Article 2: Y. Dadras, F. Mostafazadeh, M. Kavgic, M. Ghobadi, Enhancing building energy optimization efficiency: A performance analysis of simplification approaches, Journal of Building Engineering 105 (2025). https://doi.org/10.1016/j.jobe.2025.112559.
- Conference paper 1: Y. Dadras, M. Kavgic, The applicability of simplified whole-building energy model for energy-efficiency retrofit analysis, (2022). (eSim Conference in Ottawa, Ontario, Canada).
- Conference paper 2: Y. Dadras, M. Kavgic, O. Alaei, Investigation of the thermal transmittances calculated using new infrared technology developed by QEA Tech, (2022). (CCBST Conference in Vaughan, Ontario, Canada).

3.1 Introduction

Building on the broader introduction and literature review provided in Chapter 1, this chapter focuses on evaluating how commonly used simplification techniques affect the accuracy and computational efficiency of simulation-based multi-objective optimization. The study investigates thermal zone abstraction, HVAC system simplification, material property approximation, and geometric simplification using a mixed-use commercial building (Case Study 1) as the case study. It also examines how parallel computing and result-saving strategies can further reduce computational time within an NSGA-II optimization framework. By analyzing the trade-offs among model complexity, simulation speed, and prediction accuracy, this chapter provides a detailed assessment of the strengths and limitations of simplified models

for energy-efficiency retrofit optimization. The subsequent sections describe the modeling and optimization procedures and the results obtained from each simplification scenario.

3.2 Methodology

This research used a parallel computing SBMO framework to compare the time efficiency and accuracy of simplified models with a detailed model during optimization. The SBMO framework followed a methodology similar to [17,52] across its overall phases but is unique in its simultaneous simulation of simplified and detailed models, enabling an assessment of the simplified models' accuracy. Furthermore, all software tools used in this research are well-established and widely used in academic research. Thus, MATLAB [75] handled data processing, optimization, and input/output management, while EnergyPlus [68] was used for energy simulation.

Figure 3-1 illustrates the four phases of the proposed methodology framework. In Phase 1, an initial building model was developed based on audit data, and energy simulations were performed to evaluate the baseline case (Chapter 2, section 2.1.1). In Phase 2, the detailed model was simplified using four approaches: thermal zone, HVAC system, material properties, and geometric simplifications. These simplified models were calibrated against energy consumption data to ensure accuracy (Chapter 2, section 2.2). Phase 3 defined the environmental and economic objectives, specifically minimizing Primary Energy Consumption (PEC) and Net Present Value (NPV), and introduced decision variables into the baseline model to create a parametric model. In Phase 4, the NSGA-II algorithm was employed in a multi-objective optimization process to identify Energy Conservation Measures (ECMs) that balanced these competing objectives. The algorithm iteratively refined ECM combinations, yielding a set of Pareto-optimal solutions. A two-stage approach was also

implemented to compare the accuracy and computational efficiency of optimization results derived from simplified versus detailed models.

3.2.1 Simplified Model Calibration

The detailed commercial building model was simplified using four approaches introduced in Chapter 2: thermal zone aggregation (A_{10}-A_{13}), HVAC abstraction (B_{11}), material property reduction (C_{11}), and geometry simplification (D_{11} and D_{12}). These scenarios progressively reduced the spatial, mechanical, material, and geometric complexity of the baseline model while keeping all other inputs consistent. The calibrated versions of these simplified models serve as the basis for the accuracy assessment and optimization analysis presented in this chapter.

Model calibration is a necessary step because building energy simulation depends on numerous input parameters, including infiltration rates, internal load schedules, HVAC performance, material properties, and weather data, each of which carries inherent uncertainty. In this study, simplified building models were calibrated to improve their applicability for optimization processes aimed at exploring various ECMs. TMY weather file was adjusted using measured data, including solar radiation, air pressure, relative humidity, wind speed and direction, and ambient temperature collected from a nearby weather station. This modification ensured that model calibration reflected the weather conditions experienced during the available year (2018), providing a more accurate representation of local climate [76]. The actual energy demand was compared with the modeled monthly energy demand derived from the calibrated simplified models. Following ASHRAE Guideline 14 [69], the CV(RMSE) and the NMBE were used to evaluate model calibration accuracy.

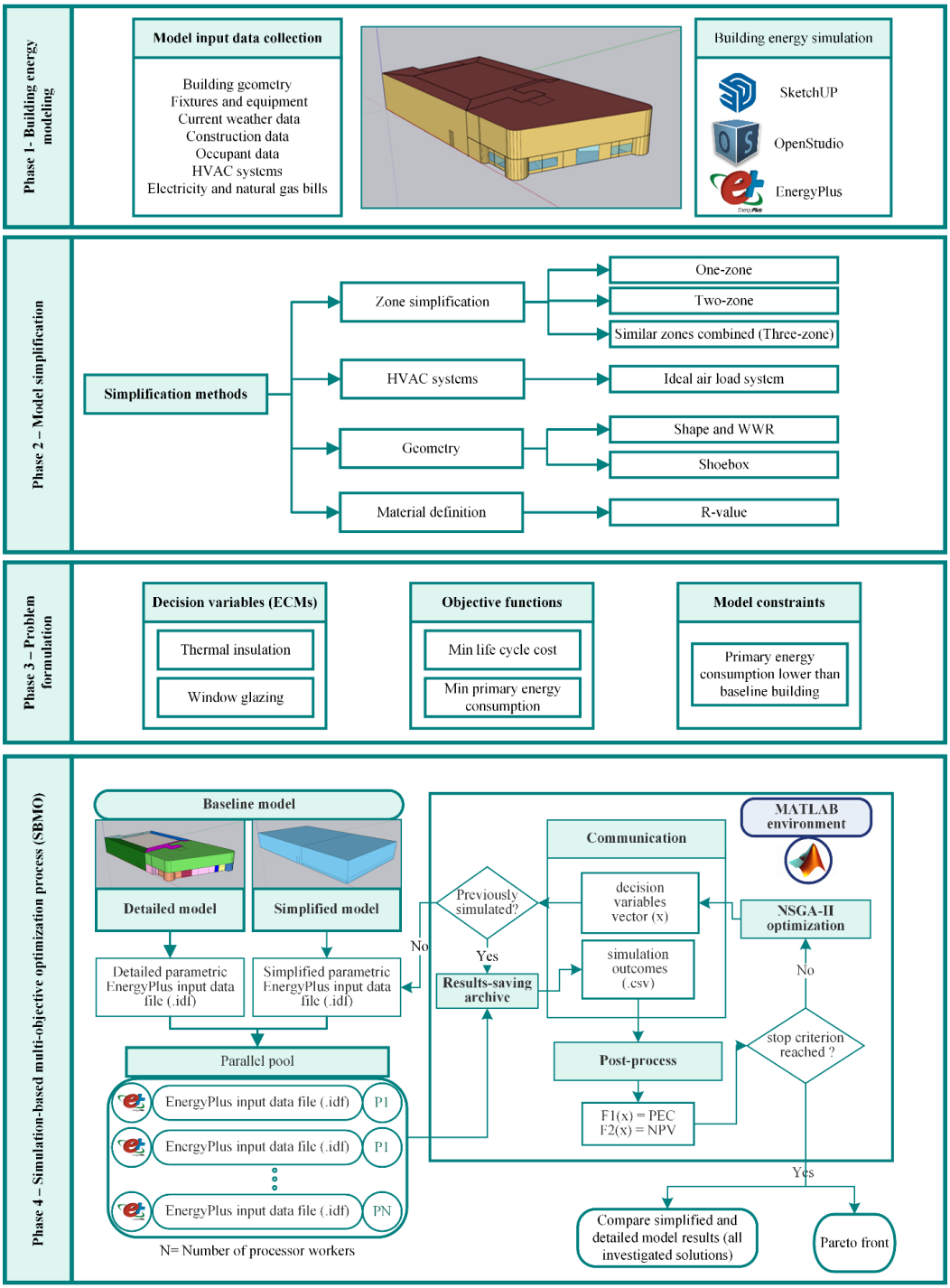

Figure 3-1: Methodology framework (Chapter 3).

3.2.2 Objective Functions

Building energy retrofit projects should address environmental and economic objectives to promote sustainability [77–86]. In this research, the environmental objective is to minimize Primary Energy Consumption (PEC) in line with sustainable energy practices. Simultaneously, the economic objective is to minimize life cycle costs, ensuring the project's financial viability.

These dual objectives are essential for balancing sustainability with cost-effectiveness, enhancing the project's long-term impact and feasibility.

This framework assessed the environmental impact of building energy retrofitting PEC, as recommended by the Energy Performance of Buildings Directive recast [87]. Hence, PEC is calculated by converting natural gas and electricity demands into primary energy values, applying specific primary energy factors [88]. Furthermore, an economically viable energy retrofit project aims to minimize life cycle costs by investing in ECMs and reducing natural gas and electricity expenses. Therefore, this study applied the Net Present Value (NPV) method to perform an economic analysis over an assumed building service life of 50 years. NPV evaluated the project's total cost by discounting all future cash flows to their present value using a specified discount rate. This method provides a comprehensive financial overview, facilitating comparison between projects or investment options based on long-term cost implications [89–92]. The Life Cycle Cost (LCC) using the NPV method is calculated as follows:

$$LCC = I + q(EC + GC) \quad \text{Equation 3-1}$$

where q is a present value factor, I is the investment cost, and EC and GC are electricity and gas costs, respectively. Energy price discounts and escalation rates are incorporated to enhance the precision of LCC assessments. This approach enables more accurate calculation of the present value of expenses and revenues over the project's lifespan. Specifically, the present value of electricity and natural gas costs is calculated as:

$$q = \begin{cases} \frac{\left[1-\left(\frac{1+g}{1+d_r}\right)^t\right]}{d_r-g} & if\ d_r \neq g \\ \frac{t}{1+d_r} & if\ d_r = g \end{cases} \quad \text{Equation 3-2}$$

where t denotes the lifespan of the building, g represents the annual energy price escalation rate, and d_r is the actual discount rate, which is determined as shown in Equation 5:

$$d_r = \frac{1+d_n}{1+e} - 1$$ Equation 3-3

where e is the inflation rate, and d_n is the nominal discount.

3.2.3 Multi-Objective Optimization

This research formulated a simulation-based multi-objective optimization framework to evaluate the accuracy and computational efficiency of simplified building energy models while identifying optimal ECMs for building retrofits. The optimization balanced two objectives: minimizing PEC and NPV, subject to a constraint that ensures the selected retrofit strategy improves energy efficiency relative to the baseline building ($PEC \leq PEC_0$). A genetic algorithm, specifically NSGA-II, is employed due to its proven efficacy in building energy optimization problems, offering a favorable balance between solution reliability and computational efficiency [17,93]. The NSGA-II algorithm is implemented in MATLAB and coupled with EnergyPlus for detailed building energy simulations. MATLAB and EnergyPlus rely on text-based input/output formats, facilitating smooth data exchange. A key feature of MATLAB used in this study is its parallel computing capability, which addresses the computational intensity of the optimization by dividing the task into smaller sub-tasks that run concurrently across multiple processors. This parallelization significantly reduces computation time by enabling simultaneous processing of various parts of the optimization workflow.

The NSGA-II process begins with an initial population of potential solutions (chromosomes), each representing different building configurations or retrofit strategies based on the decision variables (x). The evolutionary process is driven by genetic operators such as crossover and mutation, with elitism and diversity criteria guiding the selection of superior solutions. Each solution's performance is evaluated using building energy simulations, where EnergyPlus calculates each chromosome's objective functions (PEC and NPV). A parametric EnergyPlus model (see Figure 14) is used as a template to generate specific building configurations based

on decision variables representing the various retrofit scenarios. A dedicated coupling agent facilitates the interaction between NSGA-II and EnergyPlus by converting decision variables into corresponding EnergyPlus input files (.idf) and automating the simulation process. After each simulation, the results are extracted from the output files (.csv), and the post-processing agent calculates the objective function values, which are then fed back to NSGA-II to guide the evolutionary process. NSGA-II iteratively refines the population of building models based on the simulation feedback, improving the solutions over successive generations. This process continues until a predefined stopping criterion is met, yielding a Pareto front of optimal solutions that represent the best trade-offs between minimizing PEC and NPV.

This study executed the optimization process for all models on a computer with an Intel Core i9 processor (2.60 GHz, 24 MB cache). The algorithm was configured with a population size of 50 individuals and mutation and crossover rates of 0.7 and 0.4, respectively. These parameters were selected to ensure reliable results within a reasonable computational timeframe, with a stopping criterion of 50 generations.

3.2.4 Energy Conservation Measures (ECMs)

Potential Energy Conservation Measures (ECMs) were identified and evaluated through an energy audit, stakeholder consultations, and market research. In this respect, envelope assessment via thermographic inspection revealed thermal bridges, insufficient thermal insulation in several wall areas, and air leakage around the inefficient windows. Consequently, the specific ECMs included the application of various thicknesses and types of thermal insulation materials, along with the evaluation of several window replacement options, given their considerable influence on the envelope's thermal energy performance. These measures, summarized in Table 3-1, were defined as decision variables within the EnergyPlus and MATLAB simulation environments for multi-objective optimization.

Table 3-1: Characterization of investigated ECMs.

Decision Variables	Components	Parameter	Options
Insulation	• Office and warehouse walls, floors and roofs	Material	Base model; Stone wool; Fiberglass; Extruded polystyrene; Mineral wool
		Thickness [in]	0 - 6 [in]
Window glazing	• Office windows • Warehouse added windows	Glass material	Clear; Bronze; Reflex
		Glass thickness [mm]	Base; 4;6;10
		Gas type	Air, argon

3.2.5 Two-Stage Model Comparison in Optimization

A two-stage methodology is employed to examine the trade-off between computational efficiency and the accuracy of a simplified model in a simulation-based optimization framework. In the first stage, the optimization process utilizes a simplified building model. A corresponding detailed simulation is conducted for each configuration generated during the optimization using the same set of decision variables. The purpose of the detailed simulation is solely to evaluate the accuracy of the simplified model's predictions. It is not involved in guiding the optimization process. The accuracy of the simplified model is quantified by calculating the percentage error between the simplified and detailed models, as expressed in the following equation:

$$error = \frac{E_d - E_s}{E_d} * 100 \qquad \text{Equation 3-4}$$

where E_d and E_s represent the annual natural gas or electricity consumption of detailed and simplified models, respectively.

Since running both the simplified and detailed models in parallel affects the overall computational time, the second stage of the analysis focuses solely on optimizing with the simplified model. This approach enabled an independent assessment of the computational time

when using the simplified model. A separate optimization is also conducted using only the detailed model for comparison. The Pareto fronts generated from both the simplified and detailed models are then compared to assess the influence of model fidelity on the optimization results. Additionally, comparing computational times between the two models highlights the efficiency gains achieved using the simplified model. This two-stage process provided insights into the trade-off between accuracy and computational cost, guiding model selection for future optimizations tailored to project-specific requirements.

3.2.6 Energy Modeling Practices and Preferences Survey

This study employed a structured survey questionnaire to investigate current practices, preferences, challenges, and opportunities for simplification in building energy modeling among professionals in academia and industry. The questionnaire was designed to gather comprehensive data, which is provided in Appendix A. A total of 42 energy modelers participated in the survey, offering diverse insights into the field. The questionnaire was organized into three key categories to address the research objectives systematically:

- Experience: The first category focused on capturing the respondents' professional backgrounds, including their primary roles in energy modeling, years of experience, and the software tools they predominantly use. Understanding the diversity of experience and expertise is essential for contextualizing the findings and identifying trends in professional roles and software preferences.
- Energy modeling challenges: This section aimed to identify common challenges faced by energy modelers, particularly regarding time allocation and data collection. It explored how much time participants spend on various modeling tasks, the importance they place on accuracy, and the specific stages where data collection is most challenging.

- Willingness and benefits of simplification in building energy modeling: The third category delved into energy modelers' attitudes toward the use of simplified models. It examined their willingness to adopt models with reduced accuracy for efficiency, the frequency with which they used such models, and the perceived benefits in terms of time savings.

3.3 Results and Discussion

3.3.1 Calibrated Simplified Model Predictions

Table 3-2 compares the annual natural gas and electricity energy consumption of the calibrated simplified models against the predictions of the validated detailed model, simulated using the Actual Meteorological Year (AMY) weather file. Compared with the measured data, all calibrated simplified models achieved monthly NMBE and CV(RMSE) values within ASHRAE's acceptable ranges [69], except for electricity consumption in the model using the ideal air load system.

Figures 3-2 and 3-3 compare their monthly electricity and natural gas consumption predictions based on Typical Meteorological Year (TMY) weather files to further evaluate the calibrated simplified models. The calibrated zone-simplified and simple-geometry models exhibited a consistent trend in electricity consumption compared with the detailed model. However, they overestimated electricity consumption during the summer, likely due to increased cooling demand. For example, in July, the two-zone model overestimated electricity consumption by 4% (5129 kWh compared to 4930 kWh from the validated detailed model), and the simple geometry model overestimated it by 4.4%. In contrast, the shoebox model consistently overestimated electricity consumption throughout the year, with overestimations more pronounced in summer, reaching 18.9% in July.

In the case study, the HVAC system operated with fans year-round, contributing significantly to electricity consumption. The ideal air load system did not capture this aspect, resulting in notable discrepancies between the validated detailed and the ideal loads air system, particularly during summer. For instance, in July, the ideal air load system predicted only 1872 kWh, 62.0% lower than the detailed model. Despite these differences, all calibrated simplified models, including the ideal air load system, showed a consistent trend in natural gas consumption relative to the validated detailed model. In January, the two-zone model overestimated natural gas consumption by 7.9%, while the shoebox model overestimated it by 10.2%. Similarly, the simple geometry model overestimated natural gas consumption by 6.5% in January.

Table 3-2: Annual electricity and natural gas consumption: detailed vs. calibrated simplified models.

	Measured data	Detailed	Three-zone	Two-zone	One-zone	HVAC	R-value	Simple geometry	Shoebox
Electricity [MWh]	94	98	98	96	95	15	97	94	93
Natural gas [MWh]	301	287	295	314	305	278	291	309	316

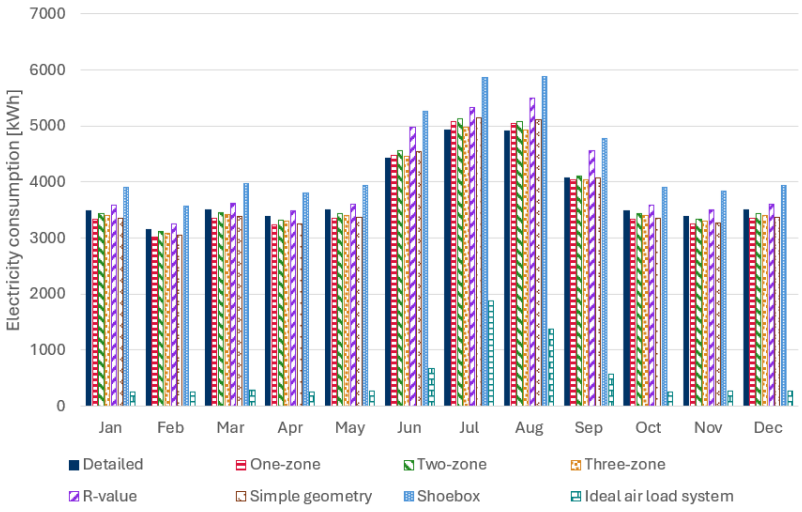

Figure 3-2: Comparison of electricity consumption: validated detailed model vs. calibrated simplified models.

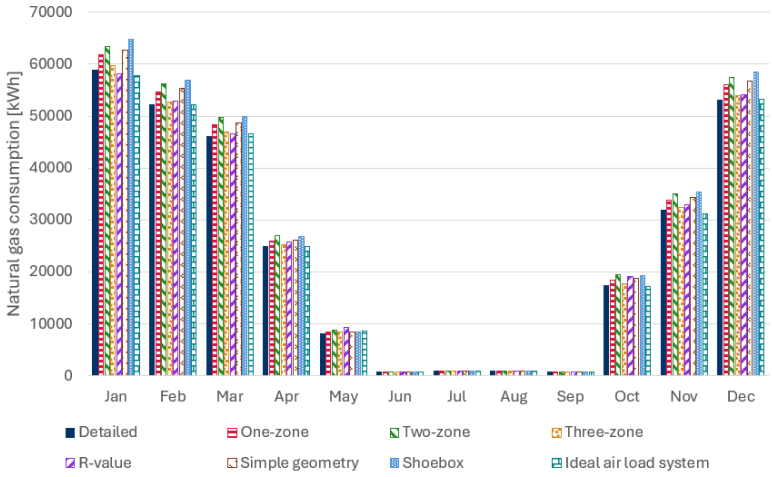

Figure 3-3: Comparison of natural gas consumption: validated detailed model vs. calibrated simplified models.

3.3.2 Optimization

The optimization process yielded a total computational time of 10.65 hours when parallel computing was used for the detailed case study model. In contrast, re-executing the optimization with a single-threaded NSGA-II algorithm required 21.65 hours. This 51% reduction in computational time demonstrates significant efficiency gains from parallel computing, particularly for large-scale building performance optimization.

3.3.2.1 Comparative Analysis: Time Efficiency and Accuracy Assessment in Optimization

A corresponding detailed simulation was conducted with the same parameters for each building configuration generated during the optimization process using the simplified model. The detailed simulation evaluated only the accuracy of the simplified model's results and was not part of the optimization process. The optimization was repeated using only the simplified model to evaluate the processing time. Table 3-3 presents the mean annual natural gas and electricity errors for the simplified models across all assessed solutions relative to the corresponding detailed model. Additionally, the table provides a comparative analysis of computational times between the simplified and detailed models.

The shoebox, simple geometry, and one-zone models exhibited comparable levels of underestimation to the detailed, validated model due to their similar parameterizations, with only minor discrepancies caused by geometry changes in the simple geometry and shoebox models. Hence, compared to the detailed model, the one-zone model showed mean errors of -10.70% for natural gas and -21.80% for electricity. Similarly, the simple geometry model exhibited mean errors of -10.71% for natural gas and -22.95% for electricity. Furthermore, the shoebox model predicted 11.64% and 21.16% lower natural gas and electricity use than the detailed model. In contrast, the two-zone and three-zone models performed better by accurately representing the building's functional zones and HVAC systems. The two-zone model underestimated natural gas and electricity consumption by 9.90% and 20.90%, respectively. By incorporating the plenum space, the three-zone model improved accuracy, yielding errors of -7.20% for natural gas and -14.50% for electricity. The results align with findings from previous studies [14,15,30,73]. For instance, Alhedad's study on zone simplification reported an underestimation of energy demand ranging from 10.9% to 35.8% in simplified models compared to the detailed model [14]. Similarly, Picco et al. observed a 9% underestimation when zones were merged [30]. However, it is important to recognize that results across different case studies depend heavily on the characteristics of the buildings analyzed. For example, simplifications in complex buildings may introduce greater inaccuracies than in simpler structures. Consequently, direct numerical comparisons between different case studies may not be meaningful. Despite these variations, a clear trend of underestimation of energy demand due to zone simplification is evident, reinforcing the findings of the present study.

An analysis of the simplified models indicates that internal walls facing exterior windows are more sensitive to solar radiation, particularly during the summer when solar gains are higher. These interior walls absorb the solar heat, store it, and release it into the zone later. This phenomenon is more pronounced in models with more complex zoning configurations, leading

to higher cooling energy consumption in the three-zone model than in the two-zone and one-zone models. Additionally, previous studies [15,73] investigated the underestimation of heating energy consumption in simplified models. The increased convective heat gain on internal surfaces in heating seasons leads to a higher convection coefficient, increasing conduction losses through the building envelope. This dynamic raises the overall heating demand, contributing to the underestimation observed in the more extensive zone-simplified models compared to the three-zone model.

The R-value (material simplification) model produced results closest to those of the detailed model. It showed minimal underestimation of natural gas consumption (0.39%) and a slight overestimation of electricity consumption (1.41%). The thermal mass of building materials, which influences the building's ability to absorb, store, and release heat, impacts energy consumption and cooling demand. Buildings with high thermal mass tend to have reduced energy demand because thermal mass dampens temperature fluctuations, creating a more stable indoor environment. This effect is particularly pronounced during cooling periods, as materials absorb excess heat, reducing the need for active cooling systems. In the R-value model, omitting thermal mass led to overestimating cooling requirements because the material's capacity to moderate heat was not accounted for.

Regarding computational time, a clear trade-off emerged between speed and accuracy. The shoebox model was the fastest (0.39 hours) but the least accurate, while the detailed model offered the highest precision at the cost of significantly longer processing times (10.65 hours). HVAC system simplification also had varying impacts on time efficiency, with the extent of the impact heavily influenced by the system's configuration. The simulation times for the ideal air-load system and the detailed model were comparable in the case-study building, where the HVAC system was relatively simple. The primary time savings from the ideal air load system stemmed from reduced data collection and model development rather than computational

efficiency. A notable discrepancy was observed in electricity consumption: the ideal air load system underestimated consumption by 80% because it did not account for year-round fan operation. However, the ideal air-load system accurately predicted heating energy consumption, with only 3.28% error compared to the detailed model for natural gas. These findings align with the study by Al-Janabi et al., which also reported considerable discrepancies when using an ideal air-load system rather than a detailed HVAC model in EnergyPlus. Their study found 11.8% and 96.9% errors in total heating and cooling energy consumption, respectively, further confirming that while the ideal air load system can provide reasonable heating energy estimates, it significantly miscalculates electricity consumption [29]. Due to significant errors in electricity consumption associated with the ideal air load system in the case study building, it is not feasible to compare the retrofit results from the ideal air load system model with those from the detailed model. Consequently, the following section does not include the HVAC simplification in the comparative analysis of the optimization results.

Table 3-3: Comparison of mean annual natural gas and electricity errors across 50 Pareto front solutions between the detailed and simplified models and computational time analysis for both models.

Model	Annual natural gas error (%)	Annual electricity error (%)	Computational time (hours)
Detailed	Baseline	Baseline	10.65
Three-zone	-7.20	-14.50	6.34
Two-zone	-9.90	-20.90	6.13
One-zone	-10.70	-21.80	5.30
R-value	-0.39	+1.41	10.37
Simple geometry	-10.71	-22.95	1.16
Shoebox	-11.64	-21.16	0.39
Ideal air load system	-3.28	-80.00	11.00

3.3.2.2 Comparative Analysis: Optimization Results

This section evaluates the accuracy of simplified models by comparing their objective function values and ECMs on the Pareto fronts to those from the detailed model, as shown in Figure 3-4. The detailed model served as a benchmark, yielding NPV values of 831 kCAD to 873 kCAD and PEC values of 214 MWh to 225 MWh. The differences in energy predictions of detailed and simplified models drive the discrepancy in their NPV and PE values. Owing to its minimal

discrepancy in energy prediction compared to the detailed model (See Table 3), the R-value model solutions closely align with those of the detailed model, exhibiting NPV deviations of approximately 0.27% to 0.94% and PE consumption deviations of 0.18% to 0.81%. The three-zone model shows a moderate deviation, underestimating NPV by 7.83%-9.56% and PE consumption by approximately 10% compared to the detailed model. Significant discrepancies are observed in the shoebox, simplified geometry, one-zone, and two-zone models, which underestimate NPV by 11% to 14% and PE consumption by 13% to 16%. The shoebox model shows substantial divergence, with NPV differences exceeding 12% and PE consumption variations approximately 15% lower than the detailed model.

The lower PE observed in the simplified zone and geometry models is mainly due to their inability to fully capture the effects of convective heat gains and conduction losses on internal surfaces during heating seasons. These models underestimate heat transfer through the building envelope, leading to lower predicted heating energy demand. Additionally, these models underestimate the effects of solar heat absorption and delayed release by internal walls facing exterior windows, leading to discrepancies in heating and cooling energy predictions compared to more detailed models.

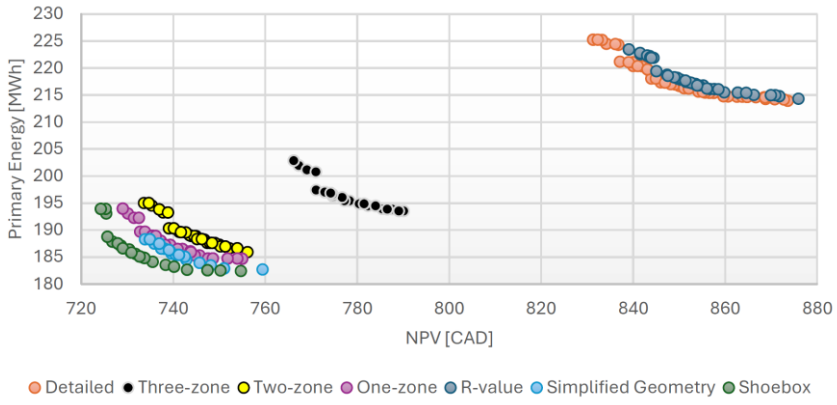

Figure 3-4: Comparison of Pareto fronts in detailed and simplified models.

The boxplots in Figures 3-5 and 3-6 display the distribution of 50 optimal results from the Pareto fronts for each model type. NPV and PE exhibit higher median values in the detailed

model, consistently predicting higher costs and energy consumption than the simplified ones. The detailed model also shows a wider Interquartile Range (IQR), suggesting it captures more dynamic interactions and introduces more significant variation in optimal solutions, revealing a more complex set of strategies. As the model's complexity reduces, median NPV and PE values tend to decrease. Hence, the shoebox and simplified-geometry models significantly reduce NPV and PE values, indicating more optimistic cost and energy estimates than the detailed model. However, outliers, particularly in the simpler models, suggest underperformance in certain conditions, potentially leading to suboptimal retrofit strategies. These outliers highlight the risk of relying on overly simplified models, which may overlook fundamental dynamics captured by the detailed model, resulting in overly optimistic or less effective outcomes.

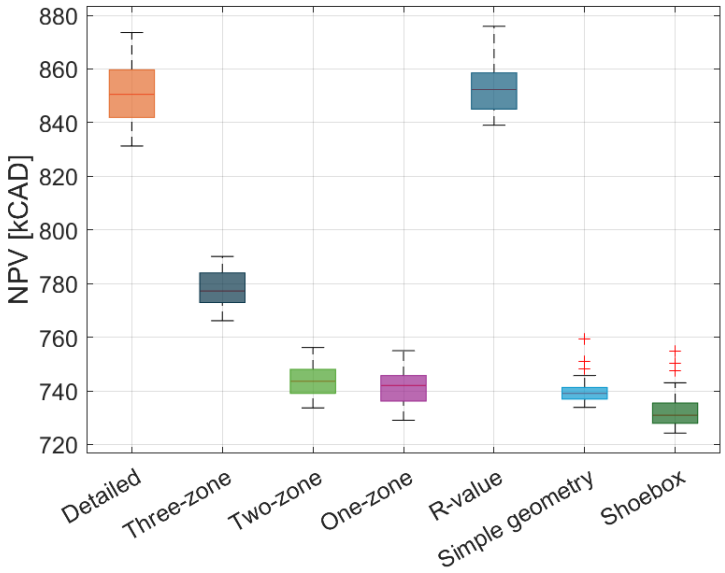

Figure 3-5: Comparison of net present values from Pareto front results for detailed and simplified models.

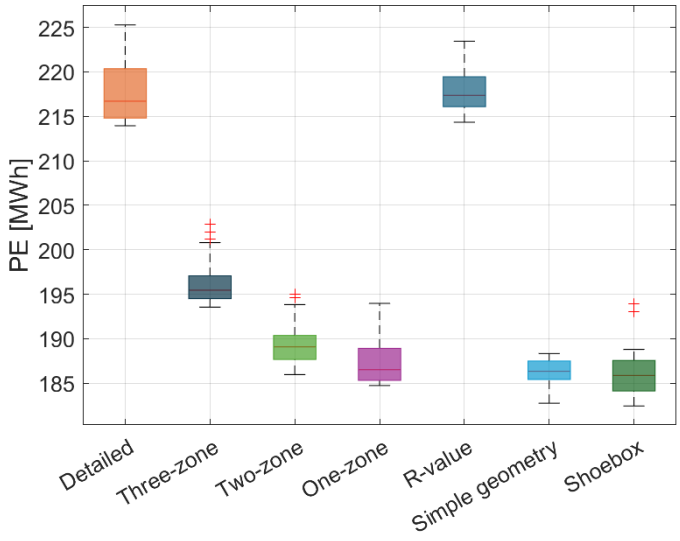

Figure 3-6: Comparison of primary energy consumption values from Pareto front results for detailed and simplified models.

The statistical analysis in Tables 3-4 and 3-5 compares NPV and PEC of the optimal results on the Pareto fronts for the detailed and simplified BEMs. For both metrics, the detailed model exhibits the highest mean values, with an NPV of kCAD 850.91 and a PEC of 217.91 MWh, indicating higher predicted financial costs and energy consumption for optimal retrofitting strategies compared to simplified models, such as the shoebox and simple geometry models, which have the lowest mean values for NPV (kCAD 733.04 and kCAD 740.11, respectively) and PEC (186,255 MWh and 186,098 MWh, respectively). The detailed model also shows the highest Standard Deviation (SD), variance, and Coefficient of Variation (CV) for NPV and PEC, reflecting a broader range of Pareto-optimal solutions. This wider spread emphasizes the detailed model's capacity to capture a more diverse set of optimal strategies, offering greater flexibility in balancing cost and energy efficiency when making retrofitting decisions. Skewness analysis reveals that most models exhibit near-symmetrical distributions. However, the shoebox and simple-geometry models exhibit higher positive skewness in NPV. In PEC, the shoebox and detailed models show positive skewness, reflecting more instances of higher energy consumption. In contrast, the simple geometry model shows negative skewness, indicating a tendency toward lower PEC values.

Table 3-4: Statistical analysis of NPV for the detailed and simplified models based on Pareto front results.

	Detailed	Three-zone	Two-zone	One-zone	R-value	Simple geometry	Shoebox
Mean (average) [kCAD]	850.91	778.00	743.74	741.48	853.62	740.11	733.04
Standard Deviation (SD) [kCAD]	11.80	7.24	5.68	7.09	9.50	4.88	7.21
Variance $[kCAD]^2$	139.26	52.39	32.24	50.20	90.17	23.83	51.95
Median [kCAD]	850.54	777.24	743.57	742.00	852.33	739.08	730.91
Coefficient of Variation (CV)	1.39	0.93	0.76	0.96	1.11	0.66	0.98
Skewness	0.17	-0.03	0.15	0.11	0.57	1.91	1.20

Table 3-5: Statistical analysis of PE for the detailed and simplified models based on Pareto front results.

	Detailed	Three-zone	Two-zone	One-zone	R-value	Simple geometry	Shoebox
Mean (average) [MWh]	217.91	196.63	189.81	187.35	218.02	186.10	186.26
Standard Deviation (SD) [MWh]	3.52	3.01	2.68	2.73	2.70	1.48	3.07
Variance $[MWh]^2$	12.39	9.07	7.16	7.46	7.29	2.20	9.41
Median [MWh]	216.70	195.45	189.08	186.51	217.35	186.34	185.86
Coefficient of Variation (CV)	1.62	1.53	1.41	1.46	1.24	0.80	1.65
Skewness	0.92	1.01	0.75	1.21	0.74	-0.66	1.22

Figures 3-7 and 3-8 compare the performance of the simplified models with that of the detailed model using selected ECMs. The shoebox model partially aligns with the detailed model for warehouse wall insulation (38% vs. 58% for StoneWool-5.5 in), but significantly diverges from the detailed model for office wall insulation (0% vs. 40%) and east office windows (10% vs. 100%). The simplified geometry model shows closer agreement, particularly in warehouse wall insulation (76% vs. 58%), though it differs in floor insulation (76% vs. 34%). The one-zone model exhibits considerable deviations in insulation and window choices, while the two-zone model demonstrates moderate alignment, especially in window selection (74% vs. 86% for the south office window). The three-zone model aligns well with the detailed model, including

warehouse wall insulation (66% vs. 58%), but differs in office wall insulation. The R-value model shows the greatest deviations, particularly in warehouse wall insulation and window selection. It frequently selects double-glazed, advanced Low-E, argon-filled windows for the south and west office windows in about 60% of its solutions, an option not selected by any other model. These discrepancies highlight the distinct approach of the R-value model in optimizing thermal performance.

Table 3-6 compares the cost-effective (lowest NPV) and energy-efficient (lowest PE) scenarios between the detailed and three-zone models, focusing on selected ECMs. The ECM selections show broad consistency across both scenarios, indicating strong alignment despite minor variations in performance metrics. In the cost-effective scenario, the three-zone model reports an NPV 7.8% lower than the detailed model, while in the energy-efficient scenario, it shows an NPV 9.6% lower. The three-zone model underestimates PE by 9.9% in the cost-effective scenario and by 9.5% in the energy-efficient scenario. The ECM selections further support this alignment, with the only difference in the energy-efficient scenario being warehouse floor insulation, where the detailed model selects StoneWool-5.5 in, and the three-zone model opts for Fiberglass-6 in. In the cost-effective scenario, both models mostly agree, except for warehouse floor insulation, where the detailed model retains the base insulation and the three-zone model upgrades to Fiberglass-3.5 in. Minor differences also arise in the ECMs for the office wall and east office window in the cost-effective scenario, reflecting slightly different optimization priorities.

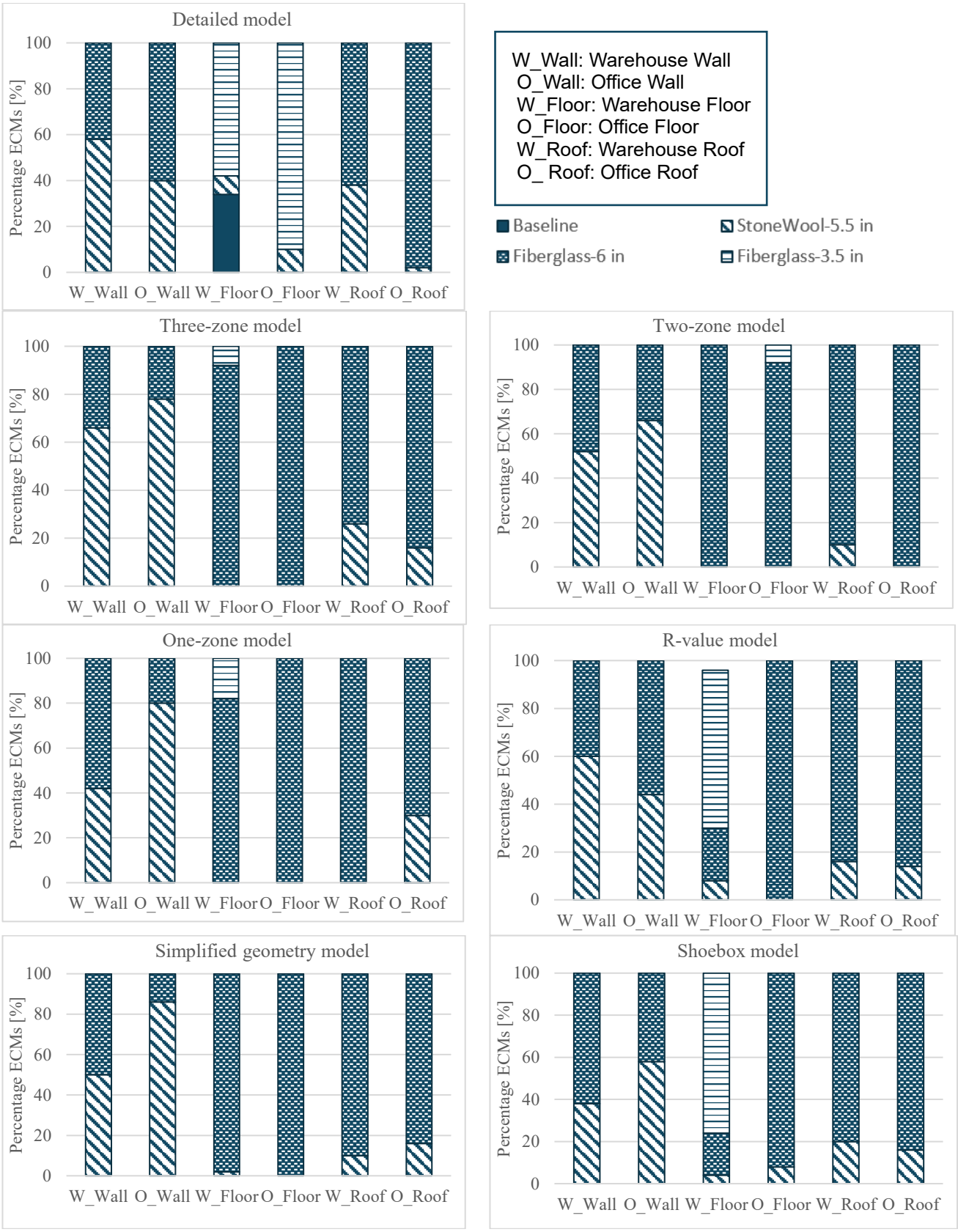

Figure 3-7: Selected ECMs in detailed and simplified models: insulation selection.

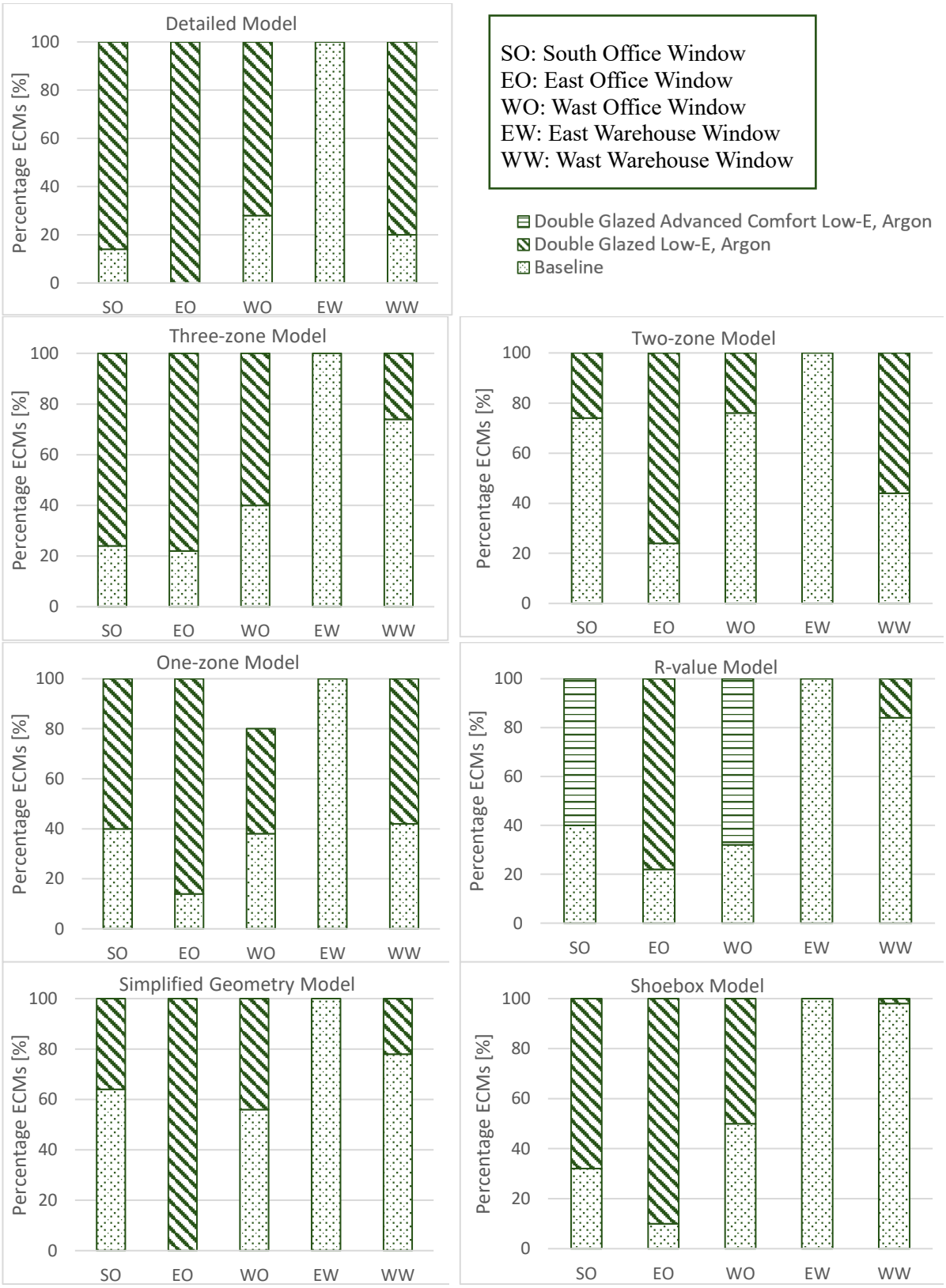

Figure 3-8: Selected ECMs in detailed and simplified models: glazing selection.

Table 3-6: Comparison of the cost-effective and energy-efficient scenarios in the detailed and three-zone models.

	Min NPV detailed model	Min NPV three-zone model	Min PE detailed model	Min PE three-zone model
NPV [kCAD]	831	766	874	790
PE [MWh]	225	203	214	194
Warehouse Wall	Fiberglass-6 in	Fiberglass-6 in	StoneWool-5.5 in	StoneWool-5.5 in
Office Wall	Fiberglass-6 in	StoneWool-5.5 in	StoneWool-5.5 in	StoneWool-5.5 in
Warehouse Floor	base model	Fiberglass-3.5 in	StoneWool-5.5 in	Fiberglass-6 in
Office Floor	Fiberglass-6 in	Fiberglass-6 in	Fiberglass-6 in	Fiberglass-6 in
Warehouse Roof	Fiberglass-6 in	Fiberglass-6 in	StoneWool-5.5 in	StoneWool-5.5 in
Office Roof	Fiberglass-6 in	Fiberglass-6 in	StoneWool-5.5 in	StoneWool-5.5 in
West Office Window	Baseline	Baseline	Double Glazed Low-E, Argon	Double Glazed Low-E, Argon
South Office Window	Baseline	Baseline	Double Glazed Low-E, Argon	Double Glazed Low-E, Argon
East Office Window	Double Glazed Low-E, Argon	Baseline	Double Glazed Low-E, Argon	Double Glazed Low-E, Argon
East Warehouse Window	Baseline	Baseline	Baseline	Baseline
East Warehouse Window Length [m]	Baseline	Baseline	Baseline	Baseline
West Warehouse Window	Baseline	Baseline	Double Glazed Low-E, Argon	Double Glazed Low-E, Argon
West Warehouse Window Length [m]	Baseline	Baseline	1	1

Overall, the three-zone model, which divides spaces by usage (warehouse, office, and plenum), effectively captures the key characteristics of the detailed model, making it a reliable alternative for energy modeling when both accuracy and efficiency are critical. The model performs well by simplifying internal spaces without losing important functional distinctions. Consolidating similar zones reduces computational time while maintaining acceptable accuracy by accounting for varying usage patterns and HVAC systems within the building. The findings suggest that when simplifying building models, it is crucial to consider the impact of space

usage when merging zones. Different spaces, such as offices, warehouses, and plenum areas, have unique thermal characteristics and energy demands. Overlooking these distinctions can lead to inaccurate predictions of energy performance.

3.3.3 Energy Modeling Practices and Preferences Survey

The resource-intensive nature of building energy modeling poses barriers to efficient project execution and innovation. Simplification reduces simulation time and lowers the effort and time required for modeling. However, the effects of simplification on the time required to generate the base model, such as data collection, geometry creation, and HVAC system definition, remain underexplored. Therefore, a comprehensive survey was conducted to explore current practices, preferences, challenges, and opportunities for simplification in building energy modeling, targeting a diverse group of professionals, including engineers and energy modelers. Figure 3-9 provides a comprehensive breakdown of the time distribution professionals dedicate to various stages of building energy modeling.

The data highlights that over 40% of participants spend 10-25% of their total time on data collection, with an additional 20% allocating 25-40% to this task. In creating detailed geometries, approximately 30% of professionals report spending 10-25% of their time, while about 15% dedicate 40-50%, demonstrating the intensive nature of this step. For HVAC system modeling, the time distribution shows more variability. Around 20% of participants spend 10-25% of their time on this task, while roughly 10% allocate 40-50% to it, reflecting the complexity of HVAC modeling in energy simulation workflows. In contrast, addressing simulation errors appears less time-intensive for many respondents, with nearly 50% spending less than 10% of their total time on this activity. However, a smaller portion (about 20%) reported spending more than 25% of their time resolving errors, highlighting the variability in the challenge posed by simulation troubleshooting. These activities represent critical initial

steps in the modeling process, often labor-intensive and requiring significant attention to detail. This highlights the substantial effort needed during the early phases of model development, suggesting that strategies to streamline these tasks could improve overall efficiency in building energy modeling workflows.

Given the substantial time investment required for detailed building energy modeling, many professionals expressed a strong willingness to adopt simplified modeling approaches. As shown in Figure 3-10, 62% of respondents are moderately willing to accept reduced accuracy in exchange for faster simulations, while 19% are very willing to make such trade-offs, even with noticeable reductions in accuracy. This indicates growing industry acceptance of balancing accuracy and efficiency to meet time and resource constraints. The survey revealed that professionals with over four years of experience are similarly inclined toward simplified models, with around 60% accepting a reduction in accuracy for improved efficiency. Simplifications in complex tasks, such as detailed geometry creation and HVAC system specifications, proved particularly effective, as illustrated in Figure 3-11. For 42% of respondents, these simplifications reduced modeling time by more than 40%, highlighting the potential for significant time savings in labor-intensive processes. In contrast, less complex tasks, such as defining materials, construction elements, lighting systems, and operational schedules, yielded only 5-10% time savings for about half of the participants. These findings underscore the industry's readiness to shift to more efficient modeling techniques that prioritize speed and resource optimization without compromising the integrity of simulations.

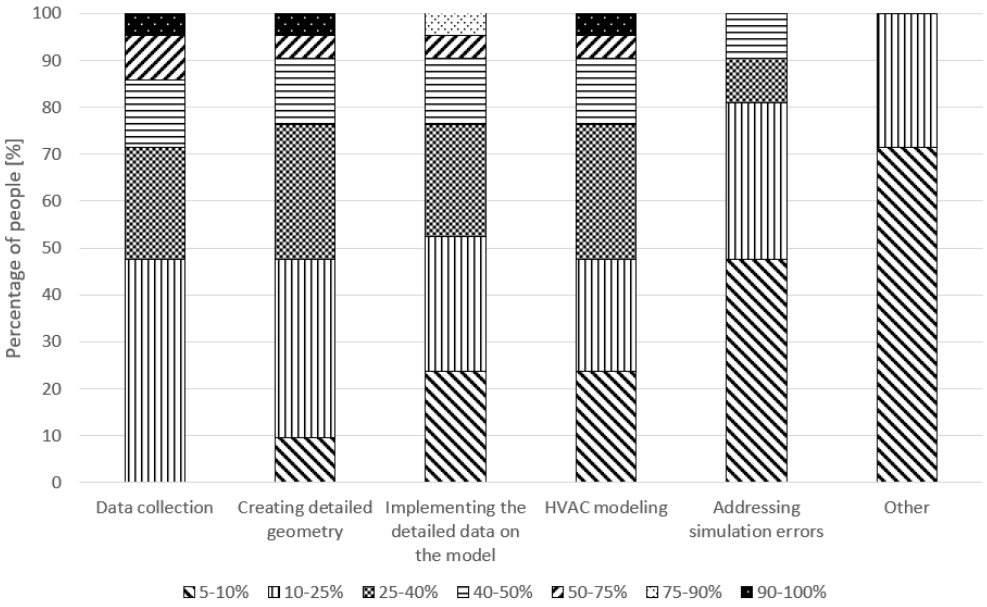

Figure 3-9: Distribution of total modeling time spent on key tasks by energy modelers.

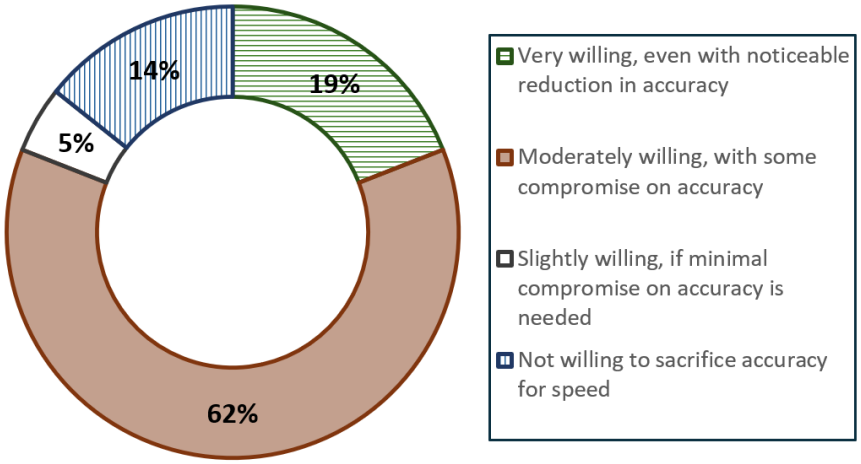

Figure 3-10: Willingness to use simplified models by energy modelers.

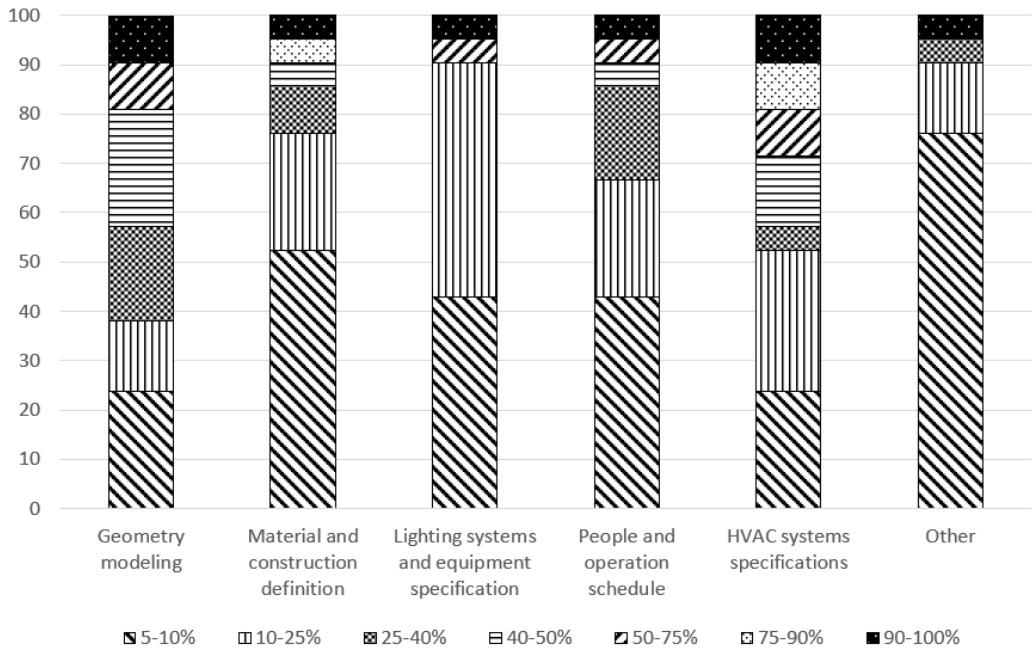

Figure 3-11: Simplified modeling process components and their impact on reducing modeling time.

3.4 Conclusion

This study provides a comprehensive evaluation of building model simplifications in the context of multi-objective energy retrofit optimization, aiming to balance computational efficiency and predictive accuracy. The novelty of this work lies in identifying which simplification strategies can most effectively balance computational efficiency and accuracy, while leveraging parallel computing to enhance the optimization process for building energy retrofits. A survey of energy modelers was conducted to understand current practices, followed by an assessment of thermal zone abstraction, HVAC simplification, material property approximations, and geometric simplifications applied to a mixed-use commercial building using a parallel NSGA-II framework.

The results demonstrate that simplified models significantly reduce computational time, especially when combined with parallel processing. In the detailed model, parallel computing halved the simulation time, reducing it from 21.65 hours to 10.65 hours. Among the simplified models, the shoebox approach was the fastest (0.39 hours) but introduced notable energy

consumption underestimations (11% for gas and 21% for electricity). The three-zone model, which divided spaces by usage, provided the best balance between efficiency and accuracy. It required 6.34 hours while maintaining a 7% underestimation for gas and 14% for electricity. These discrepancies in energy estimates, particularly in zone- and geometry-simplified models, stem from the sensitivity of internal walls to solar radiation, which increases cooling demand, and from convective heat gains on internal surfaces during heating seasons, leading to an underestimation of heating demand. Similarly, the HVAC simplification model performed well in predicting gas consumption (3% error) but considerably underestimated electricity use by 80%. This discrepancy arises because the detailed HVAC model accounts for year-round fan operation, whereas the ideal air load system ignores fan energy consumption, leading to inconsistencies between the models.

Further analysis of objective function values and ECM recommendations showed that the detailed model exhibited the widest range of Pareto-optimal solutions, offering greater flexibility for retrofit decisions. The R-value model, which simplified material properties, closely aligned with the detailed model (NPV deviation: 0.27%–0.94%, PEC deviation: 0.18%–0.81%). The three-zone model performed well, with modest deviations (8% NPV, 10% PEC), whereas the shoebox, simplified geometry, and single-zone models showed larger inaccuracies due to their inability to account for convective heat gains and conduction losses fully. The reduced predictive accuracy in the simplified zone and geometry models can be attributed to their inability to fully account for convective heat gains and conduction losses, leading to underestimations of heating and cooling energy demands compared to the three-zone and detailed models.

Overall, the three-zone model, which divides spaces by usage, emerged as the most reliable compromise, effectively capturing key characteristics of the detailed model while maintaining

reasonable computational efficiency. The shoebox model, though highly efficient, sacrifices accuracy and is better suited to large-scale applications that require rapid simulations. The R-value model, while accurate, had a computational time (10.37 hours) similar to the detailed model, making it more applicable when detailed material data is unavailable. Importantly, a survey of energy modelers revealed that 42% of participants experienced over 40% time savings by simplifying geometry and HVAC systems, highlighting the practical benefits of model simplification in early retrofit decision-making.

This study highlights several areas for future research. In this respect, while the findings demonstrate the potential benefits of model simplification, it is essential to recognize that the specific characteristics of the case study building influence the conclusions. The selected building shares architectural similarities with a large number of mixed-use office buildings in the region and across Canada. Moreover, its mixed-use functionality introduces distinct characteristics. As demonstrated in this study, merging zones with different functions, such as office, warehouse, and plenum areas, into a single-zone model significantly reduces accuracy, a limitation not observed in single-functionality buildings, such as the predominantly residential models commonly examined in the literature. However, as a mixed-use commercial facility, the building features distinct internal zoning, HVAC configurations, and occupancy patterns, presenting unique simplification challenges that may not fully represent the behavior of residential buildings, industrial facilities, or highly glazed structures. Consequently, while the findings serve as a valuable reference for similar office buildings, their applicability to other building types and retrofit scenarios may be limited. However, the proposed framework is adaptable and can be readily applied to various building types. Therefore, a more comprehensive guideline can be developed by implementing the proposed framework across different building typologies and climatic conditions. Expanding this investigation to encompass a broader range of buildings and mechanical systems would help assess the

consistency of the observed results. Future work should also consider diverse climate zones and future weather scenarios to develop resilient retrofit strategies that can adapt to changing environmental conditions. Additionally, investigating how simplification affects the accuracy of retrofit recommendations, especially for complex systems such as dynamic HVAC controls and advanced materials, would refine modeling approaches to enhance the efficiency and performance of energy retrofitting in residential and commercial sectors.

Chapter 4: Evaluating Simplified Building Models' Sensitivity to Climate Data for Energy Retrofit Optimization

This chapter has been published as:

- Article 3: Y. Dadras, F. Mostafazadeh, M. Kavgic, M. Ghobadi, Enhancing building energy optimization efficiency: A performance analysis of simplification approaches, Journal of Building Engineering 105 (2025). https://doi.org/10.1016/j.jobe.2025.112559.
- Conference paper 4: Y. Dadras, F. Mostafazadeh, M. Kavgic, Y.D. Ca, Impact of Modeling Simplification on Energy Simulation Speed and Accuracy Considering Climate Change: A Case Study of a Dormitory Building, CIB Conferences 1 (2025) 171. https://doi.org/10.7771/3067-4883.1926. (2025). (CIB Conference in West Lafayette, Indiana, USA).

4.1 Introduction

This chapter examines how simplified building energy models respond to different weather boundary conditions during retrofit optimization. While simplified models can significantly reduce computational effort, their performance may vary when diverse climate inputs, including typical meteorological years, extreme hot and cold periods, and future climate projections, drive simulations. Understanding this sensitivity is essential because retrofit decisions depend on the accuracy of model predictions across both current and future conditions.

Using the validated dormitory building introduced in Chapter 2 as the case study (Case study 2), this chapter evaluates how zoning abstraction, HVAC simplification, and material idealization influence model accuracy under eight climate scenarios. The analysis quantifies

the stability of simplification errors across weather files and assesses whether simplified models remain reliable when optimization is performed under projected future climates. The findings provide insight into when simplified models are suitable for early-stage decision-making and when higher-fidelity evaluation is necessary, especially for peak-load assessment and long-term retrofit planning.

4.2 Methodology

Figure 4-1 illustrates the methodological framework adopted in this chapter. The framework is structured into three main stages: (1) climate projection, (2) energy simulation modeling and simplification, and (3) evaluation of climate-adaptive retrofit strategies using the prNSGA-III optimization algorithm.

The first stage, climate projection, involves extracting weather data from various sources and generating weather files required for simulation. Four categories of weather files are developed to assess the building performance of simplified and detailed models under boundary climate conditions. (i) an actual weather file based on data from the year 2018, (ii) typical meteorological year (TMY) files, including EnergyPlus TMY and CWEC files from 2016 and 2020, and (iii) future weather files representing the 2020, 2050, and 2080 created using CCWorldWeatherGen and Meteonorm, and (iv) extreme weather files representing the hottest and coldest years over the past two decades.

In the second stage, building energy simulation models are developed using a combination of case study data, local climatic conditions, building energy standards, and existing literature. Both detailed (Chapter 2, section 2.1.2) and simplified (Chapter 2, section 2.2) versions of the model are created. The simplification strategies examined include: (i) thermal zone abstraction (Scenarios A_{21}–A_{24}), (ii) material property simplification (Scenario B_{21}), and (iii) HVAC system simplification (Scenario C_{21}).

The final stage involves evaluating retrofit strategies under future climate conditions using the prNSGA-III optimization algorithm. Both the simplified and detailed models are employed in a two-phase optimization process. In the first phase, the simplified model is used to identify optimal retrofit configurations. Each configuration is then simulated using the detailed model to compare the accuracy of simplified models. The second phase optimizes each model independently, enabling a direct comparison of retrofit solutions and computational time between simplified and detailed models. This dual-stage framework offers a comprehensive evaluation of how model complexity affects the selection of energy conservation measures (ECMs) in climate-adaptive retrofit planning.

The simulation engine (EnergyPlus) and optimization algorithm (prNSGA-III) used in this chapter are well-established and widely adopted in the literature. Since the objective is to systematically evaluate the impact of different weather boundary conditions on the accuracy of simplified building energy models, employing these proven tools helps isolate the effects of weather data and model simplifications. This approach ensures that observed variations are attributable to boundary conditions rather than methodological uncertainties. As a result, the study provides practical error ranges for common simplification strategies, offering guidance to practitioners seeking computationally efficient yet reliable models.

4.2.1 Weather Data Selection

4.2.1.1 Actual and Typical Meteorological Weather Files

Local weather conditions are commonly incorporated into energy models using AMY and TMY data. AMY files contain recorded weather data for a specific year, capturing the unique conditions of that period [94]. In this study, the 2018 AMY file was generated using data from the Ottawa Cda RCS station (Figure 4-2). This dataset provided hourly values for temperature,

humidity, wind, and pressure, while solar radiation was supplemented from the National Solar Radiation Database (NSRDB) [95].

To represent long-term climate trends, three TMY files were used: two Canadian Weather for Energy Calculations (CWEC) files, based on the Canadian Weather Energy and Engineering Datasets (CWEEDs) from 2016 and 2020 [96], developed by Environment and Climate Change Canada and the National Research Council (NRC) using the Sandia selection method [97]; and a third TMY file from the EnergyPlus repository, organized by the World Meteorological Organization region and country [98,99]. Table 4-1 summarizes the data periods and representative months for each TMY file, highlighting source differences that may affect simulation outcomes.

Table 4-1: Weather data periods of the typical weather years.

Weather	Period	Jan	Feb	Mar	Apr	May	Jun	Jul	Aug	Sep	Oct	Nov	Dec
TMY_EP	1953 - 1995	1966	1980	1964	1964	1968	1970	1977	1981	1979	1969	1974	1960
CWEC_2016	1998 - 2014	2011	2001	1998	2002	2014	2011	1998	2010	2012	2004	2004	2012
CWEC_2020	1998 - 2017	2011	2001	2006	2011	2014	2011	1998	2010	2001	2004	2004	2016

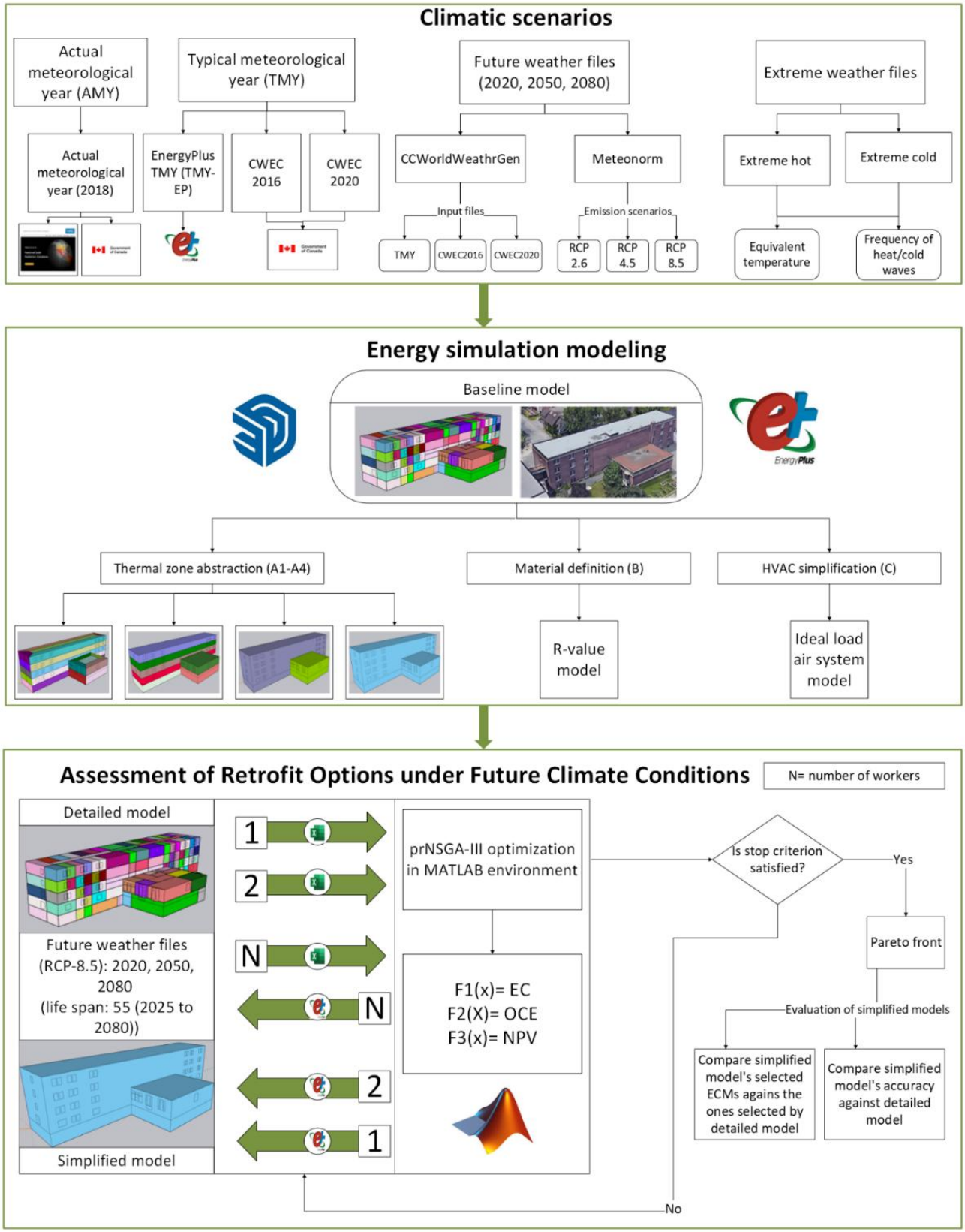

Figure 4-1: Methodology framework (Chapter 4).

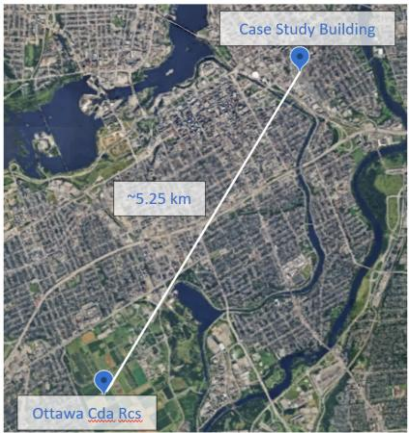

Figure 4-2: Location of the case study building and weather station in Ottawa (Canada).

4.2.1.2 Future Weather Files

To conduct a comparative analysis of future climate impacts on building energy performance, two statistical downscaling tools, Meteonorm v8 [100] and CCWorldWeatherGen v1.9 [101] were employed to generate projected weather files for the city of Ottawa. These tools are widely used in the field of building performance simulation due to their accessibility and ability to generate future climate scenarios from Global Climate Model (GCM) data [102]. The two approaches differ fundamentally in their underlying assumptions. CCWorldWeatherGen employs a morphing technique, in which monthly mean deltas from the HadCM3 [103] GCM (IPCC TAR A2 scenario) are superimposed on historical weather files such as TMY or CWEC [104]. This method preserves the original local variability and extreme events, but the results depend on a single climate model and scenario, which may introduce structural bias if the selected GCM misrepresents regional trends. Meteonorm v8, in contrast, is a stochastic weather generator that synthesizes hourly time series from long-term climate statistics and its own integrated database. It incorporates multiple Representative Concentration Pathways (RCPs 2.6, 4.5, and 8.5 from the Fifth Assessment Report), enabling the exploration of a wider range of emission futures; however, it tends to smooth short-term variability, potentially underestimating the frequency and intensity of extreme events [105]. Weather files were created for 2020, 2050, and 2080, consistent with mid- and long-term retrofit planning

horizons. Although the optimization spans from 2025 to 2080, 2020 was used as the baseline because both tools base their projections on that year and do not support intermediate years, such as 2025.

4.2.1.3 Extreme Weather Files

To further investigate the impact of weather data on energy performance across different building models, this study identifies representative extreme hot and cold periods using an advanced surface thermal metric, the equivalent temperature (T_{eq}). This parameter captures the combined thermal effects of convection, shortwave solar radiation, and longwave radiative exchange between the outdoor environment and the building envelope [106]. By integrating these mechanisms, T_{eq} provides a more comprehensive representation of outdoor thermal stress than air temperature alone.

Hourly equivalent temperature, T_{eq} [°C], is calculated over a 20-year historical dataset using four meteorological inputs: dry bulb temperature (T_{air}) [°C], dew point temperature (T_{dew}) [°C], global horizontal irradiance (GHI) [W/m²], and wind speed (v) [m/s]. The equivalent temperature accounts for the combined impact of shortwave solar radiation, longwave radiative heat exchange with the sky, and convective heat transfer with the surrounding air and is calculated using Equation 4-1 [107].

$$T_{eq} = T_{air} + \frac{1}{\alpha_e}(GHI.\alpha_{sol} + (T_{sky} - T_{air}).\alpha_r \quad \text{Equation 4-1}$$

where $\alpha_{sol} = 0.7$ is the assumed surface solar absorptivity, α_r is the radiative heat transfer coefficient [W/m²·K], and $\alpha_e = \alpha_c + \alpha_r$ is the total effective heat transfer coefficient [W/m²·K]. The sky temperature (T_{sky} [°C]) is estimated using a clear-sky emissivity model derived from the dew point temperature [108,109]. And ε_{clear} is the emissivity of a clear sky. The detailed equations used to determine emissivity, clear-sky temperature, cloud correction,

convective and radiative coefficients, and the magnitude index for extreme event detection are provided in Appendix B, Equations B.1-B.6.

Once T_{eq} is computed, daily maximum and minimum values are extracted to form a time series of extreme thermal conditions. For each year, a sliding four-day window is applied to evaluate candidate extreme periods. The severity of each of the four days is quantified in Equation 4-2 using a magnitude index (M_i), that captures the persistence and intensity of deviations from long-term statistical thresholds [110].

$$M_i = \sum_{j=1}^{4} \rho\left[\frac{T_{max,j}-T_{max,thres}}{2\times SD_{T,max}} + \frac{T_{min,j}-T_{min,thres}}{2\times SD_{T,min}}\right] \quad \text{Equation 4-2}$$

Here, $T_{max,j}$ and $T_{min,j}$ represent the daily maximum and minimum T_{eq} for each day in the window, while $T_{max,thres}$ and $T_{min,thres}$ are defined as the median of the 90^{th} and 10^{th} percentiles, respectively, from the 20-year distribution of daily maximum and minimum T_{eq}. Standard deviations $SD_{T,max,}$ and $SD_{T,min}$ are used for normalization. The $\rho = 1$ is used for hot periods and ρ = -1 for cold periods. To ensure seasonally realistic outcomes, hot events are restricted to May through September, and cold events are limited to November through March. For each year, the four days with the highest hot and cold magnitude index are selected as the representative extremes.

In addition to identifying peak intensity and the extreme temperature events, this study assesses the frequency of heat and cold waves using a dynamic threshold approach adapted from Lavaysse et al [110] and Smid et al. [111]. For each calendar day, a 31-day moving window centered on the target day is used to compute variable thresholds:

- Heat wave threshold: 90th percentile of daily maximum T_{eq}
- Cold wave threshold: 10th percentile of daily minimum T_{eq}

A heat wave is defined as a period of at least three consecutive days during which the daily maximum T_{eq} exceeds the corresponding dynamic threshold. Similarly, a cold wave is identified when the daily minimum T_{eq} remains below the cold threshold for three or more consecutive days. The total number of heat and cold waves is calculated for each year to evaluate trends in the occurrence of short-term temperature anomalies.

4.2.2 Objective Functions

This study integrates environmental and economic objectives to evaluate energy retrofit scenarios. Environmental performance is assessed by minimizing total operational energy consumption (EC) and operational carbon emissions (OCE), while economic feasibility is evaluated through Life Cycle Cost (LCC) over a 55-year service life (2025–2080) [77,78,80,81,83,90,92,112]. EC is calculated by summing annual electricity and natural gas use, and OCE is estimated using emission factors from the National Research Council Canada: 0.185 kg CO_2/kWh for natural gas and 0.0579 kg CO_2/kWh for electricity [113]. Energy simulations are conducted in EnergyPlus for three representative future years (2020, 2050, 2080). Intermediate years (2025, 2030, 2040, 2060, 2070) are estimated through linear interpolation to capture long-term energy and emissions trends under changing climate conditions [114]. The total environmental impact is expressed in Equations 4-3 and 4-4.

$$EC = \sum_i^n (EC_i + GC_i) \quad \text{Equation 4-3}$$

$$OCE = \sum_i^n (EC_i \cdot EF_{elec} + GC_i \cdot EF_{gas}) \quad \text{Equation 4-4}$$

where EC_i and GC_i are electricity and natural gas consumption in year i, and EF_{elec} and EF_{gas} are the emission factors for electricity and natural gas, respectively.

The LCC is calculated over a 55-year evaluation period (2025–2080), combining the retrofit investment cost with the present value of future electricity and natural gas expenditures. The analysis is conducted using the constant-dollar method, employing a real discount rate that

reflects the time value of money, exclusive of general inflation. The LCC is defined using Equation 4-5.

$$LCC = I + \sum_j (E_j^{elec}.q_j.C_{elec} + E_j^{gas}.q_j.C_{gas}) \quad \text{Equation 4-5}$$

where I is the initial investment cost of retrofit measures, E_j^{elec} and E_j^{gas} represent the estimated annual electricity and gas consumption (in kWh/year) for decade j, q_j is the present value factor for decade j, and C_{elec} and C_{gas} are the base-year (2025) unit costs of electricity and natural gas, respectively. The present value factor q_j discounts a stream of escalating annual costs over each decade and is calculated using the Modified Uniform Present Value (UPV*) [115] in Equation 4-6:

$$q_j = \begin{cases} \frac{\left[1-\left(\frac{1+g}{1+d_r}\right)^{t_j}\right]}{d_r-g} & if\ d_r \neq g \\ \frac{t_j}{1+d_r} & if\ d_r = g \end{cases} \quad \text{Equation 4-6}$$

where t_j is the duration of the evaluation period for decade j (typically 10 years, except for the first block covering 2025–2029 with 5 years, and the final year 2080 with 1 year), g is the assumed real escalation rate of energy prices (0.5%) [116], and d_r is the real discount rate, which is computed based on the nominal discount rate and general inflation in Equation 4-7.

$$d_r = \frac{1+d_n}{1+e} - 1 \quad \text{Equation 4-7}$$

where d_n = 3.29% [117] is the nominal discount rate, and e = 2.5% [118] is the annual inflation rate.

4.2.3 Multi-Objective Optimization

The optimization problem is formulated with three objectives:

- Minimize F1(x): Total energy consumption over 55 years
- Minimize F2: Operational equivalent CO_2 emissions

- Minimize F3(x): Life cycle cost (LCC) based on net present value (NPV)

Subject to x∈X, Constrains: $EC < EC_0,\ OCE < OCE_0$

where x is the vector of decision variables defining retrofit strategies, X is the feasible solution space, and EC_0 and OEC_0 are baseline operational energy consumption and CO_2 emissions, respectively. Each objective function is evaluated using results from annual energy simulations performed in EnergyPlus. A constraint is applied to enforce minimum energy performance and emission limits by excluding solutions that perform worse than the baseline case. To solve the optimization problem, this study adopts a methodology similar to [52], employing a customized version of the Non-dominated Sorting Genetic Algorithm III (NSGA-III) tailored for parallel, simulation-based optimization called prNSGA-III. Genetic algorithms, particularly their multi-objective variant, NSGA-II, have been widely applied in the literature and are recognized as established optimization methods [119–124]. More recent research has demonstrated that newer versions of multi-objective genetic algorithms, such as NSGA-III, outperform NSGA-II on problems with more than two objectives by introducing hyperplane and reference points that guide the classification and selection of high-quality solutions for subsequent populations [125,126]. In this study, a modified version of NSGA-III, called prNSGA-III, is employed, specifically tailored for improved performance in building energy optimization. To enhance computational efficiency, prNSGA-III integrates two key modifications. First, the evaluation of individual retrofit configurations is parallelized across multiple CPU cores, enabling simultaneous simulation runs and significantly reducing total computation time. Second, a result-archiving mechanism is implemented to eliminate redundant simulations. Each solution vector is assigned a unique identifier, allowing previously evaluated configurations to be retrieved from an archive rather than re-simulated.

The genetic algorithm was configured with a population size of 50, while mutation and crossover probabilities were set at 0.7 and 0.4, respectively. These parameter values, informed

by prior research [127–129], provide a balance between solution reliability and computational efficiency. The evolutionary process was carried out until the termination condition was met, defined as 100 generations. The optimization runs for all models were performed on a computer equipped with an Intel Core i9 processor operating at 2.60 GHz with a 24 MB cache.

4.2.4 Simplified Models Evaluation Framework

The detailed dormitory model was simplified using the abstraction strategies outlined in Chapter 2, including thermal zone aggregation (A_{21}-A_{24}), HVAC simplification (B_{21}), and material property reduction (C_{21}). These scenarios reduce spatial, mechanical, and material detail while preserving the model inputs required for energy and retrofit evaluation. The simplified versions of the model serve as the basis for the accuracy and sensitivity analyses presented in this chapter.

Modeling accuracy is evaluated by first conducting optimization using only simplified building energy models. The resulting ECMs are then re-simulated with a detailed model to assess long-term performance. The detailed model is not involved in the optimization itself but serves as a post-optimization benchmark. The deviation in predicted objective functions is quantified by comparing them over a 55-year simulation horizon in simplified models against the benchmark detailed model's results. The percentage error is calculated using Equation 4-8:

$$error = \frac{Obj_s - Obj_d}{Obj_d} * 100 \qquad \text{Equation 4-8}$$

where Obj_d and Obj_s denote the objective function values from the detailed and simplified models, respectively.

Additionally, a separate optimization is performed using the detailed model to generate its own optimal ECM set. These results are compared to those from each simplified model to examine how model fidelity influences retrofit selection under future climate conditions. Furthermore,

separate optimization runs are conducted for all models to assess their efficiency relative to the detailed model.

Energy conservation strategies were developed based on a detailed energy audit, stakeholder input, and an assessment of locally available options. Thermographic imaging revealed key envelope deficiencies, including thermal bridging, inadequate insulation, and air leakage around aging windows. Retrofit measures focused on improving envelope performance through various insulation types and thicknesses, as well as evaluating high-performance window systems. Although physically connected, the residential and mixed-use sections differ in function, occupancy, internal loads, and HVAC systems, requiring tailored retrofit approaches for each. This separation ensures more realistic and effective optimization compared to applying uniform measures across both areas.

To account for the potential use of the dormitory building during the summer as rental accommodation for summer camps and students, cooling was added to the retrofit scenario via portable window air-conditioning units. The selected ECMs, outlined in Table 4-2, were included as decision variables in the EnergyPlus [68] and MATLAB [75] optimization framework.

Table 4-2: Characterization of investigated ECMs.

Components	Decision Variables	Investigated options
Exterior wall	Add exterior insulation to the RB. Add exterior insulation to the MB.	10 insulation options (rigid insulation and foam insulation with R-values between 0.8 and 3.5 [m^2.K/W])
Basement wall	Replace insulation in the RB. Replace insulation in the MB.	
Roof	Add roof insulation to the RB. Add roof insulation to the MB.	
Floor	Replace floor insulation in the RB. Replace floor insulation in the MB.	
Window	Replace windows in the RB. Replace windows in the MB.	6 window options: Glass material: clear, bronze, and reflex. Glass thickness [mm]: base case, 4, 6, 10 Gas: air, argon

4.3 Results and Discussion

4.3.1 Impact of AMY and TMY Weather Files on Detailed and Simplified Models

This section evaluates the suitability of three TMY datasets (TMY_EP, CWEC 2016, and CWEC 2020) against the AMY 2018 file using weather parameters (dry-bulb temperature, global horizontal irradiance, and relative humidity) and thermal demand indicators (HDD and CDD), showing that while mean values are similar across datasets, differences exist in temperature ranges, solar radiation distributions, and humidity variability, with AMY capturing the widest extremes and CWEC datasets reflecting more overcast conditions (Table 4-3). Moreover, in Table 4-4 energy demand assessed through HDD (18 °C) and CDD (23 °C) shows that while CWEC 2016 and 2020 align more closely with AMY in heating demand, all TMY datasets misrepresent cooling demand by up to 43%, with TMY_EP overestimating HDD by 6% and underestimating CDD by more than 60%, which may lead to biased retrofit recommendations for passive cooling strategies or cooling system sizing under future climates.

Table 4-3: Summary statistics of dry-bulb temperature, global horizontal radiation, and relative humidity for TMY and AMY weather files.

Weather file	Dry bulb temperature [°C]				Global Horizontal Radiation [W/m^2]				Relative humidity [%]			
	Mean	Median	Min	Max	Mean	Median	Min	Max	Mean	Median	Min	Max
AMY_2018	7	6	-28	35	155	4	0	986	71	73	14	99
TMY_EP	6	7	-25	33	153	10	0	1005	68	69	16	107
CWEC_2016	7	7	-30	33	156	1	0	965	73	75	20	100
CWEC_2020	7	8	-30	33	156	1	0	965	72	74	18	104

Table 4-4: Annual HDD and CDD were calculated for each weather file using hourly temperatures, with base temperatures of 18 °C and 23 °C, respectively.

Weather File	HDD (°C·day)	CDD (°C·day)
AMY_2018	4482.8	140.0
TMY_EP	4746.9	53.3
CWEC 2016	4393.5	81.5
CWEC 2020	4406.8	79.5

The impact of different weather files on energy predictions was assessed using both a detailed model and several simplified configurations. Table 4-5 reports total natural gas consumption across four weather files during the occupied season (September–April). Zone-simplified models consistently underpredict energy use compared to the detailed model, although the magnitude of the deviation depends on the level of simplification and the weather file used. During colder months, zone-simplified models may underestimate heating loads because they fail to account for increased convective exchange and dynamic heat losses through the envelope [15,130]. This trend of underprediction in zone-simplified models is consistent with findings reported in the literature [14,15,30,130,131].

In the one-zone model, energy consumption varied by weather file, with TMY_EP producing a 16.3% deviation from the detailed model, compared to 14.9% for AMY and 14.6% for CWEC 2016. These results highlight how oversimplified zoning can amplify the impact of climatic assumptions, particularly under colder profiles, such as TMY_EP. More granular models (e.g., two-, seven-, and thirty-five-zone) exhibited smaller and more consistent errors; for instance, the thirty-five-zone model had a stable deviation of 10.9% across AMY and TMY files. These findings indicate that greater spatial detail reduces sensitivity to weather-file variability, thereby enhancing the robustness of energy predictions across different climate conditions.

HVAC simplification consistently led to an underestimation of approximately 21%, regardless of the weather file used. This finding highlights the dominance of system-level assumptions over climatic inputs for this type of HVAC. The ideal HVAC system ignores part-load inefficiencies and the transient dynamics inherent in actual HVAC performance, leading to substantial discrepancies in energy predictions. The R-value simplification model showed greater weather sensitivity, overestimating demand by 1.5% to 3.3% across files. This behavior can be attributed to the omission of thermal mass in the simplified model. Thermal mass enables building materials to absorb, store, and gradually release heat, thereby moderating

indoor temperature swings and reducing reliance on mechanical systems. Without representing these dynamic thermal interactions, the R-value model overlooks an essential passive mechanism of heat regulation [130].

Table 4-5: Total natural gas consumption [MWh] predicted by detailed and simplified models across weather files during the occupied heating season (September–April).

Weather File	Detailed	One-zone	Two-zone	Seven-zone	Thirty-five-zone	R-value	HVAC
AMY_2018	663.4	564.6	577.0	586.7	590.8	673.2	523.2
TMY_EP	679.5	569.0	590.7	601.4	605.0	694.2	535.9
CWEC 2016	627.1	535.5	549.7	555.7	559.2	648.0	491.8
CWEC 2020	631.0	535.8	551.3	558.8	562.3	651.3	495.4

An additional analysis examined monthly percentage errors in predicted natural gas consumption across TMY and AMY scenarios to assess the weather sensitivity of simplified models. As shown in Figure 4-3, the one-zone model exhibited the highest variability, with errors ranging from 1.2% (TMY_EP) to 17.8% (AMY) in September, and 8–22% during colder months. However, it is essential to note that shoulder season errors can appear exaggerated due to low baseline heating demand, where small absolute deviations result in large percentage differences. Similar fluctuations were observed in the two-zone and R-value models, indicating greater sensitivity among more abstracted configurations to changes in weather inputs. In contrast, higher-resolution models, such as the thirty-five-zone model, maintained more stable error margins of about 11% in heating months, suggesting reduced sensitivity to boundary condition variability. The HVAC-simplified model consistently underestimated by a significant amount across all months, primarily because it neglected system inefficiencies.

One- and two-zone models also experienced a seasonal bias, underpredicting in winter and overpredicting in the shoulder months, such as September. These overestimations are largely attributable to the loss of interior thermal mass. When multiple zones, including vertically stacked floors, are merged, key thermal storage elements such as floors and ceilings are

removed. This thermal mass removal reduces the model's ability to buffer short-term temperature fluctuations through thermal inertia. A practical approach to improve the performance of highly abstracted zone-simplified models is to reintroduce the unaccounted interior thermal mass using the "InternalMass" object in EnergyPlus, which requires specifying the removed construction and its equivalent area. After adding interior thermal mass (vertically stacked floors) to the one- and two-zone models, natural gas consumption in September was underestimated by only 2.3% and 0.9%, respectively, under the AMY scenario compared to the detailed model. These results represent a significant improvement over versions without interior thermal mass, which showed overestimations of 17.8% for the one-zone and 14.6% for the two-zone model. Cold-season underestimations reflect the models' inability to capture inter-zone heat transfer, especially solar gains in window-facing walls. Absorbed solar energy is often stored in interior surfaces and gradually released, moderating space temperatures over time. High-resolution models (seven- and thirty-five-zone) better represent these dynamics, maintaining errors below 12% across most months.

The R-value model performed well in peak heating months (e.g., 2.2% error in January under AMY); however, it greatly overestimated heating in the shoulder season, with errors exceeding 114% in September. This overestimation results from the lack of thermal mass, which in the detailed model tempers heat transfer during fluctuating conditions. Unlike zoning simplifications that retain most of the construction mass, the R-value model replaces all interior and exterior construction with massless layers, eliminating buffering effects and inflating demand during milder weather. Improving thermal mass in the R-value model cannot be addressed in the same way as in zone-simplified models through the "InternalMass" object, since the R-value approach is often applied when detailed, layer-by-layer material information is unavailable. Moreover, assigning thermal mass to each zone separately, with the corresponding surface area, would be complex and impractical. A more reasonable strategy is

to adopt a hybrid hypothetical approach. In this method, representative high-mass materials in the building are identified through observation, and a hypothetical material is defined with the same overall R-value as the massless layer but with specified density and specific heat capacity values characteristic of the identified material. This hypothetical material is then assigned to the construction, preserving the intended thermal resistance while reintroducing realistic thermal mass effects. After applying the hypothetical material to the external surfaces, the September heating prediction error under AMY improved from a 114.5% overestimation to a 40% overestimation. Assigning it to both external and internal surfaces further improved accuracy, resulting in an 18% underestimation of the actual value.

Finally, the HVAC-simplified model consistently underestimated heating by over 20%. These inaccuracies arise from the use of an ideal load air system, which fails to capture part-load inefficiencies, response delays, and distribution losses, factors that are particularly influential during periods of fluctuating demand.

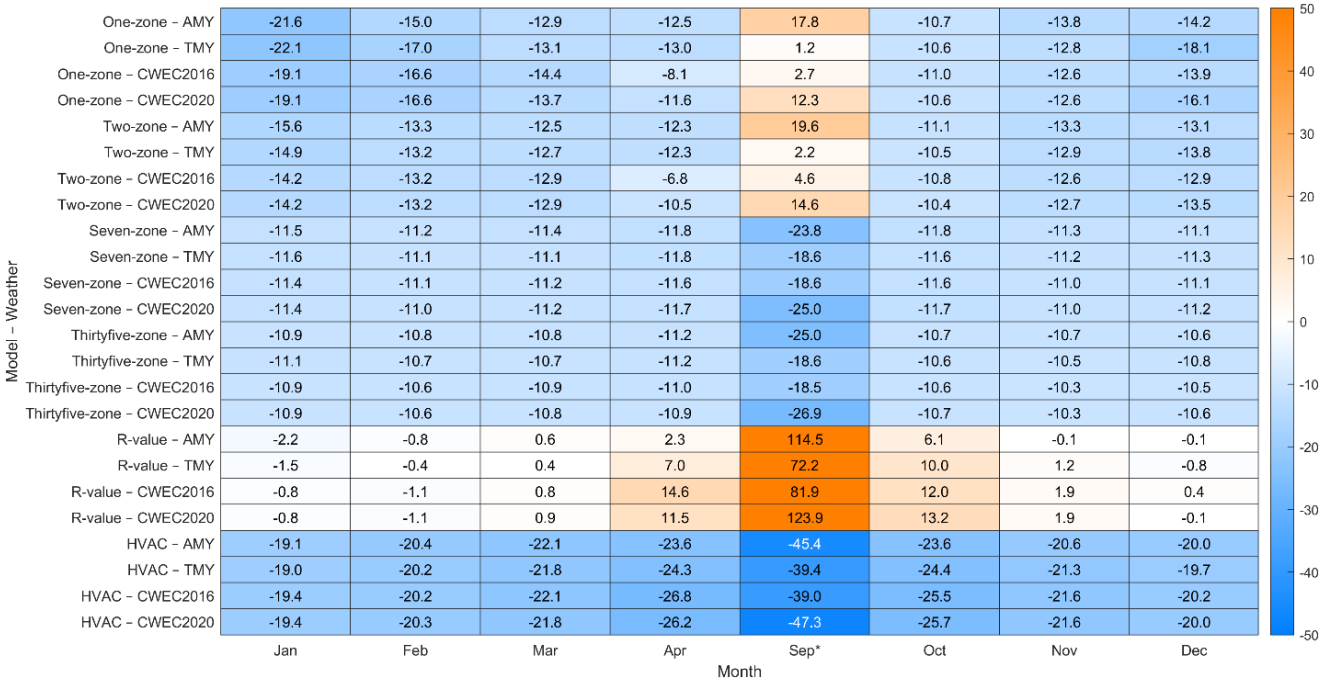

Figure 4-3: Monthly heating error of simplified models compared to detailed baseline across TMY and AMY weather scenarios. (*September is a key transition month)

Table 4-6: Monthly average weather conditions in September across different weather files.

Weather File	Temp (°C)	Temp standard deviation (°C)	RH (%)	GHI (Wh/m²)
AMY	16.84	6.12	76.1	155.1
TMY_EP	14.23	5.09	74.3	156.5
CWEC_2016	14.80	5.73	77.3	162.4
CWEC_2020	15.75	5.41	75.4	170.1

4.3.2 Influence of Future Climate Scenarios on Energy Model Predictions

As presented in Table 4-7, six future weather files generated with CCWorldWeatherGen and Meteonorm were analyzed to assess changes in annual mean dry-bulb temperature, HDD, and CDD from 2020 to 2080, showing a consistent warming trend with CCWorldWeatherGen projecting a 3.91 °C rise by 2080. Meteonorm varies by emissions trajectory (0.91 °C under RCP 2.6, 2.57 °C under RCP 4.5, and 4.57 °C under RCP 8.5), leading to reductions in HDD (−1,145.7 °C·days) and increases in CDD (+313.7 °C·days), particularly under high-emission futures.

Table 4-7: Change in annual temperature, HDD, and CDD from 2020 to 2080.

Scenario	ΔTemperature (°C)	ΔHDD (°C·day)	ΔCDD (°C·day)
CCWorld_TMY_EP	3.91	−924.00	284.71
CCWorld_CWEC2016	3.91	−874.80	317.78
CCWorld_CWEC2020	3.91	−880.70	315.31
Meteonorm_RCP2.6	0.91	−303.30	1.42
Meteonorm_RCP4.5	2.57	−604.30	185.94
Meteonorm_RCP8.5	4.57	−1145.70	313.72

As shown in Figure 4-4, across future climate scenarios, all models project reductions in annual natural gas use from 2020 to 2080, ranging from 6% to 8% under RCP 2.6 to 24% to 27% under RCP 8.5. Simplified models closely track the detailed model in capturing these climate-driven reductions, supporting their application in early-stage retrofit decision-making. Simplified models can replicate the detailed model's ability to capture long-term reductions in heating demand under the RCP 8.5 scenario (Figure 4-4), as climate-driven warming exerts a dominant influence on overall energy use. As average outdoor temperatures rise, the relative

differences introduced by simplifications such as zone aggregation, omission of thermal mass, or HVAC idealization become less pronounced in terms of annual energy demand. In other words, the large-scale decline in heating requirements over several decades is consistently reflected across both simplified and detailed models. By contrast, short-term behavior, such as monthly results during transitional seasons or hourly profiles under extreme conditions, reveals more noticeable discrepancies. These arise from the inherent simplifications, including merged zones, massless envelope representations, and idealized system dynamics, which limit the models' ability to reproduce fine-grained thermal interactions. Consequently, while simplified models differ from the detailed model in their short-term performance, they align in long-term percentage changes in heating demand between 2020 and 2080, thereby producing similar overall trends under future climate scenarios.

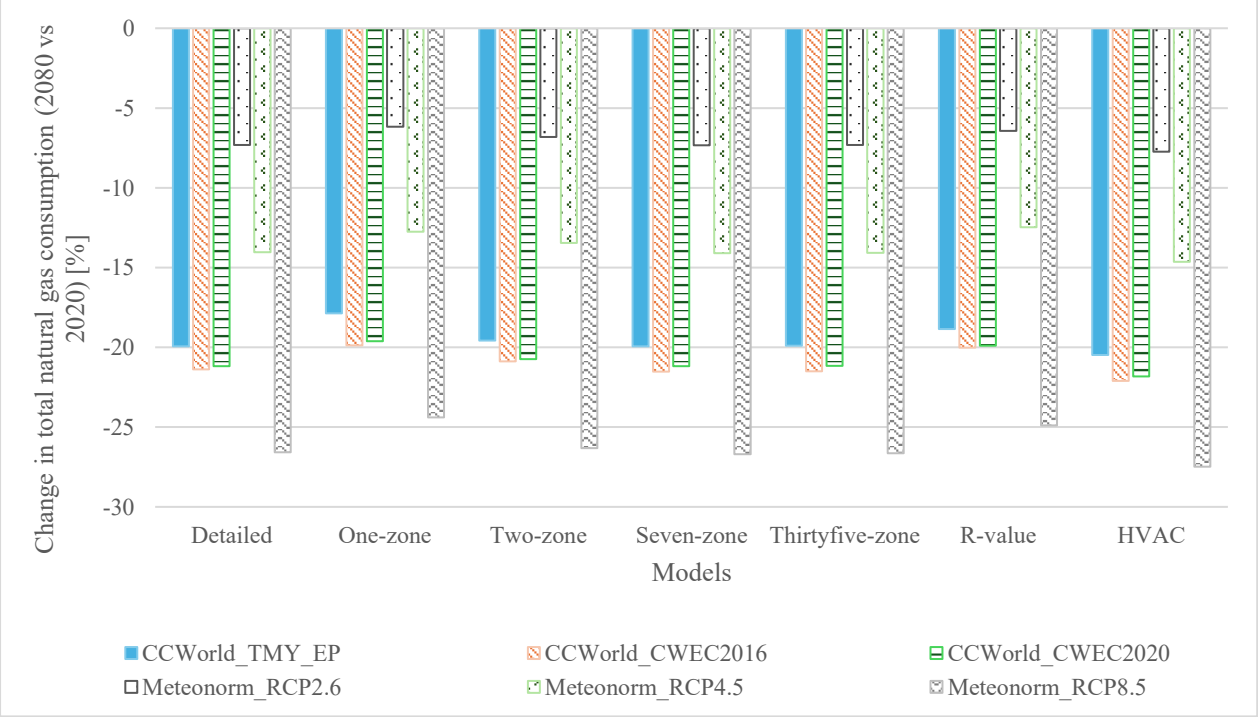

Figure 4-4: Projected change in total natural gas consumption (2080 vs 2020) across models and climate scenarios.

4.3.3 Model Performance Under Extreme Climatic Conditions

Model performance under boundary conditions was assessed by analyzing predicted heating demand during extreme hot and cold years, identified using the equivalent temperature-based

method. This investigation is especially relevant for long-term retrofit planning, where robustness to extremes is critical. The analysis identified 2020 as the hottest year, with a 4-day heat event from May 9 to 12, and 2010 as the coldest year, with a cold spell from February 4 to 7. These years represent the most thermally challenging conditions in terms of combined air and radiative loading, making them ideal candidates for stress-testing building models under non-typical boundary conditions. The annual frequency of 3-day (or longer) thermal events was also evaluated. Figure 4-5 shows that cold waves occurred regularly, with some years (e.g., 2013, 2015) experiencing up to three events. In contrast, heat waves were rare, with only 2009 and 2016 each registering one. This asymmetry highlights Ottawa's continued heating-dominated climate despite observed warming trends in Section 4.3.2.

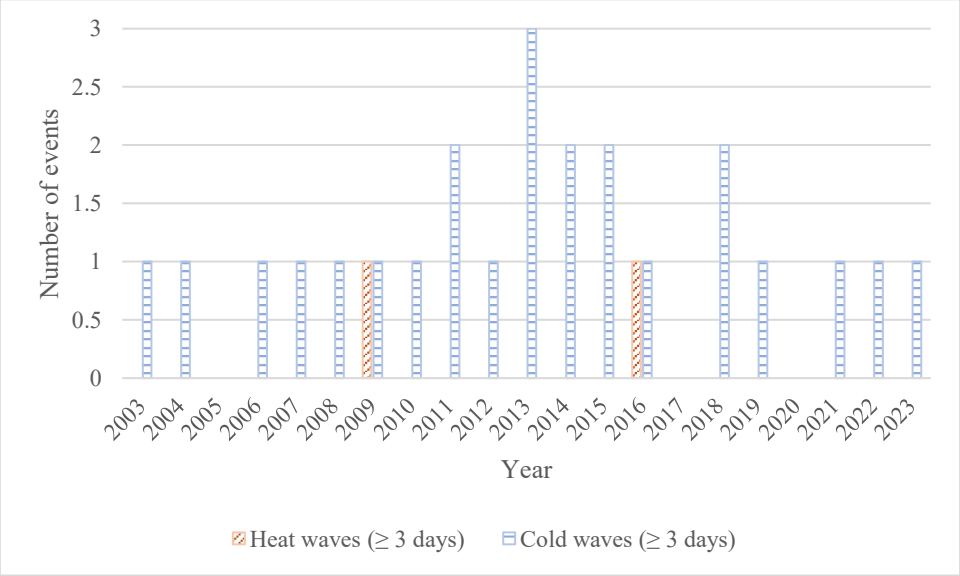

Figure 4-5: Annual frequency of heat and cold waves in Ottawa based on equivalent temperature (2003–2023).

Short-term behavior of simplified models under boundary climate conditions was further examined by analyzing hourly heating demand during the extreme cold period from February 4 to 7, 2010. This 96-hour window corresponds to the most thermally challenging cold wave in Ottawa over the past two decades, as determined by T_{eq} analysis. Figure 4-6 presents the hourly natural gas consumption predicted by the detailed model and six simplified configurations over four days. The detailed model reveals pronounced diurnal variations in gas

use, with peak heating demands exceeding 225 kWh during the early morning hours and troughs dropping below 150 kWh in the afternoon. By contrast, the one-zone model significantly underrepresents these fluctuations. Its predictions remain relatively flat, particularly during peak demand periods, where hourly consumption levels off around 173 kWh. This smoothing effect is attributed to the extreme spatial aggregation in the one-zone model, which neglects inter-zone thermal gradients and underestimates perimeter-zone losses. Over the 96-hour window, the one-zone model underpredicts peak demand by up to 52 kWh (24.1% underestimation at 6:00 AM on February 6), which limits its suitability for capturing short-term extremes. Across the entire cold event, the hourly load profiles of the two-, seven-, and thirty-five-zone models closely track the detailed model, capturing both the morning ramp-up and afternoon decline in heating demand.

The R-value simplified model consistently underestimates heating demand during off-peak periods by as much as 34%, particularly during midday hours when solar gains and internal loads help reduce space-heating needs. This underestimation is primarily due to the model's lack of thermal mass, which prevents it from capturing the delayed thermal response and heat storage effects inherent in real building materials. As a result, the model exhibits a more immediate energy use profile, failing to reflect how buildings with thermal mass can store heat during active heating hours and release it gradually throughout the day. As noted by Kosny [132], buildings with significant thermal mass cool down more slowly during setback periods and take longer to reach the heating setpoint after setback, shifting part of the energy demand to early and late hours. In contrast, the R-value model tends to overestimate heating during peak demand hours by up to 13% compared to the detailed model, due to its assumption that all heating must be supplied instantaneously to meet setpoints.

The HVAC-simplified model exhibits a relatively consistent underestimation of approximately 20% across various weather scenarios, as evident in both the hourly results (Figure 4-6). While

the magnitude of this error is notable, its consistency indicates a degree of predictability for this type of HVAC configuration. Such predictability can be useful in practice; however, the decision to use a simplified model ultimately depends on the practitioner's priorities, project type, the stage of the decision-making process, the acceptable level of risk, the availability of data, and the modeling team's expertise.

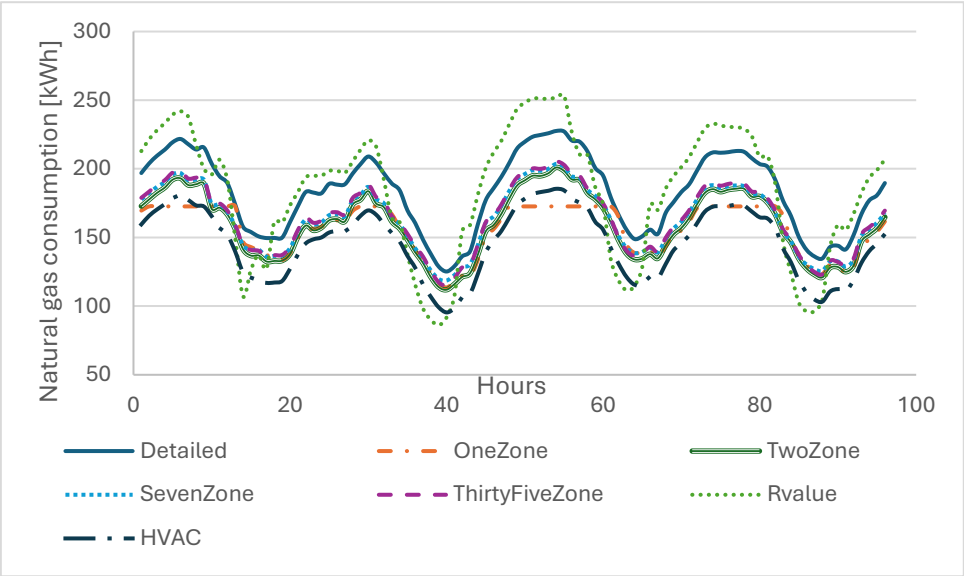

Figure 4-6: Hourly natural gas consumption comparison across detailed and simplified models during extreme cold conditions (Feb 4–7, 2010).

Under-sizing retrofit solutions based on underestimated peak loads can result in inadequate system capacity, increased risk of occupant discomfort, and additional stress on electrical grids during extreme cold events. In addition, utility pricing structures and demand-response programs increasingly depend on accurate peak demand estimation, so misrepresentation of peaks can lead to miscalculated economic outcomes for electrification strategies. Consequently, highly abstracted models, such as the one-zone configuration, should be interpreted with caution when peak demand predictions are central to the analysis. Mid-resolution models (two- and seven-zone) showed stronger agreement with the detailed model in capturing diurnal load fluctuations during extreme events, providing a more reliable balance between computational efficiency and accuracy. Simplified models remain useful for exploratory analyses and assessing long-term trends. However, for resilience planning, where

performance during short-duration but high-impact events is critical, such as in retrofit planning under electrification pathways, higher-fidelity models or the application of correction factors are necessary to address predictable underestimations in peak load predictions.

4.3.4 Comparative Evaluation of Optimization Outcomes

Despite global climate pledges, recent reports confirm that emissions continue to rise, aligning more with RCP 8.5 than with optimistic scenarios [133]. Accordingly, Meteonorm RCP 8.5 was selected to represent future climate conditions from 2025 to 2080. RCP 8.5 represents a high-emissions pathway aligned with current global trends, characterized by insufficient climate action and a continued failure to meet the Paris Agreement targets [134]. As discussed in Section 4.3.2 and illustrated in Figure 4-4, RCP8.5 leads to a substantial (~24–27%) reduction in heating demand due to accelerated warming. Notably, all simplified models in this study exhibit a similar percentage reduction in heating demand from 2020 to 2080 under the RCP8.5 scenario, suggesting their potential to approximate long-term climate-driven trends.

Figure 4-7 and Table 4-8 show that under RCP 8.5, Pareto-optimal retrofit solutions range from CAD 2.37 million to CAD 2.66 million in NPV, with total energy use declining from 41.2 GWh to 36.9 GWh and CO_2 emissions decreasing from 6.23 million kg to 5.46 million kg. These results indicate that an 11% increase in NPV enables an 11% reduction in energy consumption and a 14% reduction in emissions, demonstrating that significant environmental benefits can be achieved without prohibitive financial costs.

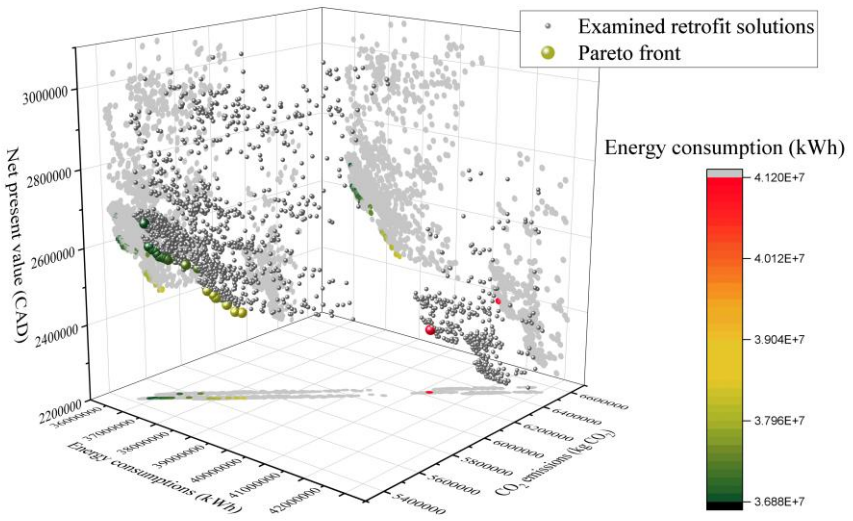

Figure 4-7: 3D Pareto front for solutions in the detailed model under the RCP 8.5 weather scenario.

Table 4-8: Statistical analysis on Pareto front optimal solutions in the detailed model under the RCP 8.5 weather scenario.

	Energy consumption [kWh]*10^3	CO_2 Emissions [kg]*10^3	NPV [CAD]*10^3
Minimum	36,890	5,464	2,370
Maximum	41,195	6,233	2,661
Mean	37,620	5,591	2,529
Median	37,219	5,573	2,560
Standard Deviation	853	148	65

Figures 4-8 and 4-9 compare the Pareto-optimal solutions obtained from each simplified and detailed model under the RCP 8.5 weather scenario (see Tables B.1–B.3). Zone aggregation models, including one-zone, seven-zone, and thirty-five-zone, shift the Pareto front downward and to the left under RCP 8.5, underestimating both energy use and retrofit costs. On average, these models predict 10–15% lower energy consumption and 5–11% lower NPV compared to the detailed front.

A secondary validation was performed to assess the predictive reliability of each simplified model. While the simplified models were used during the optimization process to identify Pareto-optimal retrofit configurations, each selected ECM package was subsequently re-simulated using the detailed model to evaluate accuracy. For each model, the average

percentage error between the simplified and detailed models was calculated across all Pareto-optimal solutions for NPV, EC, and OCE. The one- and two-zone models exhibited the largest deviations, underestimating NPV by 10.2% and 8.8%, respectively, and energy use by 14.6% and 13.7%, respectively. Additionally, they underestimated CO_2 emissions by 15.6% and 14.9%. The two-zone model also showed the widest range of outcomes among its Pareto-optimal solutions. The difference between the minimum and maximum NPV values exceeded 42%, compared to 12.3% in the detailed model. The wide NPV range observed in the two-zone model reflects its tendency to underpredict energy use, leading the optimization process to favor more aggressive, costly envelope upgrades. The R-value model shifts the Pareto front slightly upward, marginally overestimating both NPV and energy use. It demonstrates the lowest average deviation from the detailed model, with values below 2% across all metrics, indicating strong predictive accuracy. In contrast, the HVAC-ideal model significantly underestimates energy use (20.7%) and CO_2 emissions (26.6%), leading to overly optimistic performance projections. This level of abstraction fails to capture system-level inefficiencies, making it unsuitable for reliable retrofit planning.

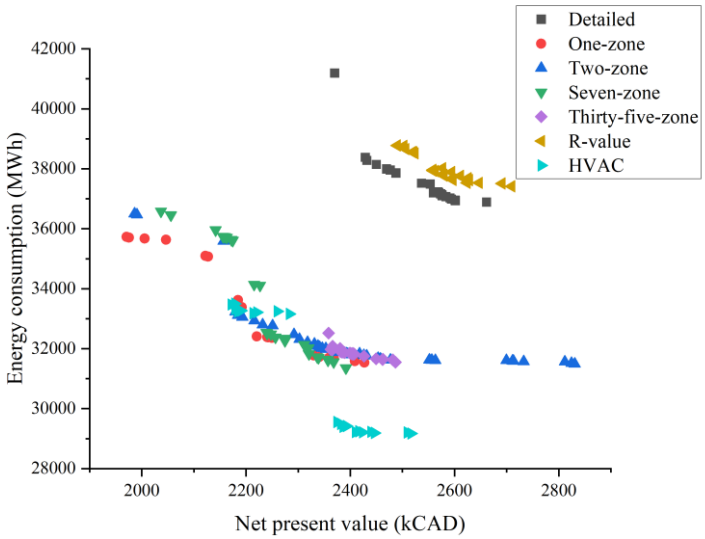

Figure 4-8: NPV-EC Pareto front solutions in the detailed and simplified models under the RCP 8.5 weather scenario.

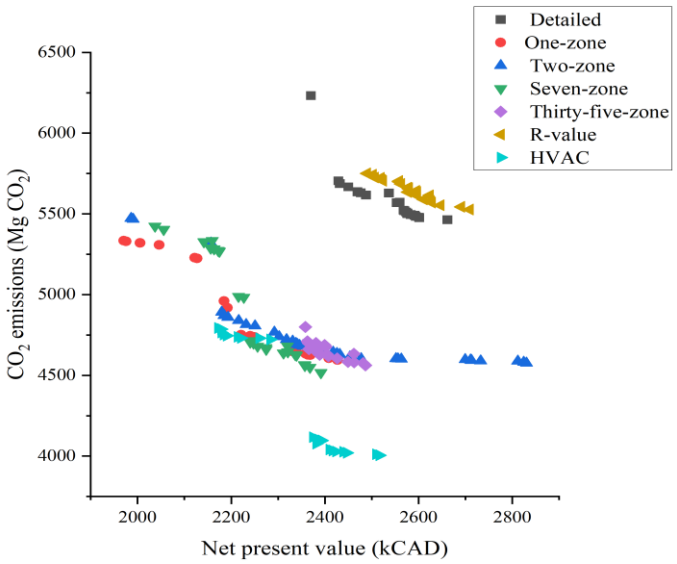

Figure 4-9: NPV-OCE Pareto front solutions in the detailed and simplified models under the RCP 8.5 weather scenario.

Model simplification introduces errors in energy performance predictions, which propagate into the objective function values. As a result, for the same building configuration, changes in objective function values can alter both the ranking of solutions and the identification of optimal solutions. As optimal solutions are sometimes only marginally better than near-optimal alternatives, even small errors, as observed in the previous sections, may influence which solutions are classified as optimal. It is therefore necessary to examine whether such changes in the selected solutions are substantial enough to affect decision-making. To quantify this effect, the analysis examines how frequently each decision variable is selected for retrofit across the optimization results of various simplified models.

Comparing Pareto-front selections between the detailed model and zone-simplified variants (one-, two-, seven-, and thirty-five-zone) reveals consistent prioritization of envelope upgrades. As shown in Table 4-9, exterior wall insulation in the residential building and roof upgrades in both buildings are selected in more than 99% of cases across all models, confirming their cost-effectiveness regardless of spatial simplification. However, the selection of basement wall insulation increases sharply, from just 2% in the detailed model to 39% in the simplified cases.

This shift suggests that lumped zoning tends to overestimate heat loss through below-grade assemblies by smoothing out temperature gradients between conditioned spaces and surrounding soil. Similarly, window retrofits are overrepresented, with mixed-use glazing selections increasing by 21.5 points and residential glazing selections increasing by 4.5 points. These deviations likely stem from the averaging of solar exposure, internal gains, and occupancy patterns across larger aggregated zones. In the detailed model, such variations create localized conditions that reduce the apparent benefit of glazing improvements. Once these dynamics are homogenized through simplified zoning, the perceived effectiveness of window upgrades is overstated.

The R-value simplified model aligns closely with the detailed model in envelope-related ECMs, with all major upgrades selected in 100% of solutions, demonstrating that simplifying material thermal properties does not alter the priority of the dominant retrofits. Window retrofits are slightly more frequent in the R-value model, at 64% versus 34% for mixed-use building windows and 86% versus 62% for residential building windows, suggesting that removing material variability marginally amplifies the benefits of glazing. In contrast, the HVAC-simplified model exhibits more pronounced deviations in basement and fenestration-related selections. While key exterior envelope measures remain prominent, the selection frequency for the exterior wall of the mixed-use building decreases from 96% to 72%, and basement wall selections increase from 2% in the detailed model to 30% and 18% for the two basement zones. Window upgrades also became nearly universal, rising to 98% and 100% for mixed-use and residential building windows, respectively. These shifts indicate that simplifying the HVAC system alters the balance between passive and active strategies. By replacing detailed system components with abstract representations, the model neglects part-load inefficiencies, distribution losses, and equipment-level performance variations. As a result, passive measures, especially those affecting thermal loads, appear more effective than

they would under realistic system operations, potentially leading to overestimated benefits in early-stage assessments. Overall, findings show that while simplified models tend to over-select measures in two of the decision variables, they provide reliable results for most others. This supports their use in the first stage of retrofit decision-making, where rapid exploration of multiple options is required. However, because simplified models may misrepresent the cost-effectiveness of specific ECMs, additional analysis is essential before final investment choices are made. At this stage, engineering judgment and rigorous cost analysis should guide decisions to ensure that retrofit budgets are allocated to the most impactful and robust measures.

Table 4-9: Percentage of Pareto-optimal solutions retrofitted with a specific option.

	Residential building [%]					Mixed-use building [%]				
	Floor	Roof	Basement wall	Exterior wall	Window	Floor	Roof	Basement wall	Exterior wall	Window
Detailed	0	100	2	100	34	0	100	2	96	62
Average of zone-simplified models	4	99	39	100	55.5	4	100	14.5	85	66.5
R-value	0	100	2	100	64	0	100	4	100	86
HVAC	0	96	30	100	98	0	100	18	72	100

The main benefits of model simplification include: (i) applicability in cases where detailed data are not available, (ii) reduction in model preparation effort and time, and (iii) shorter simulation runtimes [130]. In this study, the reductions in simulation time achieved by different simplification methods are compared. Table 4-10 reports the average optimization runtime for each model configuration. As expected, higher levels of zone simplification substantially reduced runtime, decreasing from approximately 39.8 hours for the detailed model to less than 2.5 hours for the most simplified configurations. The R-value model exhibited a runtime nearly identical to that of the detailed case, whereas the HVAC-simplified configuration required 16.8 hours, representing a notable reduction compared to the detailed baseline. However, simulation

runtime alone does not fully capture the total modeling effort. In practice, some of the most resource-intensive tasks involve collecting and cleaning building data as well as developing and calibrating the initial detailed model, particularly for large or complex buildings with many thermal zones and systems.

Table 4-10: Percentage of Pareto-optimal solutions retrofitted with a specific option.

	Detailed	One-zone	Two-zone	Seven-zone	Thirty-five-zone	R-value	HVAC
Time	39.8	2.1	2.3	3	5.7	39.3	16.8

4.4 Conclusion

To the best of our knowledge, this study is the first to quantify errors resulting from common model simplifications (zoning, material property, and HVAC) across actual, typical, extreme, and future climate files, and to investigate whether these errors persist after retrofit optimization under future extreme conditions. A multi-objective optimization using prNSGA-III examined the influence of simplification on both prediction accuracy and retrofit solution selection under a high-emissions scenario (RCP 8.5), considering net present value, total energy use, and operational carbon emissions. By employing established simulation and optimization tools, the analysis isolated the effects of model abstraction and weather assumptions, providing practical error ranges and guidance for selecting models that balance efficiency and reliability. The case study, a validated model of a five-story 1965 dormitory in Ottawa, shares the massing, envelope/system configuration, and area-to-volume ratios with typical mid-rise Canadian dwellings of the same period, thereby supporting the transferability of findings to similar building types.

Results show that the accuracy of simplified models may vary depending on the weather file used (actual, typical, extreme, or future climate). Highly abstracted models (one-zone) were the most weather-sensitive, underestimating cold-season heating by 8–22% across weather

files. In contrast, the thirty-five-zone model maintained narrower, more stable error bands across the same inputs. All models showed increased errors during transitional months, while highly simplified versions overestimated loads, as removing thermal mass increased diurnal peaks and seasonal energy use. Restoring interior mass improved the one- and two-zone variants, and assigning a high-mass envelope reduced errors in the R-value-only model. The HVAC-simplified variant consistently underpredicted heating because it omits distribution losses, cycling/defrost penalties, and part-load inefficiencies.

Under extreme climate conditions, simplified models displayed limitations in representing short-term thermal dynamics and hourly heating fluctuations. The one-zone model, which cannot represent inter-zone gradients and dynamic behavior, underestimated peak hourly heating demand by up to 24.1%. The R-value model exhibited a dual-error pattern, with overestimation during the morning ramp-up and underestimation at midday, primarily because of the missing thermal mass. In contrast, mid-resolution models, such as the seven- and thirty-five-zone variants, more closely matched detailed model behavior. These findings suggest that since peak and hourly errors are decision-critical for grid integration and demand planning, simplified models are useful for identifying trends, but capacity sizing and demand-response commitments should rely on mid- to high-fidelity models.

In multi-objective retrofit optimization, simplified models altered the Pareto front, with the one-zone model underestimating energy use and lifecycle costs by 10–15%, thereby affecting ECM ranking and selection. The R-value model demonstrated the highest accuracy, with errors of less than 2% for cost, energy, and emissions. In contrast, the HVAC-simplified model underestimated energy demand by 20.7% due to unaccounted system inefficiencies. Although simplified models are effective in capturing broad optimization trends, they can misrank individual retrofit strategies and should be interpreted cautiously for building-level decisions. Their strengths lie in exploratory, pre-screening, and large-scale scenario analyses, where rapid

comparison of multiple options is needed. For final investment decisions, promising ECMs identified by simplified models should be validated using detailed models and known error ranges. Ultimately, the choice of simplification strategy should reflect the availability of data, the analysis context, and project requirements. When detailed material data are available, explicit modeling is preferable to an R-value approach. HVAC systems can often be reasonably simplified in early or envelope-focused planning, while zoning simplifications are most reliable when mid-resolution models are used rather than highly abstracted ones.

The results of this study can inform analyses in heating-dominated regions, such as Northern Europe. Although the specific outcomes may not be directly applicable to countries with climatic conditions substantially different from Canada's, the findings still provide valuable insights across diverse contexts. Deviations in simplified models were most pronounced during transition months, when thermal mass and system dynamics had a stronger influence. Comparable challenges are expected in mixed or cooling-dominated climates, including those in Southern Asia, North Africa, and other warm regions, where models must capture both heating and cooling loads. In particular, R-value–based models may be less suitable for cooling-dominated climates, as they neglect thermal inertia, which plays a crucial role in moderating indoor temperatures and peak loads [135]. As climate change increases the frequency and intensity of heatwaves, future research should also assess the ability of simplified models to predict thermal comfort and overheating risks, especially in buildings with low thermal mass or limited passive cooling strategies. Expanding this framework across multiple case studies with different building types, occupancy patterns, construction characteristics, and weather scenarios could further support statistical decision-making and risk analysis in large-scale retrofit.

Chapter 5: Enhancing Retrofit Optimization with ANN-Corrected Simplified Building Energy Models

This chapter is ready to be published as:

- Article 4: Y. Dadras, F. Mostafazadeh, M. Kavgic, M. Ghobadi, Improving the Accuracy of Simplified Building Energy Models Using Neural Networks in Retrofit Decision-Making: *Submitted to Applied Energy*.

5.1 Introduction

Energy model simplification plays an important role in accelerating simulation-based optimization, yet these abstractions often introduce prediction biases that can affect the selection and evaluation of retrofit measures. While previous chapters examined the trade-offs between computational efficiency and accuracy under various simplification strategies, improving the reliability of simplified models without increasing their complexity remains a key challenge. This chapter introduces a neural network–based adjustment method that enhances the predictive performance of simplified models while preserving their structure. The approach generates external corrections to hourly heating and electricity profiles and can be integrated directly into optimization workflows. The methodology, results, and implications for retrofit decision-making are presented in the following sections.

5.2 Methodology

This chapter employs an innovative approach to enhance the accuracy of retrofit decision-making by integrating ANNs within an SBMO framework. Building upon methodologies adapted from prior studies [130,136], this study uniquely addresses the challenge of aligning simplified model outputs with actual building performance data, ensuring computational efficiency without compromising accuracy. Multi-Layer Feedforward Neural Networks

(MFNNs), also known as Multilayer Perceptrons (MLPs), are adopted due to their demonstrated suitability and flexibility for building performance simulation tasks, as noted by [75]. Their capacity to represent complex, nonlinear relationships makes them well suited for correcting discrepancies caused by simplification. After training and validation, the ANN is integrated into the optimization workflow to dynamically adjust the simplified model outputs, providing a consistent and reliable foundation for evaluating energy conservation measures (ECMs).

Figure 5-1 outlines the five key phases of the proposed methodology framework. In Phase 1, an initial detailed energy model of the case study buildings (chapter 2, sections 2.1.2 and 2.1.3) was developed based on audit data, establishing a baseline case with accurate energy performance data. Phase 2 involved creating simplified models using three techniques: thermal zoning abstraction, HVAC idealization, and material property adjustments (chapter 2, section 2.2). Phase 3 involved training and evaluating the MFNN using hourly data from the simplified model, including electricity and natural gas consumption, along with weather inputs such as temperature, global horizontal irradiance, relative humidity, and wind speed. The detailed model's hourly energy consumption served as the target output for network learning. Phase 4 defined the environmental and economic objectives, specifically minimizing total energy consumption (EC), net present value (NPV), and carbon emissions (CE), and introduced decision variables into the baseline model to create a parametric model. Finally, in Phase 5, the trained and validated ANN was integrated into the multi-objective optimization algorithm (prNSGA-III) to refine the simplified model outputs during the evaluation of retrofit scenarios. This integration enabled the identification of Pareto-optimal solutions while maintaining a balance between accuracy and computational efficiency and accounting for uncertainties inherent in simplified model predictions. Through this methodology, the study enhances the reliability of simplified models and provides a pathway for their practical application in large-

scale, computationally intensive retrofit decision-making scenarios. The case study follows the methodology described in Sections 2.1.2 and 2.1.3; the building simplification methods align with Section 2.2; and the weather generation approach corresponds to Section 4.2.1.1.

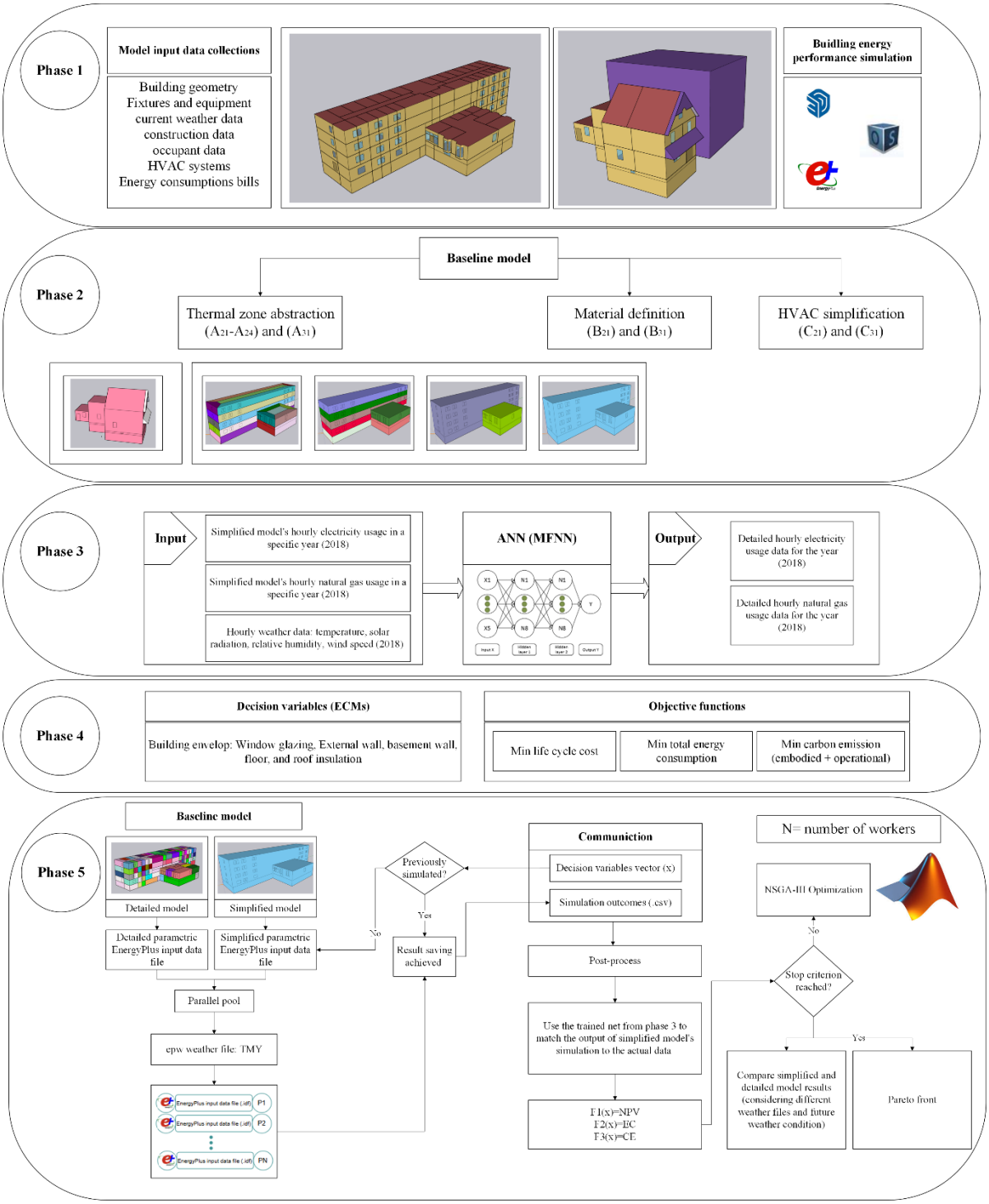

Figure 5-1: Methodology framework (Chapter 5).

5.2.1 Artificial Neural Network

Artificial Neural Networks (ANNs) were used in this study to improve the predictive accuracy of simplified building energy models by learning the nonlinear relationships between simplified model's outputs, weather conditions, and the corresponding detailed model results. Consistent with the formulation presented by Haykin [137], an ANN comprises interconnected processing units arranged in layers and trained to approximate complex functional relationships.

The ANN architecture adopted in this work is a multilayer feedforward neural network (MFNN), also referred to as a multilayer perceptron (MLP) (see Figure 5-2). This network type is widely used in surrogate modeling and energy prediction tasks due to its universal approximation capability [138]. The MFNN implemented here consists of an input layer, two fully connected hidden layers with eight neurons each, and an output layer, with *tanh* activation functions applied in the hidden layers to capture nonlinear patterns. The output layer uses a linear activation, appropriate for continuous regression targets.

Separate networks were trained for electricity and natural gas, reflecting their distinct patterns and weather sensitivities. For each ANN, the input vector included the hourly simplified model output and four weather variables (dry-bulb temperature, relative humidity, global horizontal irradiance, and wind speed). All training data were based on hourly data from 2018, ensuring consistent temporal alignment across simplified, detailed simulations, and weather inputs. The target variable for each network was the corresponding hourly output from the detailed model.

The datasets were randomly partitioned into 70% training, 15% validation, and 15% testing subsets, ensuring robust generalization while preventing overfitting. Both models were trained with the Adam optimizer for 50 epochs, using a mini-batch size of 128. Training progress was

monitored via validation loss, and training was terminated when performance plateaued, preventing unnecessary iterations.

The MATLAB Deep Learning Toolbox was used to implement the network, and the trained models, along with their normalization parameters, were saved for integration into the optimization framework [139]. The performance of each ANN was evaluated using common regression metrics, namely Mean Squared Error (MSE), Root Mean Squared Error (RMSE), and the coefficient of determination (R^2), defined as:

$$MSE = \frac{1}{n}\sum_{i=1}^{n}(y_i - \hat{y})^2 \quad \text{Equation 5-1}$$

$$RMSE = \sqrt{\frac{1}{n}\sum_{i=1}^{n}(y_i - \hat{y})^2} \quad \text{Equation 5-2}$$

$$R^2 = 1 - \frac{\sum(y_i - \hat{y})^2}{\sum(y_i - \bar{y})^2} \quad \text{Equation 5-3}$$

Where $\hat{y}$ is the predicted value of y, and $\bar{y}$ is the mean value of y.

This ANN configuration provides a balance between computational efficiency and predictive capability, enabling effective correction of simplified model outputs without altering the physical structure of the underlying energy model.

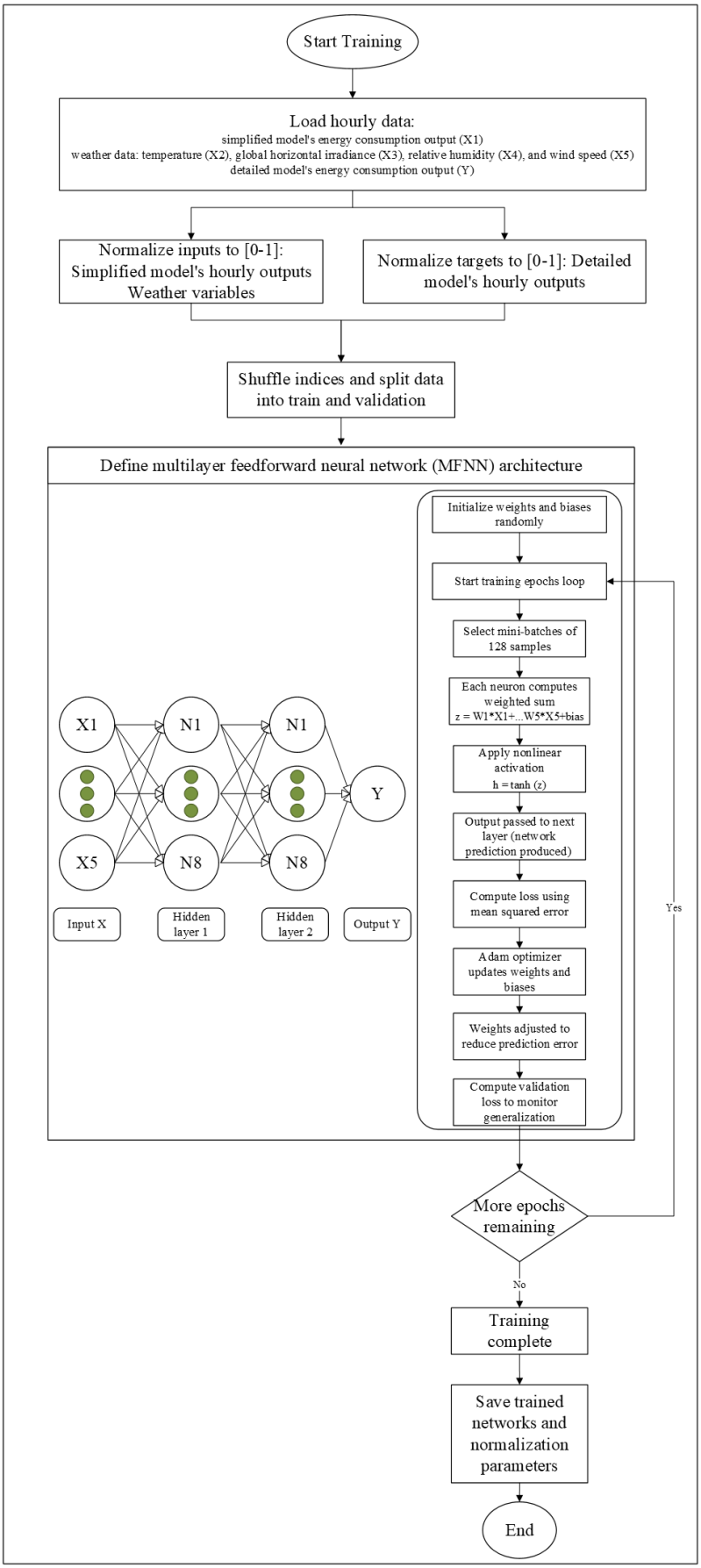

Figure 5-2: MFNN architecture and training workflow used for correcting simplified model outputs.

5.2.2 Objective Functions

This chapter integrates environmental and economic objectives to evaluate energy retrofit scenarios. Environmental performance is assessed by minimizing total operational energy consumption (EC) and life cycle carbon emissions (CE), while economic feasibility is evaluated through Life Cycle Cost (LCC) over a 55-year service life (2025–2080) [77,78,80,81,83,90,92,112]. The study defines EC as the total annual input of electricity and natural gas. CE is derived by applying the National Research Council Canada's conversion factors of 0.185 kg CO_2/kWh (natural gas) and 0.0579 kg CO_2/kWh (electricity) [113]. These operational emissions are combined with embodied carbon values derived from Athena to account for cradle-to-grave impacts, ensuring that both operational and material-related emissions are represented in the assessment [140]. Energy simulations are conducted in EnergyPlus using TMY weather files. The total environmental impact is expressed in Equations 5-4 and 5-5.

$$EC = \sum_i^n (EC_i + GC_i) \quad \text{Equation 5-4}$$

$$CE = \sum_i^n (EC_i \cdot EF_{elec} + GC_i \cdot EF_{gas}) + ECO_2 \quad \text{Equation 5-5}$$

where EC_i and GC_i are electricity and natural gas consumption in year i, and EF_{elec} and EF_{gas} are the emission factors for electricity and natural gas, respectively and ECO_2 is the embodied carbon.

To determine the economic viability of the interventions, the study calculates the Life Cycle Cost (LCC) over 55 years, from 2025 to 2080. This calculation combines the upfront retrofit investment with the net present value of projected energy expenditures. A constant-dollar approach is employed, using a real discount rate to account for economic changes independent of general inflation. The LCC is defined using Equation 5-6.

$$LCC = I + \sum_j (E_j^{elec}.q_j.C_{elec} + E_j^{gas}.q_j.C_{gas}) \quad \text{Equation 5-6}$$

where I is the initial investment cost of retrofit measures, E_j^{elec} and E_j^{gas} represent the estimated annual electricity and gas consumption (in kWh/year) for decade j, q_j is the present value factor for decade j, and C_{elec} and C_{gas} are the base-year (2025) unit costs of electricity and natural gas, respectively. The present value factor q_j discounts a stream of escalating annual costs over 55 years is calculated using the Modified Uniform Present Value (UPV*) represented in section 4.2.2.

5.2.3 ANN- Integrated Multi-Objective Optimization

The multi-objective optimization framework is designed to assess and improve the accuracy and computational efficiency of simplified building energy models, while simultaneously identifying optimal retrofit ECMs. The approach integrates trained ANNs into the optimization process, enhancing the accuracy of simplified models' predictions for retrofit scenarios and enabling an efficient exploration of the decision space. The optimization focused on minimizing EC, CE, and NPV while ensuring that the selected retrofit strategies improve energy efficiency compared to the baseline case ($EC \leq EC_0$). In this regard, a modified version of the NSGA-III algorithm, prNSGA-III [52], was employed due to its robustness in solving multi-objective optimization problems.

In this implementation, prNSGA-III was implemented in MATLAB, and the trained neural networks were incorporated directly into the evaluation of each candidate retrofit solution. The optimization begins by generating a population of decision vectors, which are passed to a communication module that automatically updates the parametric EnergyPlus model and produces the corresponding input files (.idf). EnergyPlus simulations are then run to obtain hourly simplified-model predictions of natural gas and electricity consumption.

Immediately after each simulation, the trained ANNs are invoked to adjust these simplified predictions. For every candidate solution, the simplified hourly outputs and concurrent weather

variables are fed into the trained electricity and natural gas networks. The networks return adjusted energy-use values that approximate the detailed model's response without requiring a full simulation. MATLAB then uses the ANN-adjusted outputs to evaluate the environmental and economic objective functions, rather than relying on the raw simplified results.

prNSGA-III iteratively refines the population by evaluating each solution with this ANN-enhanced prediction workflow until the termination criterion, defined as the maximum number of generations, is reached. The outcome is a Pareto front of optimal retrofit solutions, with trade-offs evaluated using ANN-adjusted performance estimates. This workflow enhances the accuracy and stability of the optimization process while preserving the computational efficiency gained from model simplification.

The genetic algorithm was configured with a population size of 50 individuals. Based on recommendations from prior literature [127–129], the crossover and mutation rates were set to 0.4 and 0.7, respectively. These parameters were selected to achieve an optimal trade-off between thorough exploration of the search space and computational efficiency. All simulations were conducted on a workstation equipped with an Intel Core i9 processor (2.60 GHz, 24 MB cache).

5.2.4 Evaluation Framework for Simplified Models

The dormitory building was represented using several abstraction levels derived from the methodological foundations in Chapter 2. These included reductions in spatial resolution through zoning aggregation (A_{21}–A_{24}), the replacement of detailed HVAC configurations with an idealized representation (B_{21}), and simplified envelope constructions that retain only overall thermal resistance (C_{21}). Because the dormitory is a large, highly zoned, and computationally intensive model, these abstraction levels were essential for reducing simulation time while maintaining the inputs required for retrofit analysis. In contrast, the single-family house, which

is considerably smaller and less complex, served as a complementary case to examine how simplification affects buildings with minimal functional diversity. Together, these models provide a balanced basis for evaluating the trade-offs between accuracy and efficiency across different simplification strategies.

To investigate how these simplifications influence retrofit decision-making, the optimization process was executed using the ANN-adjusted simplified model rather than the raw simplified outputs. The trained ANN generated adjusted hourly predictions of natural gas and electricity for each candidate solution, and these adjusted values were used to compute the environmental and economic objective functions. The retrofit measures evaluated during optimization correspond to the ECMs listed in Table 4-2, which include options for improving envelope insulation, upgrading window systems, and adding cooling capacity where appropriate. After identifying the optimal ECM sets, the selected measures were re-simulated using the detailed model. This post-processing step enabled a direct comparison among simplified, ANN-adjusted, and detailed predictions over the 55-year evaluation horizon, with deviations quantified using Equation 4-8.

5.3 Results and Discussion

5.3.1 Impact of Building Complexity on Simplification Errors

In large and mechanically complex buildings, model simplification can introduce substantial inaccuracies because diverse zone functions, heterogeneous internal loads, and intricate HVAC interactions influence thermal behavior. This effect was clearly observed in Case Study 2, the dormitory building, where reductions in spatial resolution, zone aggregation, and HVAC idealization introduced noticeable deviations in hourly, monthly, and annual predictions of natural gas and electricity consumption, as illustrated in Figures 5-3 and 5-4. As shown in Section 4.3, these deviations propagated directly into the retrofit optimization process, since

the objective functions are calculated from energy consumption metrics. Consequently, simplification affected not only the predicted performance of candidate retrofit packages but also the selection of optimal energy conservation measures.

The behavior of the R-value-based material simplification used in case study 1 provides additional insight into the effects of reducing envelope detail. In this approach, all envelope assemblies were replaced with massless layers that preserve only the overall thermal resistance. While this approach substantially reduces modelling complexity, it removes the building's thermal storage capacity. As shown in [136], the annual predictions remain generally consistent with the detailed model; however, the hourly load profile exhibits clear deviations because the simplified construction cannot buffer heat or moderate fluctuations in outdoor conditions. This behaviour is evident in Figure 5-5, where the R-value model produces elevated heating demand across most hours and exhibits a steeper response during peak heating periods.

These discrepancies arise from the lack of thermal inertia. Since massless layers cannot store or release heat, the model responds immediately to changes in temperature. This creates two characteristic effects. First, during early-morning and peak-load hours, the simplified model overestimates natural gas demand because it assumes that all heating must be supplied instantaneously to meet the indoor setpoint. Second, during midday and shoulder-season hours, the simplified model fails to capture the delayed heat-release behaviour typical of real, massive constructions. As highlighted by Kosny [132], buildings with appreciable thermal mass cool down more slowly during setback periods and exhibit a smoother, shifted heating profile—patterns that the R-value model cannot reproduce.

To address these limitations, a hybrid material correction method was applied. Instead of reintroducing full, multi-layer constructions, a hypothetical material was defined that maintains the same overall R-value but includes realistic density and heat capacity parameters

representative of the dominant mass in the actual assembly. Assigning this material to the envelope reinstates thermal storage effects while preserving the simplicity that makes the R-value approach attractive for early-stage modelling. As shown in Figure 5-5, the hybrid model substantially improves agreement with the detailed hourly profile, reduces peak-time overestimation, and more accurately reflects the diurnal variation in heating demand. Furthermore, this adjustment reduced the annual energy deviation. The original R-value model differed from the detailed model by 5.3%, while the hybrid configuration reduced this difference to only 0.73%.

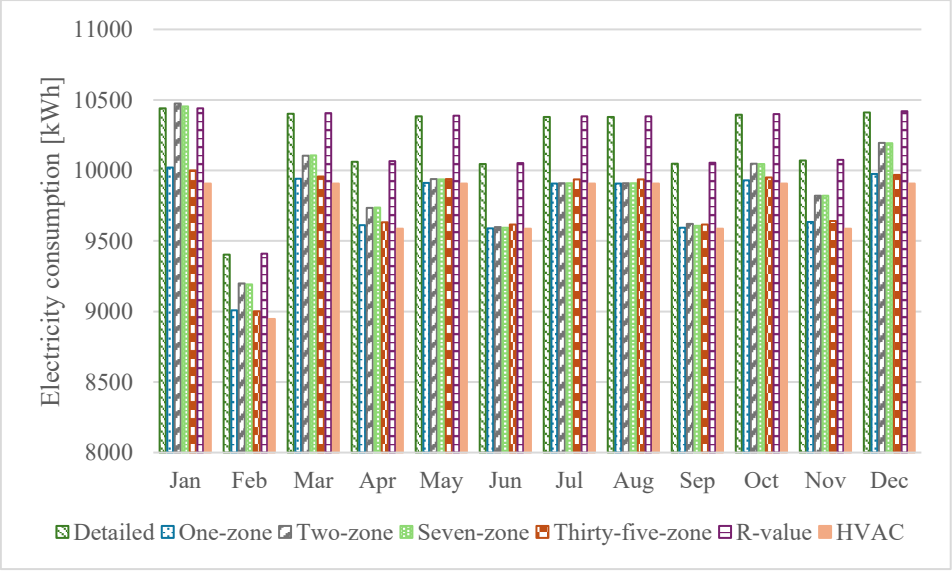

Figure 5-3: Monthly electricity consumption comparison between detailed and simplified models in the dormitory building.

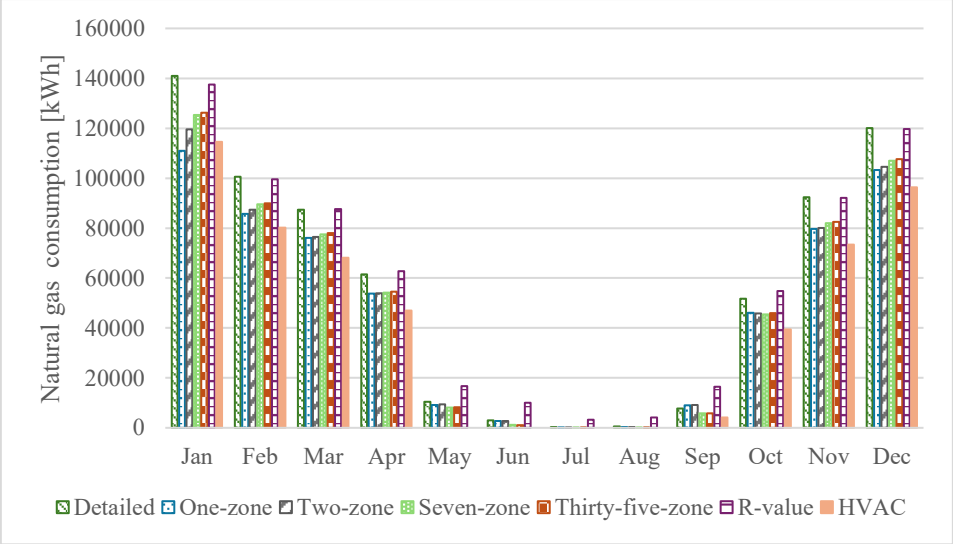

Figure 5-4: Monthly natural gas consumption comparison between detailed and zone-simplified models in the dormitory building.

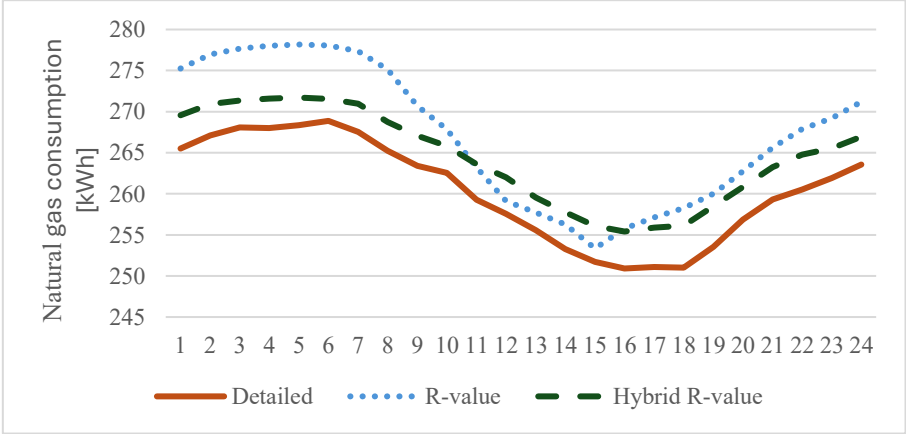

Figure 5-5: Hourly natural gas consumption comparison across detailed, R-value, and Hybrid R-value simplified models during extreme cold conditions (Jan 6th, 2018).

The single-family house, characterized by minimal functional diversity and a simple thermal configuration, showed only minor differences between the zone-simplified and detailed models (see Figures 5-6 and 5-7). The annual electricity consumption obtained from the detailed model was 2,204 kWh in 2022, and the corresponding zone-simplified model produced a value that was only 2.4% lower. Natural gas use followed the same pattern. The detailed model predicted an annual demand of 56,684 kWh, whereas the simplified configuration yielded a result

approximately 6% lower. These differences remain relatively small and fall within acceptable calibration thresholds for residential buildings with uniform thermal behavior. Part of this discrepancy can be attributed to thermophysical mechanisms identified in prior research. Previous studies [15,73] demonstrated that simplified models tend to underestimate heating energy use, particularly during colder months. When spatial resolution is reduced, internal surfaces experience elevated convective heat gains, which increases the effective convection coefficient. This strengthens heat transfer to the envelope and heightens conductive losses to the outdoor environment. As a result, heating demand in simplified models is underestimated relative to more detailed zoning configurations. Moreover, statistical indicators aligned with the observed level of consistency between the two models. The CV(RMSE) was 11.35% for natural gas and 3.6% for electricity, and the NMBE values were 6% for natural gas and 2.3% for electricity. These results indicate that the simplified one-zone model accurately represents the thermal behavior of small residential buildings.

Because of this close agreement, the single-family house does not require adjustment of the artificial neural network for the simplified zoning and envelope configurations, and these models can be used directly in the optimization process without reducing result quality. The HVAC simplified configuration, however, behaves differently as shown in Figures 4-5 and 5-5. Idealizing the mechanical system results in noticeably larger deviations in natural gas and electricity consumption, leading to greater discrepancies in the objective function values compared to the detailed model. This systematic underestimation indicates that the simplified HVAC representation omits key aspects of system behaviour that influence heating and electricity demand. As a result, the HVAC simplified model requires an ANN adjustment to achieve reliable predictions and restore consistency with the detailed benchmark.

Overall, these results demonstrate that the requirement for ANN adjustment is directly correlated with building typology and system complexity. In the case of the dormitory, the

combination of a large floor area, diverse internal loads, and intricate mechanical systems necessitates ANN correction for all investigated simplification strategies, excluding the R-value modification. However, the single-family house remains accurate under zoning and thermal resistance simplifications, requiring correction only when the HVAC system is idealized.

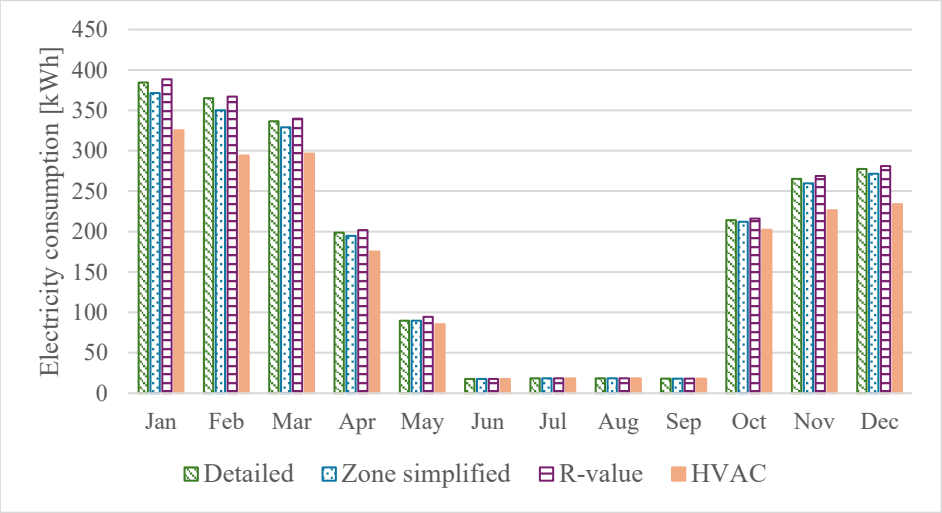

Figure 5-6: Monthly electricity consumption comparison between detailed and simplified models in single-family house.

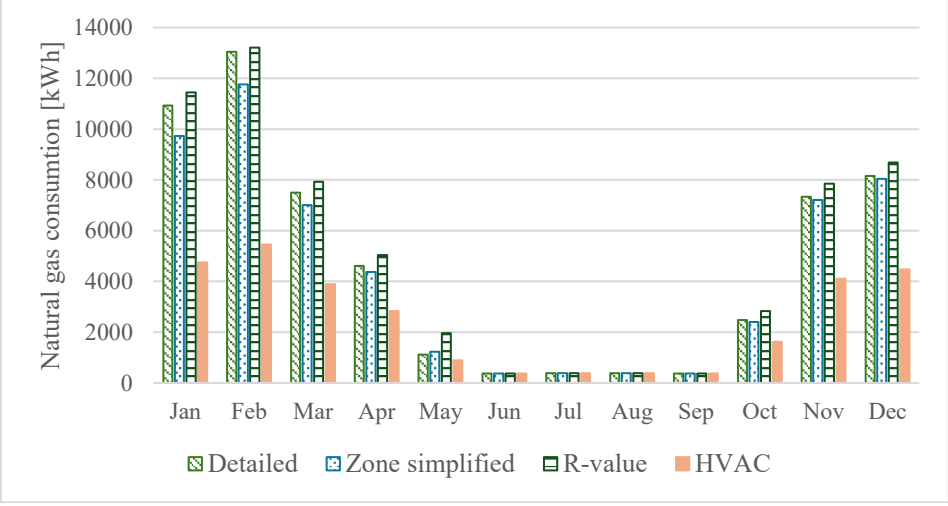

Figure 5-7: Monthly natural gas consumption comparison between detailed and zone-simplified models in a single-family house.

These results demonstrate that the requirement for ANN correction is directly correlated with building typology and system complexity. For the dormitory, the combination of a large floor

area, diverse internal loads, and intricate mechanical systems necessitates ANN correction for all investigated simplification strategies, except for the R-value modification. However, the single-family house remains accurate under zoning and thermal resistance simplifications, requiring correction only when the HVAC system is idealized.

5.3.2 ANN Training Performance

The artificial neural networks developed for the dormitory building were trained using the hourly 2018 dataset, which included simplified model outputs and four exogenous weather variables (dry-bulb temperature, relative humidity, global horizontal irradiance, and wind speed). The dataset was randomly divided into 70% for training, 15% for validation, and 15% testing to ensure robust generalization and avoid overfitting. Separate networks were trained for electricity and natural gas, each using the MFNN architecture described in Section 5.2.

The performance metrics for electricity and natural gas prediction are presented in Tables 5-1 and 5-2, respectively. The results demonstrate that the ANN models learned the relationships between simplified outputs, weather drivers, and detailed model energy use with high accuracy across all simplification levels. For the thirty-five-zone model, which has the highest physical fidelity among the simplified configurations, RMSE values were approximately 4.2 kWh for the training set, 4.1 kWh for the validation set, and 4.4 kWh for the test set. These errors are small relative to the detailed model's hourly natural gas load, which ranges from 34 to 273 kWh during colder months, with a colder-month mean of 149 kWh. Corresponding MSE values (17.4, 17.2, and 19.1 kWh^2) reflect the squared magnitude of these deviations. R^2 values were greater than 0.996 for all data subsets, indicating that more than 99% of the variance in the detailed model was captured.

As model abstraction increased, errors rose moderately but remained within acceptable bounds. For the seven-zone and two-zone models, RMSE values ranged from 5.2 to 5.8 kWh, with R^2

values near 0.995. Even for the more reduced one-zone configuration, the RMSE remained between 7.6 and 8.1 kWh, with R^2 values greater than 0.988. The HVAC-simplified model showed slightly higher errors, with RMSE values of 8.5-9.1 kWh, yet the R^2 values still exceeded 0.985, confirming reliable predictive capability. Overall, the results confirm that the MFNN architecture effectively captures the nonlinear relationships between simplified model outputs, weather inputs, and the detailed model's hourly energy use.

Table 5-1: Performance of ANN models for electricity prediction across different model simplifications using MSE, RMSE, and R^2.

	Train			Validation			Test		
	MSE $[kWh]^2$	RMSE [kWh]	R^2	MSE $[kWh]^2$	RMSE [kWh]	R^2	MSE $[kWh]^2$	RMSE [kWh]	R^2
Thirty-five zone	0.0526	0.2294	0.9991	0.0555	0.2356	0.9990	0.0441	0.2100	0.9992
Seven zone	0.0448	0.2117	0.9992	0.0417	0.2041	0.9993	0.0465	0.2155	0.9991
Two zone	0.0566	0.2379	0.9990	0.0607	0.2463	0.9980	0.0647	0.2543	0.9989
One zone	0.0404	0.2009	0.9993	0.0394	0.1986	0.9993	0.0388	0.1969	0.9993
HVAC	0.0859	0.2931	0.9985	0.0833	0.2886	0.9985	0.0839	0.2897	0.9986

Table 5-2: Performance of ANN models for natural gas prediction across different model simplifications using MSE, RMSE, and R^2.

	Train			Validation			Test		
	MSE $[kWh]^2$	RMSE [kWh]	R^2	MSE $[kWh]^2$	RMSE [kWh]	R^2	MSE $[kWh]^2$	RMSE [kWh]	R^2
Thirty-five zone	17.4299	4.1749	0.9968	17.2136	4.1489	0.9970	19.1255	4.3733	0.9968
Seven zone	28.0199	5.2934	0.9950	28.3253	5.3222	0.9949	26.8195	5.1788	0.9951
Two zone	31.0045	5.5682	0.9945	28.9333	5.3790	0.9948	33.0936	5.7527	0.9942
One zone	64.8338	8.0519	0.9885	60.2864	7.7644	0.9888	58.2982	7.6353	0.9897
HVAC	75.7736	8.7048	0.865	72.0057	8.4856	0.9872	82.1292	9.0625	0.9856

5.3.3 Accuracy Improvement of Monthly Predictions in ANN-Corrected Models

The influence of the ANN-adjustment on monthly outputs was assessed by examining two representative retrofit solutions: the configuration yielding the lowest life-cycle cost (economic-optimal case) and the configuration minimizing life-cycle carbon emissions and total energy use (environmental-optimal case). For each of the five simplified dormitory models, monthly natural gas and electricity loads were compared across three datasets: raw simplified outputs, ANN-adjusted predictions, and detailed-model results, as illustrated in Figure 5-8. Accuracy was evaluated using monthly CV(RMSE) and NMBE values.

The results show a consistent and substantial improvement once the ANN adjustments are applied. Table 5-3 summarizes the monthly CV(RMSE) and NMBE for natural gas across all models and both retrofit solutions. In the economic-optimal case, the raw simplified models exhibited CV(RMSE) values ranging from 14.6% to 34%, depending on the level of abstraction, with NMBE values as high as 27.47% in the HVAC simplified model. After applying the ANN-adjustment, the errors dropped dramatically across all models. The thirty-five-zone case's CV(RMSE) improved from 14.6% raw to 0.34% adjusted, and similar trends were observed across other simplifications, such as the one-zone model where CV(RMSE) fell from 18.30% to 10.69% and NMBE decreased from 13.07% to -7.78%. The HVAC-simplified configuration showed the most pronounced correction, with CV(RMSE) decreasing from 34% raw to 5.3% adjusted.

A similar pattern appeared in the environmental-optimal case. Raw simplified predictions produced CV(RMSE) values between 18.5% and 30.95%, with NMBE values ranging from 13.8% to 25.08%, indicating both substantial random error and pronounced bias. After ANN-adjustments, monthly CV(RMSE) values dropped from 18.8 to 1.39% for the thirty-five-zone model and from 30.95% to 3.77% for the HVAC model. NMBE values also enhanced, with

improvements such as 15.18% raw to 0.98% adjusted for the thirty-five-zone model and 25.08% raw to -2.39% adjusted for the HVAC model.

These corrections demonstrate several key outcomes. First, the ANN effectively captured nonlinear interactions between retrofit-driven changes, outdoor conditions, and the detailed thermal response of the building, relationships that simplified physics-based models alone cannot reproduce. Second, accuracy improvements were strongest for highly abstracted models, indicating that the ANN provides the greatest benefit where simplification removes essential thermal or operational dynamics. Overall, the ANN serves as an effective correction layer that substantially enhances hourly and monthly accuracy across all simplified configurations. This improved fidelity forms a more reliable basis for annual calculations and objective-function evaluations within the optimization process.

Table 5-3: Monthly CV(RMSE) and NMBE [%] of natural gas consumption for ANN-adjusted and raw simplified models at the minimum-cost and minimum-environmental-impact Pareto-optimal solutions.

	Min cost				Min environmental impact			
	CV(RMSE)		NMBE		CV(RMSE)		NMBE	
	Adjusted	Raw	Adjusted	Raw	Adjusted	Raw	Adjusted	Raw
Thirty-five zone	0.60%	3.82%	-0.14%	3.81%	0.64%	3.69%	-0.27%	3.69%
Seven zone	0.64%	0.03%	-0.25%	2.8%	0.68%	3.24%	0.03%	3.14%
Two zone	0.74%	3.01%	-0.50%	2.74%	0.90%	3.17%	-0.2%	3.06%
One zone	0.80%	3.94%	-0.62%	3.93%	0.81%	3.98%	-0.58%	3.97%
HVAC	0.71%	4.07%	-0.64%	4.07%	0.49%	4.31%	-0.39%	4.31%

Min cost	Min environmental impact

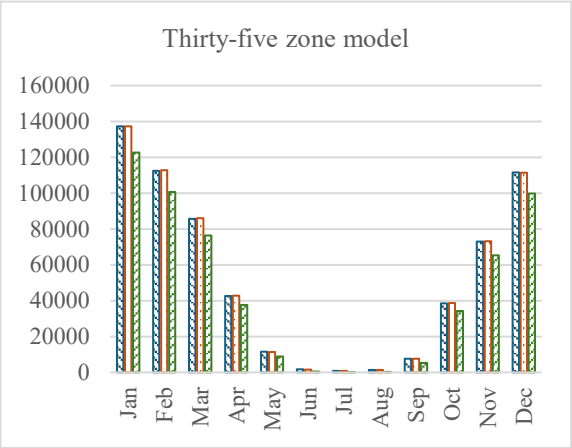

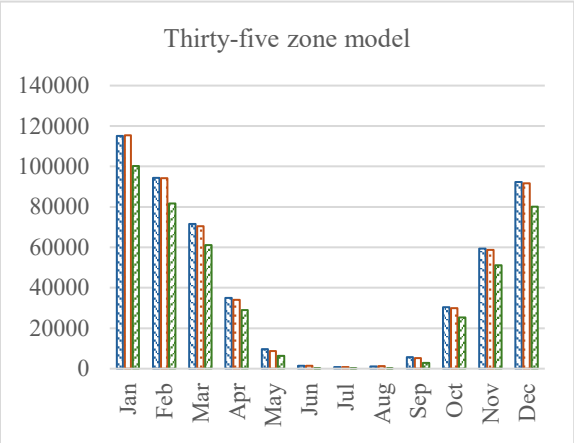

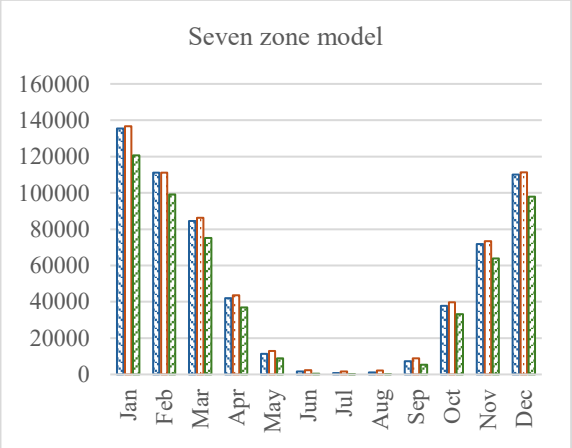

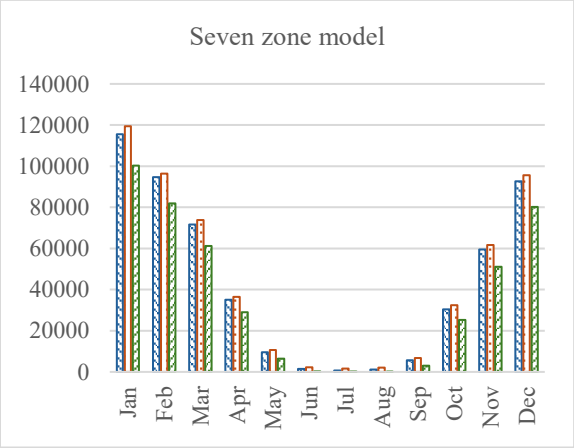

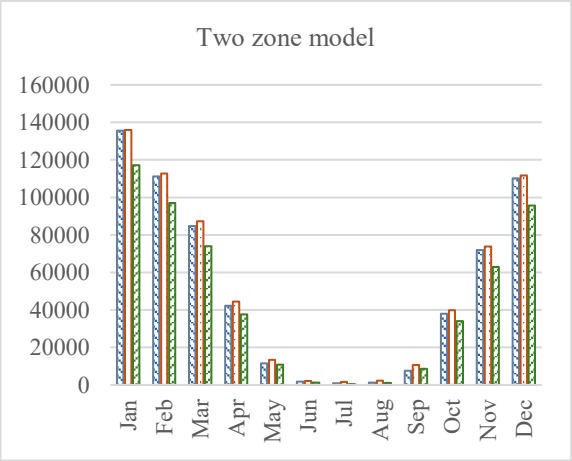

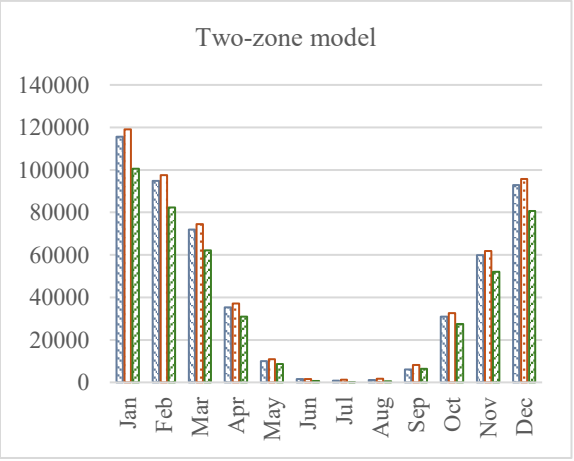

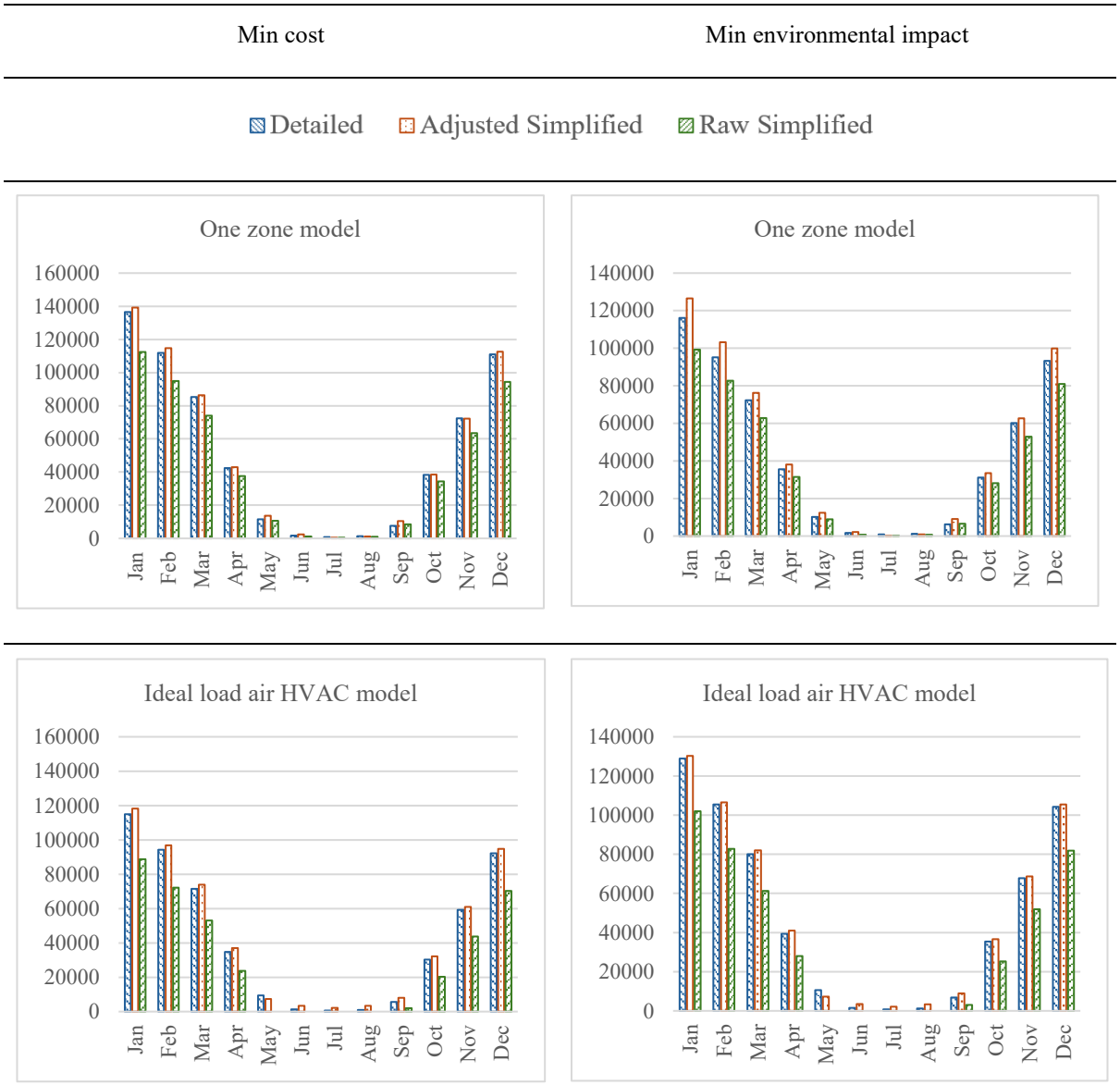

Figure 5-8: Monthly natural gas consumption [kWh] comparison between the detailed, ANN-adjusted, and raw simplified models at the minimum-cost and minimum-environmental-impact Pareto-optimal solutions.

Although the ANN-adjustment has the greatest impact on natural gas predictions due to the dominance of heating in the dormitory's annual energy profile, electricity consumption also benefits from the adjustment. Since the building has no mechanical cooling and uses natural gas for space heating, monthly electricity demand is primarily driven by lighting, plug loads, and the HVAC supply fan. These end uses exhibit limited seasonal variation, and retrofit measures do not substantially alter their temporal pattern. Consequently, the raw simplified

models already achieved low monthly CV(RMSE) and NMBE values that fall within ASHRAE Guideline 14 thresholds [69].

Even with this relatively uniform load profile, integrating the ANN further reduced residual bias and improved the monthly agreement with the detailed model across all simplification levels. The magnitude of improvement is smaller than that observed for natural gas, but the adjustment nonetheless enhances consistency in the simplified models and reduces systematic deviation, strengthening the reliability of subsequent objective-function evaluations in the optimization framework. The performance metrics for electricity across the minimum-cost and minimum-environmental-impact solutions are summarized in Table 5-4.

Table 5-4: Monthly CV(RMSE) and NMBE [%] of electricity consumption for ANN-corrected and raw simplified models at the minimum-cost and minimum-environmental-impact Pareto-optimal solutions.

	Min cost				Min environmental impact			
	CV(RMSE)		NMBE		CV(RMSE)		NMBE	
	Adjusted	Raw	Adjusted	Raw	Adjusted	Raw	Adjusted	Raw
Thirty-five zone	0.60	3.82	-0.14	3.81	0.64	3.69	-0.27	3.69
Seven zone	0.64	0.03	-0.25	2.80	0.68	3.24	0.03	3.14
Two zone	0.74	3.01	-0.50	2.74	0.90	3.17	-0.20	3.06
One zone	0.80	3.94	-0.62	3.93	0.81	3.98	-0.58	3.97
HVAC	0.71	4.07	-0.64	4.07	0.49	4.31	-0.39	4.31

5.3.4 Accuracy Improvement of Objective-Function Predictions in ANN-Corrected Models

5.3.3.1 Objective-Function Accuracy in the Dormitory Building

The improvement in hourly accuracy achieved through the ANN directly enhanced the reliability of the three objective functions used in the optimization framework: annual energy consumption (EC), carbon emissions (CE), and net present value (NPV). Since EC and CE are derived from annualized electricity and natural gas use, and NPV incorporates these annual totals into a 55-year financial projection, any systematic hourly bias in the simplified models propagates into the long-term performance indicators. Table 5-5 summarizes the average

absolute relative errors in the objective functions for both the ANN-adjusted and raw simplified models across all simplification levels, relative to the detailed model's values at the Pareto-optimal solutions.

Across all cases, the ANN substantially reduced the error magnitudes for NPV, EC, and CE. In the most detailed configuration (thirty-five-zone model), raw errors ranged from 6.9% to 13.12% across objectives. After ANN adjustment, these errors dropped to approximately 0.37-0.44%, indicating that the corrected predictions aligned closely with the detailed model. A similar improvement was observed in the other simplified models. Even in the more aggressive simplifications, such as the single-zone model, the adjusted errors remained consistently below 4%, demonstrating that the ANN effectively compensated for the loss of spatial detail.

The HVAC-simplified case showed the largest discrepancies before adjustment, with raw errors reaching 22.74% for EC, 24.89% for CE, and 10.91% for NPV. These high values reflect the substantial impact of oversimplifying HVAC system behavior on predicted heating loads and associated energy use. After applying the ANN adjustment, errors decreased to below 4% for all objectives, demonstrating the network's effectiveness in capturing and correcting the systematic biases introduced by the idealized HVAC assumptions.

Overall, ANN adjustment reduced error magnitudes by roughly 70-95% relative to the raw simplified outputs, and this improvement was consistent across all simplification levels. Before adjustment, the simplified models systematically underestimated energy use, leading to lower EC and CE values and distorted financial projections. The ANN correction resolved these biases by learning the systematic errors associated with each simplification strategy and applying adjustments to the hourly predictions. After modification, annual EC, CE, and NPV estimates aligned closely with the detailed model, and the remaining errors were small, stable, and insensitive to the degree of simplification. This consistency indicates that the ANN not

only enhances accuracy but also preserves the relative performance of candidate retrofit solutions.

Table 5-5: Average absolute relative [%] for NPV, EC, and CE from ANN-adjusted and raw simplified models across different simplification levels over the building's 55-year life span.

	NPV		EC		CE	
	Adjusted	Raw	Adjusted	Raw	Adjusted	Raw
Thirty-five zone	0.39	6.9	0.37	12.17	0.44	13.12
Seven zone	1.31	6.32	3.23	12.39	3.66	13.52
Two zone	1.01	6.02	2.95	11.29	3.25	12.04
One zone	1.59	8.07	3.3	12.14	3.63	13.05
HVAC	1.53	10.91	3.22	22.74	3.52	24.89

The Pareto-front comparisons highlight how the ANN-integrated optimization framework improved the quality and consistency of retrofit solutions across the various simplification levels of the dormitory building, as illustrated in Figure 5-9. In all configurations, the raw simplified models produced Pareto fronts that were systematically shifted downward along the energy axis. This reflects the underprediction of total energy consumption observed in the raw simplified hourly outputs, leading to overly optimistic trade-offs between NPV and energy use. After applying the ANN adjustment, the Pareto fronts realigned more closely with the detailed reference. In the thirty-five-zone model, where the physical representation is already relatively rich, the ANN-adjusted solutions nearly overlapped with the detailed model. The correction reduced the small residual bias that persisted in the raw results and restored the characteristic curvature of the cost-energy trade-off.

The improvements were most pronounced in the two-zone, one-zone, and HVAC-simplified models, where the raw Pareto fronts were compressed, shifted, and often distorted, misrepresenting both achievable energy savings and the relative performance of retrofit options. Idealizing the HVAC system produced the largest deviations, with raw fronts showing unrealistically low energy use and an incorrect overall shape. After ANN adjustment, the

corrected fronts regained an appropriate slope and structure, shifted upward, and formed clusters that closely followed the detailed model's trajectory.

Across all cases, the ANN improved absolute accuracy and restored the structure of the Pareto fronts. The corrected fronts reproduced the curvature, spread, and clustering of the detailed model, indicating that the ANN preserved both the magnitude and direction of trade-offs among retrofit options. This alignment is essential, as multi-objective optimization depends on accurate objective values and correct relationships among competing solutions. By recovering these patterns, the ANN allows simplified models to emulate the optimization behavior of the detailed simulation while maintaining their computational efficiency.

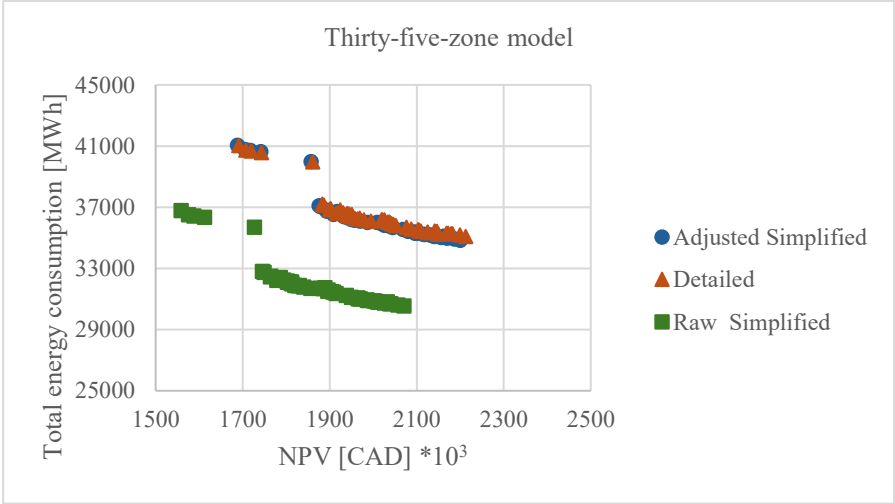

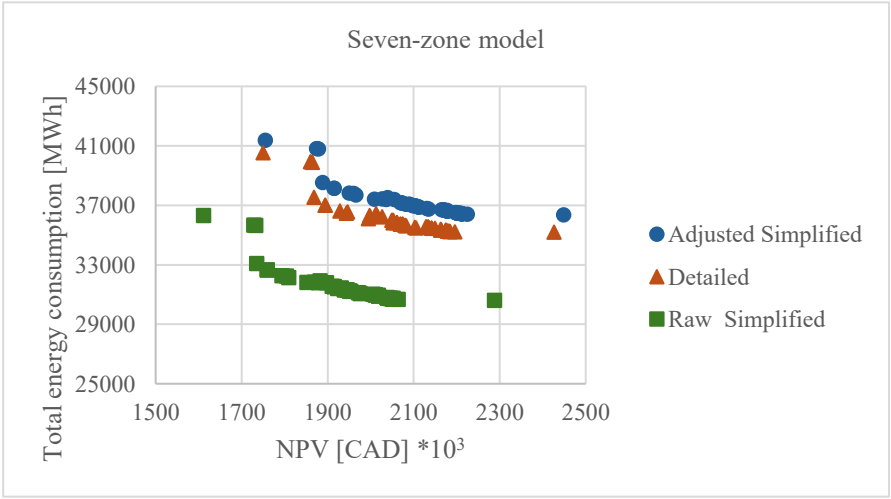

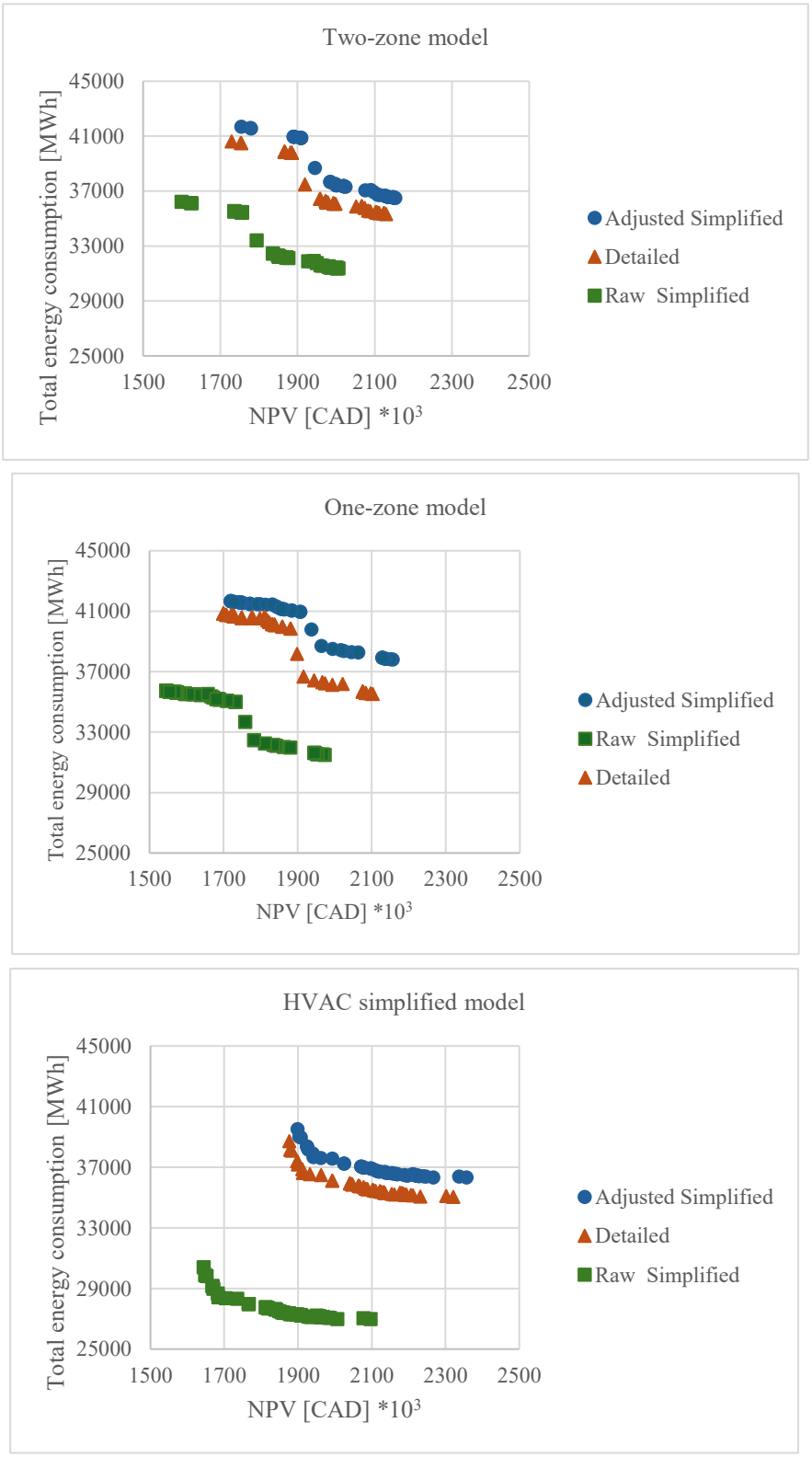

Figure 5-9: Comparison of Pareto-optimal NPV–energy trade-offs across detailed, raw simplified, and ANN-adjusted models.

5.3.4.2 Objective-Function Accuracy in the Single-Family House

As discussed previously, the single-family house's small size, uniform occupancy, and limited internal-load diversity reduce its sensitivity to zoning and material simplifications. Consequently, the Pareto-optimal solutions obtained from the simplified zone and material configurations closely align with those produced by the detailed model. However, the HVAC simplification introduced discrepancies that necessitated ANN-based modification.

Table 5-6 summarizes the average absolute relative errors for NPV, EC, CE, natural gas, and electricity consumption. The one-zone model shows low deviations, all below 5%. NPV differs by 2.22%, and EC and CE differ by 4.46% and 4.50%. Natural gas and electricity use also remain close to the detailed results, indicating that the simplified configuration captures the building's thermal behavior well enough for dependable comparison of retrofit options. Moreover, R-value simplified model shows small, and consistent deviations across all objectives. NPV differs by 2.12%, while EC and CE differ by 5.74% and 5.77%. Natural gas consumption is approximately 6.01% higher than the detailed model, and electricity differs by 0.68%.

Idealizing the HVAC system eliminates fan energy and distribution-related loads, leading to simplified predictions that underestimate energy use and result in large deviations in NPV, EC, CE, and fuel consumption. The magnitude of these discrepancies far exceeds those observed in the one-zone and R-value configurations, as reflected in the raw simplified HVAC errors that reach 18.63% for NPV, roughly 45% for EC and CE, and more than 47% for natural gas.

Applying ANN adjustment substantially reduces these errors, shifting the HVAC-simplified results toward the detailed model and restoring a coherent Pareto front. After correction, deviations drop to approximately 2% for NPV and 4% to 4.5% for EC, CE, and natural gas,

indicating that the ANN successfully recovers the missing system effects that were excluded in the idealized configuration.

Table 5-6: Average absolute relative errors [%] for NPV, EC, CE, natural gas, and electricity use comparing simplified and detailed models over the 55-year evaluation period.

	One-zone	R-value	HVAC	
			Adjusted	Raw
NPV	2.22	2.12	1.95	18.63
EC	4.46	5.74	4.35	45.38
CE	4.50	5.77	4.26	45.64
Natural gas	4.61	6.01	4.35	47.29
Electricity	1.41	0.68	4.29	9.11

5.3.5 Sensitivity Analysis of Economic Assumptions for LCC

A sensitivity analysis was completed to quantify how uncertainty in long term economic inputs influences the life cycle cost (LCC) conclusions for the single family house retrofit solutions. Results are reported for both model representations, the detailed multi zone model and the simplified one zone model. The objective is checking whether the economic interpretation of the Pareto optimal retrofit set remains stable under plausible variations in discounting and energy market assumptions, while staying consistent with the constant dollar LCC framework used in this study.

5.3.5.1 LCC Formulation and Parameters Examined

The LCC was evaluated over a 55 year period (2025 to 2080) as the sum of the initial retrofit investment and the present value of future electricity and natural gas expenditures. Discounting and escalation were handled through the Modified Uniform Present Value factor (UPV*), using Equations 4-5 to 4-7. The sensitivity analysis targeted the parameters that directly affect the present value factor:

- Inflation rate, e
- Nominal discount rate, d_n

- Real discount rate, d_r, calculated from d_n and e using Equation 4-7
- Real energy price escalation rate, g

Since the analysis is performed in constant dollars, discounting is applied using the real discount rate and escalation is applied using a real escalation rate. When e or d_n changes, d_r is recomputed using Equation 4-7 in order to preserve internal consistency between nominal and real assumptions.

5.3.5.2 Ranges Used in Sensitivity Tests

Inflation rate (e). Inflation was varied within the Bank of Canada inflation control target band, which has a 2% midpoint and a control range from 1% to 3% [141]. Three values were examined: 1.0% , 2.5% as the base assumption, and 3.0%. When inflation was varied, the real discount rate was recalculated using Equation 4-7.

Nominal discount rate (d_n) and implied real discount rate (d_r). Discounting sensitivity was implemented by varying d_n and recomputing d_r using Equation 4-7 while holding e constant. This avoids double counting inflation effects and maintains a consistent constant dollar formulation. The nominal discount values tested were 3.0%, 3.29% as the base assumption, 4.0%, and 5.0%, which provide a practical bracket for residential and public style long horizon evaluations in which discounting is often tested through alternative plausible rates rather than a single fixed value. Federal guidance on cost benefit analysis emphasizes the importance of discounting assumptions and supports sensitivity testing when results depend on long run valuation of costs and benefits [142].

A low real discounting perspective is also actively used in Canadian regulatory impact analysis for long horizon environmental and economic impacts. The Regulatory Impact Analysis Statement for the proposed Oil and Gas Sector Greenhouse Gas Emissions Cap Regulations

reports a social discount rate of 2% per year, illustrating current Canadian regulatory practice applying low social discount rates for long horizon evaluations [143].

Energy price escalation (g). Energy price uncertainty was represented by varying the real escalation rate *g* across three scenarios: 0.0%, 0.5% as the base assumption, and 2.0%. These bounds span outcomes from flat real energy prices to moderately increasing real prices. A uniform *g* was applied across the evaluation period using the UPV* formulation to keep the sensitivity design interpretable and aligned with the LCC equations used in the main analysis.

5.3.5.3 Sensitivity Design and Implementation

A one at a time sensitivity design was used. Each parameter was varied independently while all other inputs were held at base values. For each variation, the UPV* factor and total LCC were recalculated using Equations 4-5 to 4-7. Post processing was performed on the Pareto optimal solutions obtained from the baseline optimization, rather than rerunning NSGA-III for each economic scenario. This isolates the impact of economic assumptions on LCC values and avoids confounding effects from optimization stochasticity or changes in convergence.

5.3.5.4 Key Findings from the Sensitivity Results

Across the Pareto-optimal solution set, variations in economic assumptions led to systematic and monotonic changes in life-cycle cost (LCC) for both the simplified one-zone model and the detailed multi-zone model. While absolute LCC values were sensitive to the assumed economic parameters, the relative structure of the Pareto-optimal solutions was preserved, indicating consistent comparative behavior across scenarios.

Inflation sensitivity. Varying the inflation rate within the tested range produced a clear and asymmetric impact on LCC. Reducing inflation from the base value of 2.5% to 1.0% resulted in a substantial decrease in LCC, with an average reduction of approximately 16.6% for the simplified model and 16.9% for the detailed model across the Pareto set. Individual solutions

exhibited reductions ranging from approximately 10% to 27%, indicating a strong dependence of long-term discounted costs on inflation assumptions.

Conversely, increasing inflation from 2.5% to 3.0% increased LCC by an average of approximately 7.7% for the simplified model and 7.8% for the detailed model, with observed increases ranging from about 4.6% to 12.9% across solutions. The asymmetric response reflects the non-linear interaction between inflation and the real discount rate in the present value formulation. Importantly, both model representations exhibited nearly identical sensitivity magnitudes, confirming consistent inflation response behavior.

Discount rate sensitivity. Changes in the nominal discount rate, with inflation held constant, also produced pronounced effects on LCC through the implied real discount rate. Increasing the nominal discount rate above the base value of 3.29% consistently reduced LCC by decreasing the present value of future operating costs.

On average, increasing the nominal discount rate to 4.0% reduced LCC by approximately 8.8% for the simplified model and 8.9% for the detailed model, while increasing it further to 5.0% reduced LCC by approximately 18.0% and 18.3%, respectively. Across individual Pareto solutions, reductions ranged from roughly 11% to 30% at the highest discounting level. These results confirm that discounting assumptions play a dominant role in shaping long-horizon retrofit cost evaluations.

Lowering the nominal discount rate to 3.0% resulted in a moderate increase in LCC, reflecting greater weight assigned to long-term operational energy costs. As with inflation sensitivity, the simplified and detailed models exhibited nearly identical response patterns and magnitudes.

Energy escalation sensitivity. Energy price escalation emerged as the most influential economic parameter affecting LCC. Reducing the real escalation rate from the base value of 0.5% to 0.0%

resulted in a modest decrease in LCC, with an average reduction of approximately 6.4% for the simplified model and 6.5% for the detailed model.

In contrast, increasing the real escalation rate to 2.0% produced the largest upward shifts in LCC across all sensitivity tests. On average, LCC increased by approximately 27.4% for the simplified model and 27.9% for the detailed model, with individual Pareto solutions showing increases ranging from about 16.5% to over 45%. This strong response reflects the dominance of long-term energy expenditures in the life-cycle cost of residential retrofits, particularly over a 55-year evaluation horizon.

Again, both model representations responded almost identically to escalation changes, reinforcing the consistency of economic sensitivity behavior between simplified and detailed models.

5.3.5.5 Implications for Interpretation

Although sensitivity analysis is most critical in the final stages of retrofit decision making, where absolute cost values and financial feasibility become decisive, the primary objective of this study is the comparative evaluation of simplified and detailed energy models under uncertainty. The sensitivity results demonstrate that both models respond in a highly consistent manner to variations in inflation, discounting, and energy price escalation assumptions.

While economic assumptions can significantly alter absolute LCC values, they do not materially change the relative positioning or trade-offs among Pareto-optimal retrofit solutions. This indicates that simplified models can reliably capture the dominant economic sensitivities of retrofit decisions and are well suited for comparative screening and uncertainty exploration in early and intermediate stages of analysis.

5.4 Conclusion

This chapter introduces a novel simulation-based multi-objective optimization framework that integrates simplified building energy models with external ANN modifications, enhancing predictive performance for retrofit decision-making while preserving the underlying physical representation of the building. The approach combines the speed of reduced order models with an external ANN correction layer that refines hourly energy predictions before objective functions are calculated. ANNs were trained using hourly simplified outputs and weather variables as inputs and detailed model results as targets, and then embedded within a prNSGA-III optimization that minimized total energy consumption, carbon emissions, and life-cycle cost over 55 years. Two case study buildings in Ottawa were used to assess the methodology. A five-story dormitory with complex zoning and mechanical systems presented a challenging case due to strong interactions among zones, schedules, and HVAC operations. A single-family detached house with simple geometry and limited internal load diversity served as a contrasting case with much lower complexity. For both buildings, detailed EnergyPlus models were created and validated, then systematically simplified by aggregating thermal zones, idealizing HVAC systems, and reducing material definitions to equivalent R-values.

Findings show that the need for ANN enhancement is closely linked to building typology and system complexity. The dormitory, with its large footprint and heterogeneous load patterns, required ANN-adjustment for nearly all simplification methods except the R-value configuration. The single-family home demonstrated greater robustness, maintaining accuracy under zoning and material simplifications and requiring adjustment only when the mechanical system was idealized. In both buildings, simplification errors propagated through the optimization process, distorting Pareto fronts and influencing the selection of energy conservation measures.

The trained ANNs achieved high predictive accuracy across all simplification levels, with R^2 values exceeding 0.985 and RMSE values that remained modest relative to typical hourly loads. Once integrated into the prNSGA-III framework, the monthly analysis of the dormitory confirmed the ANN layer's essential role in restoring fidelity across simplified configurations. Raw simplified predictions produced sizeable monthly errors, especially in models with reduced zoning resolution or idealized HVAC systems. These discrepancies were reflected in elevated monthly CV(RMSE) and NMBE values, with the HVAC-simplified case showing natural gas deviations exceeding 30%. Integrating the ANN significantly reduced these errors across all abstraction levels, lowering monthly CV(RMSE) from 14.6% to 0.34% in the thirty-five-zone model and from 34% to 5.3% in the HVAC-simplified configuration. Comparable improvements were observed in the environmental-optimal solutions. Electricity use displayed smaller baseline deviations due to its limited seasonal sensitivity in this heating-dominated building, yet the ANN still reduced residual bias and stabilized performance across simplifications. These improvements strengthen the reliability of annual energy calculations and their contributions to life-cycle cost and carbon estimates within the optimization.

The ANN's influence extended directly to the optimization objectives. Because annual energy consumption, carbon emissions, and net present value are derived from aggregated hourly loads, errors in simplified models are carried through to long-term environmental and economic indicators. The ANN layer effectively mitigated these effects. In the thirty-five-zone model, initial objective-function errors of 6.9-13.1% were reduced to well below 1%. Similar trends were observed across the seven-zone, two-zone, and one-zone configurations, where adjusted deviations remained below 4%. The HVAC-simplified case, which originally produced the largest errors, benefited most from the ANN, with EC and CE deviations reduced from more than 22–24% to roughly 3–4%. The correction preserved the relative ranking of retrofit

alternatives and restored coherent Pareto fronts, ensuring that optimization outcomes remained dependable despite substantial reductions in model detail.

The results from the single-family house results reinforce these insights. Its compact form, uniform occupancy, and limited internal-load variation allowed the one-zone and R-value simplified configurations to reproduce annual energy, carbon, and cost outcomes with small deviations, all within 5%. Such performance suggests that simplified physics can reliably support retrofit optimization in small residential buildings without ANN adjustments. HVAC idealization, however, removed HVAC supply fan and distribution-related loads, leading to substantial underestimation of energy use and large deviations in NPV, EC, CE, and natural gas consumption, exceeding 45%. ANN adjustment effectively corrected these issues, reducing objective-function errors to approximately 2% for NPV and 4–4.5% for EC, CE, and natural gas.

Overall, the proposed framework shows that simplified models, when paired with ANN-based adjustments, can emulate the optimization behavior of detailed simulations in complex buildings while retaining their computational benefits. For simple residential buildings, carefully constructed simplified models may be accurate enough for direct use, while HVAC abstraction remains the primary source of error requiring correction. This distinction underscores that the need for ANN enhancement depends on building typology, mechanical complexity, and the intended use of the model.

The study also highlights several directions that warrant further exploration. Applying the framework to additional climates and building types would broaden understanding of its applicability. Alternative machine learning architectures, hybrid physics-data approaches, and more explicit integration of uncertainty into the optimization process merit exploration. Diagnostic tools that automatically assess when ANN correction is advisable would further enhance practicality. Overall, the study establishes a structured foundation for combining

simplified models, ANN-based adjustments, and multi-objective optimization to support fast, reliable, and scalable retrofit planning for existing buildings.

Chapter 6: Conclusion, limitations, and recommendations for future work

6.1 Conclusion

This thesis developed a structured framework for evaluating and improving the efficiency and reliability of simulation-based multi-objective optimization for building retrofits. Three major contributions were established across the research phases.

First, the work demonstrated how common simplification strategies influence predictive accuracy and optimization outputs across three representative Canadian buildings. Results confirmed that simplification can substantially reduce computational cost; however, its influence on accuracy depends strongly on building complexity. Large multi-zone buildings, such as the dormitory, exhibited notable sensitivity to zoning abstraction and HVAC idealization, particularly in heating-dominated months. In contrast, the small single-family house exhibited minimal sensitivity to zoning and material simplifications due to its simple layout, more uniform internal loads, and compact envelope. These findings underline that simplification feasibility is building-specific and that not all techniques are equally transferable across typologies.

Second, the thesis examined whether simplification-induced errors remain consistent across weather datasets. Results showed that simplified and detailed models do not respond uniformly to variations in climatic conditions. Accuracy losses were more pronounced during extreme cold events, in early fall transition months, and under climate change projections that alter the distribution of heating and cooling loads. The study found that relying on a single weather file to evaluate simplified models can provide misleading conclusions about their long-term reliability. This highlights the necessity of climate-informed validation when using simplified models for retrofit decision support.

Third, the thesis introduced an external ANN-based adjustment method to enhance the accuracy of simplified models without altering their physical structure. This neural network layer effectively corrected hourly loads and objective function values across simplification levels. Importantly, the method preserved the relative shape and structure of Pareto fronts, ensuring that the optimization process continued to reflect realistic trade-offs. For complex buildings, the ANN layer was essential for restoring fidelity. This scalable approach offers a practical means to integrate simplified models into optimization tools without compromising physical transparency.

Taken together, the outcomes of this research provide a comprehensive foundation for using simplified models responsibly in optimization workflows. They offer guidance on selecting simplification strategies, highlight the importance of climate-aware performance assessment, and introduce a computationally efficient correction method that retains model interpretability. The results support more robust, efficient, and future-ready decision-making for energy retrofits.

6.2 Limitations and Future Work by Research Article

The limitations of this research are as follows:

Chapter 3: Article 1 (Performance analysis of simplification approaches)

Limitations:

- The findings are influenced by the characteristics of the selected case study building, which, although representative of many mixed-use office buildings in Canada, does not fully capture the behavior of other building types.
- The results may not generalize to buildings with fundamentally different layouts, including residential dwellings, industrial facilities, or highly glazed commercial structures.

- The study evaluates only one climate region, and simplification performance may vary under different climatic conditions or extreme weather patterns.
- Only a limited set of mechanical systems was examined; buildings with more complex or advanced HVAC configurations may exhibit different sensitivities to simplification.
- The study does not evaluate the long-term reliability of simplification strategies under projected future climate scenarios, where seasonal thermal loads may shift substantially.

Future Work:

- Apply the proposed simplification framework across a broader range of building typologies to develop more comprehensive, generalizable guidelines.
- Assess the reliability of simplification strategies under future weather projections and climate change scenarios to support long-term, climate-resilient retrofit planning.

Chapter 4: article 2 (climate robustness of simplified models (weather-file sensitivity))

Limitations:

- The findings are based on a heating-dominated climate, which limits their direct applicability to regions with substantially different climatic conditions, such as tropical or arid environments.
- The analysis does not assess the ability of simplified models to capture thermal comfort or overheating risks, which are increasingly critical as heatwaves become more frequent under climate change.
- Only one building typology was examined; results may not generalize to buildings with different operational profiles, occupancy schedules, or envelope constructions.

Future Work:

- Extend the analysis to cooling-dominated and mixed climates to evaluate how simplification methods behave under different thermal load profiles.
- Examine the performance of a simplified model during extreme heat events and assess its ability to predict overheating, thermal comfort, and peak cooling demand.
- Apply the framework across multiple building types with diverse occupancy patterns, constructions, and mechanical systems to strengthen generalizability.

Chapter 5: Article 3 (ANN-based adjustment for simplified models)

Limitations:

- The framework was evaluated using a limited set of building types and climate conditions, which may restrict the generalizability of the ANN-based correction approach.
- The approach does not explicitly incorporate uncertainty, leaving potential variations in model predictions, ANN performance, and optimization outcomes unquantified.
- No automated diagnostic mechanism is currently included to determine when ANN adjustment is necessary or when the simplified model is sufficiently accurate on its own.
- The evaluation focused on energy performance metrics and did not assess comfort indicators, load shifting, or system-level behavior that may also be affected by simplification and ANN adjustment.

Future Work:

- Apply the framework across a wider range of building types, mechanical systems, and climatic regions to assess consistency and generalizability.

- Integrate uncertainty quantification into both the ANN predictions and the optimization workflow to support risk-aware decision-making.
- Develop diagnostic tools that automatically evaluate simplified model accuracy and determine when ANN adjustment is beneficial or required.
- Expand performance assessment to include thermal comfort, peak load behavior, and other metrics relevant to advanced energy retrofits and operational resilience.

References

[1] Buildings - Energy System - IEA, (2022). https://www.iea.org/energy-system/buildings (accessed July 7, 2024).

[2] S. Barlow, D. Fiala, Occupant comfort in UK offices—How adaptive comfort theories might influence future low energy office refurbishment strategies, Energy Build. 39 (2007) 837–846. https://doi.org/10.1016/J.ENBUILD.2007.02.002.

[3] G. Aruta, F. Ascione, N. Bianco, T. Iovane, M. Mastellone, Assessment of the Incentive Rate to Favor the Energy Retrofit of Public Buildings: A Comprehensive Approach for an Italian University Facility, Energies 2023, Vol. 16, Page 4483 16 (2023) 4483. https://doi.org/10.3390/EN16114483.

[4] E.M. Malatji, J. Zhang, X. Xia, A multiple objective optimisation model for building energy efficiency investment decision, Energy Build. 61 (2013) 81–87. https://doi.org/10.1016/J.ENBUILD.2013.01.042.

[5] A. Jafari, V. Valentin, An optimization framework for building energy retrofits decision-making, Build. Environ. 115 (2017) 118–129. https://doi.org/10.1016/J.BUILDENV.2017.01.020.

[6] X. Luo, Y. Zhang, J. Lu, J. Ge, Multi-objective optimization of the office park building envelope with the goal of nearly zero energy consumption, Journal of Building Engineering 84 (2024) 108552. https://doi.org/10.1016/J.JOBE.2024.108552.

[7] H. Wu, T. Zhang, Multi-objective optimization of energy, visual, and thermal performance for building envelopes in China's hot summer and cold winter climate zone, Journal of Building Engineering 59 (2022) 105034. https://doi.org/10.1016/J.JOBE.2022.105034.

[8] S. Attia, M. Hamdy, W. O'Brien, S. Carlucci, Computational optimisation for zero energy buildings design: Interviews results with twenty eight international experts, (2013). https://www.aivc.org/resource/computational-optimisation-zero-energy-buildings-design-interviews-results-twenty-eight (accessed August 16, 2023).

[9] A.T. Nguyen, S. Reiter, P. Rigo, A review on simulation-based optimization methods applied to building performance analysis, Appl. Energy 113 (2014) 1043–1058. https://doi.org/10.1016/J.APENERGY.2013.08.061.

[10] M. Hamdy, A. Hasan, K. Siren, Optimum design of a house and its HVAC systems using simulation-based optimisation, International Journal of Low-Carbon Technologies 5 (2010) 120–124. https://doi.org/10.1093/IJLCT/CTQ010.

[11] A. Abdeen, E. Mushtaha, A. Hussien, C. Ghenai, A. Maksoud, V. Belpoliti, Simulation-based multi-objective genetic optimization for promoting energy efficiency and thermal comfort in existing buildings of hot climate, Results in Engineering 21 (2024) 101815. https://doi.org/10.1016/J.RINENG.2024.101815.

[12] R. Chen, Y.S. Tsay, S. Ni, An integrated framework for multi-objective optimization of building performance: Carbon emissions, thermal comfort, and global cost, J. Clean. Prod. 359 (2022) 131978. https://doi.org/10.1016/J.JCLEPRO.2022.131978.

[13] Y. Gao, S. Luo, J. Jiang, Y. Rong, Environmental-thermal-economic performance trade-off for rural residence retrofitting in the Beijing–Tianjin–Hebei region, Northern China: A multi-objective optimisation framework under different scenarios, Energy Build. 286 (2023) 112910. https://doi.org/10.1016/J.ENBUILD.2023.112910.

[14] S. Elhadad, C.H. Radha, I. Kistelegdi, B. Baranyai, J. Gyergyák, Model simplification on energy and comfort simulation analysis for residential building design in hot and arid climate, Energies (Basel). 13 (2020). https://doi.org/10.3390/en13081876.

[15] F. Johari, J. Munkhammar, F. Shadram, J. Widén, Evaluation of simplified building energy models for urban-scale energy analysis of buildings, Build. Environ. 211 (2022). https://doi.org/10.1016/j.buildenv.2021.108684.

[16] F. Ascione, N. Bianco, R.F. De Masi, G.M. Mauro, G.P. Vanoli, Resilience of robust cost-optimal energy retrofit of buildings to global warming: A multi-stage, multi-objective approach, Energy Build. 153 (2017) 150–167. https://doi.org/10.1016/J.ENBUILD.2017.08.004.

[17] M. Tavakolan, F. Mostafazadeh, S. Jalilzadeh Eirdmousa, A. Safari, K. Mirzaei, A parallel computing simulation-based multi-objective optimization framework for economic analysis of building energy retrofit: A case study in Iran, Journal of Building Engineering 45 (2022) 103485. https://doi.org/10.1016/J.JOBE.2021.103485.

[18] C. Baker, S. Goel, N. Wang, M. Rosenberg, D. Wolf, P. Henderson, A SIMPLIFIED ENERGY MODELING APPROACH FOR BUILDINGS, n.d. www.ashrae.org.

[19] M. Shin, J.S. Haberl, Thermal zoning for building HVAC design and energy simulation: A literature review, Energy Build. 203 (2019) 109429. https://doi.org/10.1016/J.ENBUILD.2019.109429.

[20] 2019 Update of Standard 90.1 | ashrae.org, (n.d.). https://www.ashrae.org/news/hvacrindustry/2019-update-of-standard-90-1 (accessed August 5, 2024).

[21] B. Banville, A. École, É. Catholique De Barrhaven, B. Martel, A. Clemann, A. Ltd, EE4 Software Version 1.7 Modelling Guide, 2008. http://ecoACTION.gc.ca/buildingshttp://sbc.nrcan.gc.ca/software_and_tools/ee4_soft_e.aspAussidisponibleenfrançais.

[22] P. Shen, W. Braham, Y. Yi, Development of a lightweight building simulation tool using simplified zone thermal coupling for fast parametric study, Appl. Energy 223 (2018) 188–214. https://doi.org/10.1016/J.APENERGY.2018.04.039.

[23] J. Xie, X. Lu, Measuring Impact: Evaluating Thermal Zoning Simplification on Energy Efficiency Measures Analysis, (2024).

[24] M. Klimczak, J. Bojarski, P. Ziembicki, P. Kęskiewicz, Analysis of the impact of simulation model simplifications on the quality of low-energy buildings simulation results, Energy Build. 169 (2018) 141–147. https://doi.org/10.1016/j.enbuild.2018.03.046.

[25] O.K. Larsen, Y. Hu, M.Z. Pomianowski, Towards feasible and credible building modelling reflecting the operational energy use and indoor environment – Nordic climate case study, Energy Build. 317 (2024). https://doi.org/10.1016/j.enbuild.2024.114346.

[26] Y. Chen, T. Hong, Impacts of building geometry modeling methods on the simulation results of urban building energy models, Appl. Energy 215 (2018) 717–735. https://doi.org/10.1016/j.apenergy.2018.02.073.

[27] M. Heidarinejad, N. Mattise, M. Dahlhausen, K. Sharma, K. Benne, D. Macumber, L. Brackney, J. Srebric, Demonstration of reduced-order urban scale building energy models, Energy Build. 156 (2017) 17–28. https://doi.org/10.1016/j.enbuild.2017.08.086.

[28] L. Santos, S. Schleicher, L. Caldas, Automatic simplification of complex building geometry for whole-Building Energy Simulations, in: Building Simulation Conference Proceedings, International Building Performance Simulation Association, 2019: pp. 2691–2698. https://doi.org/10.26868/25222708.2019.210991.

[29] A. Al-janabi, M. Kavgic, A. Mohammadzadeh, A. Azzouz, Comparison of EnergyPlus and IES to model a complex university building using three scenarios: Free-floating, ideal air load system, and detailed, Journal of Building Engineering 22 (2019) 262–280. https://doi.org/10.1016/j.jobe.2018.12.022.

[30] M. Picco, R. Lollini, M. Marengo, Towards energy performance evaluation in early stage building design: A simplification methodology for commercial building models, Energy Build. 76 (2014) 497–505. https://doi.org/10.1016/J.ENBUILD.2014.03.016.

[31] G. Ren, Y. Heo, M. Sunikka-Blank, Investigating an adequate level of modelling for retrofit decision-making: A case study of a British semi-detached house, Journal of Building Engineering 26 (2019) 100837. https://doi.org/10.1016/J.JOBE.2019.100837.

[32] S. Asadi, E. Mostavi, D. Boussaa, M. Indaganti, Building energy model calibration using automated optimization-based algorithm, Energy Build. 198 (2019) 106–114. https://doi.org/10.1016/j.enbuild.2019.06.001.

[33] K. Sun, T. Hong, S.C. Taylor-Lange, M.A. Piette, A pattern-based automated approach to building energy model calibration, Appl. Energy 165 (2016) 214–224. https://doi.org/10.1016/j.apenergy.2015.12.026.

[34] D. Guyot, F. Giraud, F. Simon, D. Corgier, C. Marvillet, B. Tremeac, Building energy model calibration: A detailed case study using sub-hourly measured data, Energy Build. 223 (2020). https://doi.org/10.1016/j.enbuild.2020.110189.

[35] A. Chong, K.P. Lam, M. Pozzi, J. Yang, Bayesian calibration of building energy models with large datasets, Energy Build. 154 (2017) 343–355. https://doi.org/10.1016/j.enbuild.2017.08.069.

[36] J.E. Pachano, C.F. Bandera, Multi-step building energy model calibration process based on measured data, Energy Build. 252 (2021). https://doi.org/10.1016/j.enbuild.2021.111380.

[37] I. Yilmaz, H. Burak Gunay, G.R. Newsham, A.D. Wills, An inquiry into the accuracy of the energy model calibration process, in: Building Simulation Conference Proceedings, International Building Performance Simulation Association, 2022: pp. 1857–1864. https://doi.org/10.26868/25222708.2021.30658.

[38] F. Herbinger, C. Vandenhof, M. Kummert, Building energy model calibration using a surrogate neural network, Energy Build. 289 (2023). https://doi.org/10.1016/j.enbuild.2023.113057.

[39] A. Cacabelos, P. Eguía, L. Febrero, E. Granada, Development of a new multi-stage building energy model calibration methodology and validation in a public library, Energy Build. 146 (2017) 182–199. https://doi.org/10.1016/j.enbuild.2017.04.071.

[40] D. Hou, I.G. Hassan, L. Wang, Review on building energy model calibration by Bayesian inference, Renewable and Sustainable Energy Reviews 143 (2021). https://doi.org/10.1016/j.rser.2021.110930.

[41] A. Chong, K. Menberg, Guidelines for the Bayesian calibration of building energy models, Energy Build. 174 (2018) 527–547. https://doi.org/10.1016/j.enbuild.2018.06.028.

[42] Z. Yang, B. Becerik-Gerber, A model calibration framework for simultaneous multi-level building energy simulation, Appl. Energy 149 (2015) 415–431. https://doi.org/10.1016/j.apenergy.2015.03.048.

[43] Y. Bichiou, M. Krarti, Optimization of envelope and HVAC systems selection for residential buildings, Energy Build. 43 (2011) 3373–3382. https://doi.org/10.1016/j.enbuild.2011.08.031.

[44] F. Ascione, N. Bianco, G.M. Mauro, G.P. Vanoli, A new comprehensive framework for the multi-objective optimization of building energy design: Harlequin, Appl. Energy 241 (2019) 331–361. https://doi.org/10.1016/J.APENERGY.2019.03.028.

[45] F. Ascione, N. Bianco, C. De Stasio, G.M. Mauro, G.P. Vanoli, Multi-stage and multi-objective optimization for energy retrofitting a developed hospital reference building: A new approach to assess cost-optimality, Appl. Energy 174 (2016) 37–68. https://doi.org/10.1016/J.APENERGY.2016.04.078.

[46] C. Waibel, R. Evins, J. Carmeliet, Co-simulation and optimization of building geometry and multi-energy systems: Interdependencies in energy supply, energy demand and solar potentials, Appl. Energy 242 (2019) 1661–1682. https://doi.org/10.1016/j.apenergy.2019.03.177.

[47] M. Ferrara, F. Prunotto, A. Rolfo, E. Fabrizio, Energy demand and supply simultaneous optimization to design a nearly zero-energy house, Applied Sciences (Switzerland) 9 (2019). https://doi.org/10.3390/app9112261.

[48] R. Gagnon, L. Gosselin, S. Armand Decker, Performance of a sequential versus holistic building design approach using multi-objective optimization, Journal of Building Engineering 26 (2019). https://doi.org/10.1016/j.jobe.2019.100883.

[49] A. Karatas, K. El-Rayes, Parallel Computing Framework for Optimizing Environmental and Economic Performances of Housing Units, Journal of Computing in Civil Engineering 30 (2015) 04015026. https://doi.org/10.1061/(ASCE)CP.1943-5487.0000505.

[50] F. Bre, V.D. Fachinotti, A computational multi-objective optimization method to improve energy efficiency and thermal comfort in dwellings, Energy Build. 154 (2017) 283–294. https://doi.org/10.1016/j.enbuild.2017.08.002.

[51] M. Tavakolan, F. Chokan, M. Dadashi Haji, Simultaneous project portfolio selection and scheduling from contractor perspective, International Journal of Construction Management 24 (2024) 298–313. https://doi.org/10.1080/15623599.2023.2222995.

[52] F. Mostafazadeh, S.J. Eirdmousa, M. Tavakolan, Energy, economic and comfort optimization of building retrofits considering climate change: A simulation-based NSGA-III approach, Energy Build. 280 (2023) 112721. https://doi.org/10.1016/J.ENBUILD.2022.112721.

[53] D.R. Liyanage, K. Hewage, S.A. Hussain, F. Razi, R. Sadiq, Climate adaptation of existing buildings: A critical review on planning energy retrofit strategies for future climate, Renewable and Sustainable Energy Reviews 199 (2024). https://doi.org/10.1016/j.rser.2024.114476.

[54] P. Shen, Building retrofit optimization considering future climate and decision-making under various mindsets, Journal of Building Engineering 96 (2024). https://doi.org/10.1016/j.jobe.2024.110422.

[55] J. Pouriya, B. Umberto, Building energy demand within a climate change perspective: The need for future weather file, in: IOP Conf. Ser. Mater. Sci. Eng., Institute of Physics Publishing, 2019. https://doi.org/10.1088/1757-899X/609/7/072037.

[56] P. Jafarpur, U. Berardi, Effects of climate changes on building energy demand and thermal comfort in Canadian office buildings adopting different temperature setpoints, Journal of Building Engineering 42 (2021). https://doi.org/10.1016/j.jobe.2021.102725.

[57] K.N. Streicher, M. Berger, E. Panos, K. Narula, M.C. Soini, M.K. Patel, Optimal building retrofit pathways considering stock dynamics and climate change impacts, Energy Policy 152 (2021). https://doi.org/10.1016/j.enpol.2021.112220.

[58] P. Shen, W. Braham, Y. Yi, The feasibility and importance of considering climate change impacts in building retrofit analysis, Appl. Energy 233–234 (2019) 254–270. https://doi.org/10.1016/j.apenergy.2018.10.041.

[59] U. Berardi, P. Jafarpur, Assessing the impact of climate change on building heating and cooling energy demand in Canada, Renewable and Sustainable Energy Reviews 121 (2020). https://doi.org/10.1016/j.rser.2019.109681.

[60] X.J. Luo, L.O. Oyedele, Life cycle optimisation of building retrofitting considering climate change effects, Energy Build. 258 (2022). https://doi.org/10.1016/j.enbuild.2022.111830.

[61] G. Tomrukcu, T. Ashrafian, Climate-resilient building energy efficiency retrofit: Evaluating climate change impacts on residential buildings, Energy Build. 316 (2024). https://doi.org/10.1016/j.enbuild.2024.114315.

[62] M. Santamouris, Cooling the buildings – past, present and future, Energy Build. 128 (2016) 617–638. https://doi.org/10.1016/J.ENBUILD.2016.07.034.

[63] C. María Calama-González, R. Suárez, Á. Luis León-Rodríguez, Mitigation of climate change in Mediterranean existing social dwellings through numerical optimization of building stock models, Energy Build. 266 (2022) 112109. https://doi.org/10.1016/J.ENBUILD.2022.112109.

[64] S. Gilani, K. Haddad, C. Kirney, P. Lopez, A. Syed, M. Stylianou, Performance of energy conservation measures in Canadian office buildings, Energy Convers. Manag. 330 (2025) 119661. https://doi.org/10.1016/j.enconman.2025.119661.

[65] Energy Use in Canada: Trends Publications | Natural Resources Canada, (n.d.). https://oee.nrcan.gc.ca/publications/statistics/trends/2016/commercial.cfm?wbdisable=true (accessed March 4, 2025).

[66] B.J. Meacham, C. Mifiree, Performance-Based Building Regulatory Systems: Structure, Hierarchy and Linkages, 2004. https://www.researchgate.net/publication/345501405.

[67] 3D Design Software | 3D Modeling & Drawing | SketchUp, (n.d.). https://www.sketchup.com/en (accessed August 6, 2024).

[68] EnergyPlus, (n.d.). https://energyplus.net/ (accessed July 20, 2024).

[69] ASHRAE Guideline 14-2014 - Measurement of Energy, Demand, and Water Savings, (2014). https://webstore.ansi.org/standards/ashrae/ashraeguideline142014 (accessed March 24, 2024).

[70] Residential Housing Stock and Floor Space | Natural Resources Canada, (n.d.). https://oee.nrcan.gc.ca/corporate/statistics/neud/dpa/showTable.cfm?type=HB&sector=res&juris=00&rn=11&page=0 (accessed September 5, 2025).

[71] National Energy Code of Canada for Buildings 2020, Canadian Commission on Building and Fire Codes, 2022.

[72] X. Faure, T. Johansson, O. Pasichnyi, The Impact of Detail, Shadowing and Thermal Zoning Levels on Urban Building Energy Modelling (UBEM) on a District Scale†, Energies (Basel). 15 (2022). https://doi.org/10.3390/en15041525.

[73] Y. Dadras, M. Kavgic, The applicability of a simplified whole-building energy model for energy-efficiency retrofit analysis, n.d.

[74] Y. Dadras, M. Kavgic, O. Alaei, Investigation of the thermal transmittances calculated using new infrared technology developed by QEA Tech, n.d.

[75] MATLAB Runtime - MATLAB Compiler - MATLAB, (n.d.). https://www.mathworks.com/products/compiler/matlab-runtime.html (accessed July 20, 2024).

[76] Historical Data - Climate - Environment and Climate Change Canada, (n.d.). https://climate.weather.gc.ca/historical_data/search_historic_data_e.html (accessed October 31, 2024).

[77] S. Chang, D. Castro-Lacouture, Y. Yamagata, Decision support for retrofitting building envelopes using multi-objective optimization under uncertainties, Journal of Building Engineering 32 (2020) 101413. https://doi.org/10.1016/J.JOBE.2020.101413.

[78] A.S. Javid, F. Aramoun, M. Bararzadeh, A. Avami, Multi objective planning for sustainable retrofit of educational buildings, Journal of Building Engineering 24 (2019) 100759. https://doi.org/10.1016/J.JOBE.2019.100759.

[79] F. Harkouss, F. Fardoun, P.H. Biwole, Multi-objective optimization methodology for net zero energy buildings, Journal of Building Engineering 16 (2018) 57–71. https://doi.org/10.1016/J.JOBE.2017.12.003.

[80] F. Ascione, N. Bianco, T. Iovane, G.M. Mauro, D.F. Napolitano, A. Ruggiano, L. Viscido, A real industrial building: Modeling, calibration and Pareto optimization of energy retrofit, Journal of Building Engineering 29 (2020) 101186. https://doi.org/10.1016/J.JOBE.2020.101186.

[81] M. Motalebi, A. Rashidi, M.M. Nasiri, Optimization and BIM-based lifecycle assessment integration for energy efficiency retrofit of buildings, Journal of Building Engineering 49 (2022) 104022. https://doi.org/10.1016/J.JOBE.2022.104022.

[82] E. Asadi, M.G. Da Silva, C.H. Antunes, L. Dias, Multi-objective optimization for building retrofit strategies: A model and an application, Energy Build. 44 (2012) 81–87. https://doi.org/10.1016/J.ENBUILD.2011.10.016.

[83] I. Costa-Carrapiço, R. Raslan, J.N. González, A systematic review of genetic algorithm-based multi-objective optimisation for building retrofitting strategies towards energy efficiency, Energy Build. 210 (2020) 109690. https://doi.org/10.1016/J.ENBUILD.2019.109690.

[84] E. Asadi, M.G. da Silva, C.H. Antunes, L. Dias, A multi-objective optimization model for building retrofit strategies using TRNSYS simulations, GenOpt and MATLAB, Build. Environ. 56 (2012) 370–378. https://doi.org/10.1016/J.BUILDENV.2012.04.005.

[85] P. Shen, Building retrofit optimization considering future climate and decision-making under various mindsets, Journal of Building Engineering 96 (2024) 110422. https://doi.org/10.1016/J.JOBE.2024.110422.

[86] K. Mirzaei, A. Safari, S. Jalilzadeh, F. Mostafazadeh, M. Tavakolan, M. Safari, Environmental, Social, and Economic Benefits of Buildings Energy Retrofit Projects: A Case Study in Iran's Construction Industry, Construction Research Congress 2020: Infrastructure Systems and Sustainability - Selected Papers from the Construction Research Congress 2020 (2020) 693–701. https://doi.org/10.1061/9780784482858.075.

[87] L_2018156EN.01007501.xml, (n.d.). https://eur-lex.europa.eu/legal-content/EN/TXT/HTML/?uri=CELEX:32018L0844&rid=7 (accessed July 20, 2024).

[88] F. Maamari, M. Andersen, J. de Boer, W.L. Carroll, D. Dumortier, P. Greenup, Experimental validation of simulation methods for bi-directional transmission properties at the daylighting performance level, Energy Build. 38 (2006) 878–889. https://doi.org/10.1016/J.ENBUILD.2006.03.008.

[89] A. Auza, E. Asadi, B. Chenari, M. Gameiro da Silva, Review of cost objective functions in multi-objective optimisation analysis of buildings, Renewable and Sustainable Energy Reviews 191 (2024) 114101. https://doi.org/10.1016/J.RSER.2023.114101.

[90] R. Batres, Y. Dadras, F. Mostafazadeh, M. Kavgic, MEVO: A Metamodel-Based Evolutionary Optimizer for Building Energy Optimization, Energies 2023, Vol. 16, Page 7026 16 (2023) 7026. https://doi.org/10.3390/EN16207026.

[91] M. Tavakolan, F. Chokan, M. Dadashi Haji, Simultaneous project portfolio selection and scheduling from contractor perspective, International Journal of Construction Management 24 (2024) 298–313. https://doi.org/10.1080/15623599.2023.2222995.

[92] F. Mostafazadeh, Y. Dadras, M. Kavgic, R. Batres, Application of Metamodel-Based Evolutionary Optimizer (MEVO) to Improve Energy Efficiency of a Dormitory Building in Canada, in: Lecture Notes in Civil Engineering, Springer Science and Business Media Deutschland GmbH, 2025: pp. 479–485. https://doi.org/10.1007/978-981-97-8309-0_65.

[93] S.A. Sharif, A. Hammad, Simulation-Based Multi-Objective Optimization of institutional building renovation considering energy consumption, Life-Cycle Cost and

Life-Cycle Assessment, Journal of Building Engineering 21 (2019) 429–445. https://doi.org/10.1016/J.JOBE.2018.11.006.

[94] J.D. Kneifel, E.G. O'Rear, An Assessment of Typical Weather Year Data Impacts vs. Multi-year Weather Data on Net-Zero Energy Building Simulations, Gaithersburg, MD, 2016. https://doi.org/10.6028/NIST.SP.1204.

[95] M. Sengupta, Y. Xie, A. Lopez, A. Habte, G. Maclaurin, J. Shelby, The National Solar Radiation Data Base (NSRDB), Renewable and Sustainable Energy Reviews 89 (2018) 51–60. https://doi.org/10.1016/j.rser.2018.03.003.

[96] Engineering Climate Datasets - Climate - Environment and Climate Change Canada, (n.d.). https://climate.weather.gc.ca/prods_servs/engineering_e.html (accessed July 25, 2025).

[97] Engineering Climate Datasets - Climate - Environment and Climate Change Canada, (n.d.). https://climate.weather.gc.ca/prods_servs/engineering_e.html (accessed May 10, 2025).

[98] EnergyPlus, (n.d.). https://energyplus.net/weather (accessed July 25, 2025).

[99] Homepage | World Meteorological Organization WMO, (n.d.). https://wmo.int/ (accessed July 25, 2025).

[100] intro - Meteonorm (en), (n.d.). https://meteonorm.com/en/ (accessed October 31, 2024).

[101] Climate Change World Weather File Generator for World-Wide Weather Data - CCWorldWeatherGen - University of Southampton Blogs, (n.d.). https://energy.soton.ac.uk/ccworldweathergen/ (accessed October 31, 2024).

[102] R.F. De Masi, A. Gigante, S. Ruggiero, G.P. Vanoli, Impact of weather data and climate change projections in the refurbishment design of residential buildings in cooling dominated climate, Appl. Energy 303 (2021) 117584. https://doi.org/10.1016/J.APENERGY.2021.117584.

[103] HadCM3 Climate Scenario Data, (n.d.). https://www.ipcc-data.org/sim/gcm_clim/SRES_TAR/hadcm3_download.html (accessed May 10, 2025).

[104] M.F. Jentsch, A.B.S. Bahaj, P.A.B. James, Climate change future proofing of buildings—Generation and assessment of building simulation weather files, Energy Build. 40 (2008) 2148–2168. https://doi.org/10.1016/J.ENBUILD.2008.06.005.

[105] J. Remund, S. Müller, M. Schmutz, P. Graf, METEONORM VERSION 8, n.d. www.meteonorm.com.

[106] V.M. Nik, Application of typical and extreme weather data sets in the hygrothermal simulation of building components for future climate – A case study for a wooden frame wall, Energy Build. 154 (2017) 30–45. https://doi.org/10.1016/j.enbuild.2017.08.042.

[107] D.R. Liyanage, K. Hewage, M. Ghobadi, R. Sadiq, Thermal resiliency of single-family housing stock under extreme hot and cold conditions, Energy Build. 323 (2024) 114809. https://doi.org/10.1016/j.enbuild.2024.114809.

[108] P. Berdahl, M. Martin, Emissivity of clear skies, Solar Energy 32 (1984) 663–664. https://doi.org/10.1016/0038-092X(84)90144-0.

[109] M. Martin, P. Berdahl, Characteristics of infrared sky radiation in the United States, Solar Energy 33 (1984) 321–336. https://doi.org/10.1016/0038-092X(84)90162-2.

[110] C. Lavaysse, C. Cammalleri, A. Dosio, G. Van Der Schrier, A. Toreti, J. Vogt, Towards a monitoring system of temperature extremes in Europe, Natural Hazards and Earth System Sciences 18 (2018) 91–104. https://doi.org/10.5194/nhess-18-91-2018.

[111] M. Smid, S. Russo, A.C. Costa, C. Granell, E. Pebesma, Ranking European capitals by exposure to heat waves and cold waves, Urban Clim. 27 (2019) 388–402. https://doi.org/10.1016/j.uclim.2018.12.010.

[112] M.R. Kaloop, F. Ahmad, P. Samui, E. Elbeltagi, J.W. Hu, H. Wefki, Predicting energy consumption of residential buildings using metaheuristic-optimized artificial neural network technique in early design stage, Build. Environ. 274 (2025) 112749. https://doi.org/10.1016/J.BUILDENV.2025.112749.

[113] Emission factors and reference values - Canada.ca, (n.d.). https://www.canada.ca/en/environment-climate-change/services/climate-change/pricing-pollution-how-it-will-work/output-based-pricing-system/federal-greenhouse-gas-offset-system/emission-factors-reference-values.html (accessed July 18, 2025).

[114] X. Zhan, W. Zhang, R. Chen, Y. Bai, J. Wang, G. Deng, Non-dominated sorting genetic algorithm-II: A multi-objective optimization method for building renovations with half-life cycle and economic costs, Build. Environ. 267 (2025) 112155. https://doi.org/10.1016/J.BUILDENV.2024.112155.

[115] J. Kneifel, D. Webb, Life cycle costing manual for the Federal Energy Management Program, 2022. https://doi.org/10.6028/NIST.HB.135e2022-upd1.

[116] Regulated Price Plan Price Report Ontario Energy Board, 2024. https://ieso.ca/en/Market-Renewal/Market-Participant-Readiness/Market-Participant-Readiness.

[117] Canada 10 Year Benchmark Bond Yield Market Daily Trends: Bank of Canada Interest Rates | YCharts, (n.d.). https://ycharts.com/indicators/canada_10_year_benchmark_bond_yield (accessed May 24, 2025).

[118] The Daily — Consumer Price Index, August 2024, (n.d.). https://www150.statcan.gc.ca/n1/daily-quotidien/240917/dq240917a-eng.htm (accessed May 24, 2025).

[119] B. Ge, Z. Fan, J. Liu, Two-stage multi-objective optimization of solar roof design for railway-station represented large-space public buildings considering thermal efficiency, carbon emissions, and daylighting, Build. Environ. 280 (2025) 113084. https://doi.org/10.1016/J.BUILDENV.2025.113084.

[120] M.A. Kamazani, M.K. Dixit, S.S. Shanbhag, Optimizing interconnected embodied and operational energy of buildings: An embodied energy factor approach, Build. Environ. 276 (2025) 112902. https://doi.org/10.1016/J.BUILDENV.2025.112902.

[121] X. Zhan, W. Zhang, R. Chen, Y. Bai, J. Wang, G. Deng, Non-dominated sorting genetic algorithm-II: A multi-objective optimization method for building renovations with half-life cycle and economic costs, Build. Environ. 267 (2025) 112155. https://doi.org/10.1016/J.BUILDENV.2024.112155.

[122] Q. Yang, F. Xu, W. zhen Lu, Z. Yang, Y. Bai, B. Wen, Green renovation and multi-objective optimization of Tibetan courtyard dwellings, Build. Environ. 279 (2025) 113071. https://doi.org/10.1016/J.BUILDENV.2025.113071.

[123] W. Li, M. Rahim, B. Wang, M. El Ganaoui, R. Bennacer, Enhancing building envelope performance via dynamic PCM Integration in biomaterial concrete walls: A numerical evaluation and multi-objective optimization study, Build. Environ. 280 (2025) 113141. https://doi.org/10.1016/J.BUILDENV.2025.113141.

[124] G. Zhang, H. Wu, J. Liu, H. Huang, Y. Liu, A multi-objective design optimization for the exterior wall coatings of residential buildings in hot summer and warm winter regions, Build. Environ. 262 (2024) 111776. https://doi.org/10.1016/J.BUILDENV.2024.111776.

[125] G. Campos Ciro, F. Dugardin, F. Yalaoui, R. Kelly, A NSGA-II and NSGA-III comparison for solving an open shop scheduling problem with resource constraints, in: IFAC-PapersOnLine, Elsevier B.V., 2016: pp. 1272–1277. https://doi.org/10.1016/j.ifacol.2016.07.690.

[126] A. Razmi, M. Rahbar, M. Bemanian, PCA-ANN integrated NSGA-III framework for dormitory building design optimization: Energy efficiency, daylight, and thermal comfort, Appl. Energy 305 (2022) 117828. https://doi.org/10.1016/J.APENERGY.2021.117828.

[127] A. Karatas, K. El-Rayes, Optimizing tradeoffs among housing sustainability objectives, Autom. Constr. 53 (2015) 83–94. https://doi.org/10.1016/J.AUTCON.2015.02.010.

[128] Y.F. Li, M. Xie, T.N. Goh, A study of project selection and feature weighting for analogy based software cost estimation, Journal of Systems and Software 82 (2009) 241–252. https://doi.org/10.1016/J.JSS.2008.06.001.

[129] Y.F. Li, S.H. Ng, M. Xie, T.N. Goh, A systematic comparison of metamodeling techniques for simulation optimization in Decision Support Systems, Appl. Soft Comput. 10 (2010) 1257–1273. https://doi.org/10.1016/J.ASOC.2009.11.034.

[130] Y. Dadras, F. Mostafazadeh, M. Kavgic, M. Ghobadi, Enhancing building energy optimization efficiency: A performance analysis of simplification approaches, Journal of Building Engineering 105 (2025). https://doi.org/10.1016/j.jobe.2025.112559.

[131] Y. Dadras, M. Kavgic, The applicability of simplified whole-building energy model for energy-efficiency retrofit analysis, 12 (2022) 0–0. https://publications.ibpsa.org/conference/paper/?id=esim2022_254 (accessed July 10, 2024).

[132] J. Kosny, D. Gawin, Thermal Mass-Energy Savings Potential in Residential Buildings, n.d. https://www.researchgate.net/publication/268411404.

[133] Emissions Gap Report - United Nations Environment Programme, (2023). https://doi.org/10.59117/20.500.11822/43922.

[134] Paris Agreement - Canada.ca, (n.d.). https://www.canada.ca/en/environment-climate-change/services/climate-change/paris-agreement.html (accessed July 4, 2025).

[135] A. Reilly, O. Kinnane, The impact of thermal mass on building energy consumption, Appl. Energy 198 (2017) 108–121. https://doi.org/10.1016/J.APENERGY.2017.04.024.

[136] Y. Dadras, F. Mostafazadeh, M. Kavgic, M. Ghobadi, Evaluating simplified building models' sensitivity to climate data for energy retrofit optimization, Build. Environ. 287 (2026) 113885. https://doi.org/10.1016/J.BUILDENV.2025.113885.

[137] S. Haykin, Neural networks: a comprehensive foundation., Prentice Hall PTR, 1998.

[138] N.D. Roman, F. Bre, V.D. Fachinotti, R. Lamberts, Application and characterization of metamodels based on artificial neural networks for building performance simulation: A systematic review, Energy Build. 217 (2020). https://doi.org/10.1016/j.enbuild.2020.109972.

[139] Deep Learning Toolbox - MATLAB, (n.d.). https://www.mathworks.com/products/deep-learning.html (accessed November 14, 2024).

[140] IE for Buildings | Athena Sustainable Materials Institute, (n.d.). https://www.athenasmi.org/our-software-data/impact-estimator/ (accessed November 29, 2025).

[141] Inflation-control target - Bank of Canada, (n.d.). https://www.bankofcanada.ca/rates/indicators/key-variables/inflation-control-target/?utm_source=chatgpt.com (accessed December 29, 2025).

[142] Canada's cost-benefit analysis guide for regulatory proposals, Treasury Board of Canada Secretariat = Secrétariat du Conseil du trésor du Canada, 2022.

[143] Canada Gazette, Part 1, Volume 158, Number 45: Oil and Gas Sector Greenhouse Gas Emissions Cap Regulations, (n.d.). https://gazette.gc.ca/rp-pr/p1/2024/2024-11-09/html/reg1-eng.html?utm_source=chatgpt.com (accessed December 29, 2025).

Appendix

Appendix A: Survey Questionnaire

1. What is your primary role in energy modeling? *

   Energy Modeler

   Architect

   Engineer

   Other

2. How many years of experience do you have in energy modeling? *

   I have no experience in energy modeling

   Less than one year

   1-3 years

   4-6 years

   7+ years

3. On average, what percentage of your total modeling time is spent on the following tasks: *

	5-10%	10-25%	25-40%	40-50%	50-75%	75-90%	90-100%
Data collection							
Creating geometry							
Implementing the detailed data on the model							
HVAC modeling							
Addressing simulation errors							
Other							

4. How important is accurate energy modeling on your projects? *

   Extremely important

   Somewhat important

   Neutral

   Somewhat not important

   Extremely not important

5. How challenging do you find the process of collecting necessary data for your energy modeling projects? *

Extremely challenging

Somewhat challenging

Neutral

Somewhat not challenging

Not challenging

6. In which stages of your modeling process do you find data collection most challenging? (Select all that apply) *

Geometry data

Material and construction selection

Lighting systems and equipment specification

People and operation schedule

HVAC systems specifications

Control systems

Other

7. Which software do you primarily use for energy modeling? *

EnergyPlus

eQUEST

OpenStudio

TRNSYS

DesignBuilder

IES VE (Virtual Environment)

Other

8. How willing are you to use simplified models with reduced accuracy to accelerate the simulation process? *

Very willing, even with a noticeable reduction in accuracy

Moderately willing, with some compromise on accuracy

Slightly willing, if minimal compromise on accuracy is needed

Not willing to sacrifice accuracy for speed

9. How frequently do you use simplified models (e.g., default templates, simplified geometry) in your energy modeling projects? *

Frequently

Occasionally

Rarely

Never

10. Please indicate which parts of your modeling process you have simplified and estimate the percentage by which these simplifications reduced the modeling time for each applicable part. Select all options that apply: *

	5-10%	10-25%	25-40%	40-50%	50-75%	75-90%	90-100%
Geometry modeling							
Material and construction definition							
Lighting systems and equipment specifications							
People and operation schedule							
HVAC systems specifications							
Other							

11. Is there anything else you would like to share about your experiences with energy modeling?

12. Please provide your email address (optional) if you would like to receive the survey results or participate in follow-up research.

Appendix B

ε_{clear} is calculated using Equation B.1:

$$\varepsilon_{clear} = 0.711 + 0.56 \cdot \frac{T_{dew}}{100} + 0.56 \cdot (\frac{T_{dew}}{100})^2 \quad \text{Equation B.1}$$

Then, the clear-sky temperature is computed as in Equation B.2:

$$T_{clear\ sky} = (T_{air} + 273.15) \cdot (\varepsilon_{clear}^{0.25}) \quad \text{Equation B.2}$$

Cloud cover is incorporated using a correction factor (β_a) which is introduced based on the cloudiness fraction β, as shown in Equation B.3:

$$\beta_a = 1 + 0.0224\,\beta + 0.0035\,\beta^2 + 0.00028\,\beta^3 \quad \text{Equation B.3}$$

Assuming clear-sky conditions ($\beta = 0$), the sky temperature is then calculated using Equation B.4.

$$T_{sky} = \beta_a^{0.25}.T_{clear\ sky} - 273.15 \quad \text{Equation B.4}$$

The convective heat transfer coefficient (α_c) [W/m²·K] is determined as a function of wind speed using Equation B.5.

$$\alpha_c = \begin{cases} 6 + 4 \cdot v, & if\ v \leq 5\ m/s \\ 7.41 \cdot v^{0.78}, & if\ v > 5m/s \end{cases} \quad \text{Equation B.5}$$

The radiative heat transfer coefficient (α_r) [W/m²·K] is calculated using Stefan–Boltzmann's law as shown in Equation A.6:

$$\alpha_r = 4.\varepsilon.\sigma.(\frac{(T_{sky}+273.15)+(T_{air}+273.15)}{2})^3 \quad \text{Equation B.6}$$

where ε = 0.9 is the surface emissivity and σ = 5.67×10^{-8} [W/m^2·K] is the Stefan–Boltzmann constant.

Table B.1. Statistical analysis of Pareto-optimal results of simplified models based on NPV ([CAD]×10^3) criterion.

	One-zone	Two-zone	Seven-zone	Thirty-five-zone	R-value	HVAC
Minimum	1971	1986	2037	2358	2490	2172
Maximum	2427	2830	2392	2487	2709	2516
Mean	2243	2409	2233	2396	2591	2370
Median	2246	2382	2248	2386	2595	2417
Standard Deviation	105	197	104	28	44	104

Table B.2: Statistical analysis of Pareto-optimal results of simplified models based on Energy consumption ([kWh]×10^3) criterion.

	One-zone	Two-zone	Seven-zone	Thirty-five-zone	R-value	HVAC
Minimum	31536	31494	31354	31546	37413	29168
Maximum	35726	36502	36585	32522	38780	33499
Mean	32677	32271	33663	31879	37855	30378
Median	32367	31863	32483	31882	37755	29243
Standard Deviation	1217	1098	1977	135	342	1806

Table B.3: Statistical analysis of Pareto-optimal results of simplified models based on CO_2 Emissions ([kg]×10^3) criterion.

	One-zone	Two-zone	Seven-zone	Thirty-five-zone	R-value	HVAC
Minimum	4594	4576	4516	4562	5527	4005
Maximum	5334	5472	5424	4800	5751	4793
Mean	4798	4723	4923	4656	5635	4237
Median	4740	4658	4700	4653	5636	4034
Standard Deviation	212	196	345	42	57	319